

Final report

# BIO-ELECTROFUELS

– hybrid fuels for improved resource efficiency

April 2022

Erik Furusjö, Sennai Mesfun – RISE Research Institutes of Sweden

Mahrokh Samavati – KTH Royal Institute of technology

Anton Larsson, Gabriel Gustafsson – BioShare

With contributions from:

Christer Gustavsson – BioShare AB

Sven Hermansson, Johanna Olsson – Södra Skogsägarna

Per Sundell, Kajsa Kairento – Vattenfall

Per-Arne Karlsson, Linda Werner – St1

Johan Ahlström, Camille Hamon and Tobias Gunneberg, RISE

A project within

**RENEWABLE TRANSPORTATION FUELS AND SYSTEMS 2018-2021**

A collaborative research program between the Swedish Energy Agency and  
f3 The Swedish Knowledge Centre for Renewable Transportation Fuels



[www.energimyndigheten.se](http://www.energimyndigheten.se)



[www.f3centre.se](http://www.f3centre.se)



## PREFACE

This project has been carried out within the collaborative research program *Renewable transportation fuels and systems* (Förnybara drivmedel och system), Project no. 50452-1. The project has been financed by the Swedish Energy Agency and f3 – Swedish Knowledge Centre for Renewable Transportation Fuels.

The Swedish Energy Agency is a government agency subordinate to the Ministry of Infrastructure. The Swedish Energy Agency is leading the energy transition into a modern and sustainable, fossil free welfare society and supports research on renewable energy sources, the energy system, and future transportation fuels production and use.

f3 Swedish Knowledge Centre for Renewable Transportation Fuels is a networking organization which focuses on development of environmentally, economically and socially sustainable renewable fuels. The f3 centre is financed jointly by the centre partners and the region of Västra Götaland. Chalmers Industriteknik functions as the host of the f3 organization (see <https://f3centre.se/en/about-f3/>).

The results presented in this report is the result of a cooperation in the project group, including the organisations RISE, KTH, BioShare, St1, Södra Skogsägarna and Vattenfall. The main authors, from RISE, KTH and BioShare, wish to express their appreciation for the additional contributions as indicated on the front page.

### **This report should be cited as:**

Furusjö, E., *et. al.*, (2022) *Bio-electro fuels – hybrid technology for improved resource efficiency*. Publ. No FDOS 45:2022. Available at <https://f3centre.se/en/renewable-transportation-fuels-and-systems/>



## SUMMARY

Sustainable biofuels will be an important part of the transition of the transport sector towards sustainability. Despite extensive electrification, primarily in road transport, the demand for gaseous and liquid fuels is expected to be significant in both 2030 and 2045.

Sustainable biomass is a limited resource and harvesting levels for forest biomass for industrial use is being intensively discussed in politics, both with respect to biodiversity trade-offs and the forest as a short-term carbon sink. Regardless of one's position in this debate, it can be concluded that obtaining maximum utility from each harvested tree is important – and will likely be increasingly important in a future with even larger demands of sustainable products to replace fossil products.

In this respect, the relatively low carbon efficiency in the transformation of lignocellulosic biomass to transportation fuels and chemicals using emerging biorefinery technologies, such as gasification, pyrolysis and fermentation, could become a challenge. It leads to lower climate benefit and lower amount of displaced fossil products from a certain amount of biomass. This research project investigates how integrated electrification of biorefinery processes can be used to improve the carbon efficiency. Process modelling of different process configurations, based on openly available data for process units' performance, was used as the main tool. The results of the modelling were used to estimate performance indicators for the configurations, such as efficiency, production cost and greenhouse gas emissions.

An initial screening of emerging biofuel production technologies for lignocellulosic feedstock shows that the carbon efficiencies that can be obtained practically, using current “state-of-the-art” process configurations, are only 25-50%. There are several reasons for this

- 1) the limitation posed by the differing elemental composition of feedstock and product
- 2) biomass feedstock is used both as carbon source and as energy source, which usually means that some of the feedstock is combusted in the process
- 3) by-product formation and side reactions, which lead to the formation of carbon-containing streams other than the main desired product

Integrated electrification can provide means to improve the carbon efficiency. Previous research studies have investigated the effects for specific combinations of biofuel production technologies and electrification options. The broader analysis done in this project for a large number of combinations show that the two most important technology categories for electrification were:

- 1) Electrolysis of water for hydrogen addition to the biomass conversion process, which can address the limitations posed by the different element composition of feedstock and product
- 2) Electric heating, which can address the use of part of the biomass feedstock as energy source, by replacing this with electric energy. For example by high temperature direct heating or heat pumps.

For some biorefinery technologies, the fraction of electric energy input can become substantial and even exceed the energy input from the biomass feedstock. This motivates the terminology bio-electrofuels for the products of such an electrified biorefinery.

Based on process modelling, techno-economic analysis and implementation scenario analysis, the following overall conclusion can be made:

- Integrated electrification of biofuel production, leading to so called bio-electrofuels, can in general greatly improve biomass resource efficiency. The potential is different for different biofuel production technologies.
- Integrated electrification can in general enable increased production capacity and improved economies of scale for a given amount of feedstock available.
- The most important electrification technologies that can lead to this improvement in efficiency are water electrolysis, high-temperature direct electric heating and heat pumps, with the specific technology or combination of technologies being dependent on the biofuel production process.
- Gasification-based biofuel production from lignocellulosic biomass shows the greatest potential for integrated electrification. The amount of transportation fuels that can be produced from the same amount of biomass can in many cases be doubled or tripled.
- Other lignocellulosic-based production technologies also show potential for integrated electrification with good efficiency improvements, but smaller than gasification
- The overall energy efficiency of the process is in general not negatively affected by the electrification. There are differences depending on the production technology with either small improvements in energy efficiency or small decreases.
- The production costs for bio-electrofuels are similar to or somewhat higher than the corresponding biofuels production costs, but lower than the corresponding electrofuels cost. This indicates that indirect electrification is cost-efficient.
- The greenhouse gas performance of all options studied – biofuels, bio-electrofuels and electrofuels – are in general good as long as the GHG footprint of the electricity used in the process is low.
- A scenario analysis for production to meet the demand of the future transport sector demand for liquid and gaseous fuels was made. The results indicate that improving biomass resource efficiency by indirect electrification leads to the possibility to meet demand based on domestic sustainable biomass resources, which was not possible using state-of-the-art biofuel production technology with lower carbon efficiency.
- Development of policy/incentives that promotes resource efficient use of limited biogenic resources in biorefineries is highly motivated in order to future-proof the biofuel production capacity being built up in the coming years. The efficient bio-electrofuel technologies may not be cost-competitive compared to pure biofuels given current market conditions.

## SAMMANFATTNING

Hållbara biodrivmedel kommer att vara en viktig del av transportsektorns omställning. Trots omfattande elektrifiering, främst inom vägtransporter, förväntas efterfrågan på gasformiga och flytande bränslen vara betydande både 2030 och 2045.

Hållbar biomassa är en begränsad resurs och avverkningsnivåer för skogsbiomassa för industriellt bruk diskuteras intensivt i politiken, både när det gäller biologisk mångfald och skogen som en kortsiktig kolsänka. Oavsett vad man ställer sig i denna debatt kan man dra slutsatsen att det är viktigt att få maximal nytta av varje avverkat träd – och sannolikt kommer att bli allt viktigare i en framtid med ännu större krav på hållbara produkter för att ersätta fossila produkter.

I detta avseende skulle den relativt låga koleffektiviteten vid omvandlingen av lignocellulosa-biomassa till drivmedel och kemikalier med hjälp av ny bioraffinadertechnik, såsom förgasning, pyrolys och fermentering, kunna bli en utmaning. Denna leder till lägre klimatnytta och lägre mängd substituerade fossila produkter från en viss mängd biomassa.

Detta forskningsprojekt undersöker hur integrerad elektrifiering av bioraffinaderiprocesser kan användas för att förbättra koleffektiviteten. Processmodellering av olika processkonfigurationer, baserat på öppet tillgängliga data för processernas prestanda, användes som huvudverktyg. Resultaten av modelleringen användes för att uppskatta prestandaindikatorer för konfigurationerna, såsom effektivitet, produktionskostnader och utsläpp av växthusgaser.

En första granskning av framväxande produktionstekniker för biodrivmedel för lignocellulosaråvaror visar att de koldioxideffektiviteter som kan erhållas praktiskt, med hjälp av nuvarande "state-of-the-art" processkonfigurationer, endast är 25–50%. Det finns flera skäl till detta:

1. Begränsningar till följd av råvarans och produktens olika grundämnessammansättning
2. Biomassaråvara används både som kolkälla och som energikälla, vilket vanligtvis innebär att en del av råvaran förbränns i processen
3. Biproduktbildning och sidoreaktioner, vilket leder till bildandet av andra kolhaltiga strömmar än den huvudsakliga önskade produkten

Integrerad elektrifiering ger goda möjligheter att förbättra koleffektiviteten. Tidigare forskningsstudier har undersökt effekterna för specifika kombinationer av produktionstekniker och elektrifieringsalternativ. Den bredare analys som gjorts i detta projekt för ett stort antal kombinationer visar att de två viktigaste teknikkategorierna för elektrifiering var:

1. Elektrolys av vatten för vätetillsats till omvandlingsprocessen, som kan motverka de begränsningar som orsakas av råmaterialets och produktens olika grundämnessammansättning.
2. Elvärme, som kan motverka användningen av en del av biomassaråvaran som energikälla, genom att ersätta denna med elektrisk energi, till exempel genom direktvärmning vid hög temperatur eller genom värmepumpar.

För vissa bioraffinadertechniker kan andelen tillförd elenergi bli betydande och till och med överstiga den tillförda energin från biomassaråvaran. Detta motiverar terminologin bioelektrobränslen för produkterna i ett sådant elektrifierat bioraffinaderi.

Baserat på processmodellering, tekno-ekonomisk analys och analys av implementeringsscenarioer kan följande övergripande slutsats göras:

- Integrerad elektrifiering av biodrivmedelsproduktion, som leder till så kallade bioelektrobränslen, kan i allmänhet avsevärt förbättra biomassans resurseffektivitet. Potentialen är olika för olika produktionstekniker.
- Integrerad elektrifiering kan i allmänhet möjliggöra ökad produktionskapacitet och förbättrade stordriftsfördelar för en viss mängd tillgängliga råvaror.
- De viktigaste elektrifieringsteknikerna som kan leda till denna effektivitetsförbättring är vattenelektrolys, direkt elektrisk uppvärmning vid höga temperaturer och värmepumpar, där den specifika tekniken eller kombinationen av tekniker är beroende av produktionsprocessen.
- Förgasningsbaserad biodrivmedelsproduktion från lignocellulosa visar störst potential för integrerad elektrifiering. Mängden drivmedel som kan produceras från samma mängd biomassa kan i många fall fördubblas eller tredubblas.
- Andra lignocellulosabaserade produktionstekniker visar också potential för integrerad elektrifiering med goda effektivitetsförbättringar, men mindre än förgasning.
- Processens totala energieffektivitet påverkas i allmänhet inte negativt av elektrifieringen. Det finns skillnader beroende på produktionsteknik med antingen små förbättringar av energieffektiviteten eller små minskningar.
- Produktionskostnaderna för bioelektrobränslen är liknande eller något högre än motsvarande produktionskostnader för biodrivmedel, men lägre än motsvarande elektrobränslekostnad. Detta indikerar att indirekt elektrifiering är kostnadseffektivt.
- Växthusgasprestandan för alla studerade alternativ – biobränslen, bioelektrobränslen och elektrobränslen – är i allmänhet bra så länge som växthusgasavtrycket från den el som används i processen är lågt.
- En scenarioanalys av produktion för att möta efterfrågan från den framtida transportsektorn på flytande och gasformiga bränslen gjordes. Resultaten tyder på att förbättrad biomassa-resurseffektivitet genom indirekt elektrifiering leder till möjligheten att möta efterfrågan baserad på inhemska hållbara biomassaresurser, vilket inte var möjligt med hjälp av produktion av biodrivmedel med lägre koldioxideffektivitet.
- Utvecklingen av politik/incitament som främjar resurseffektiv användning av begränsade biogena resurser i bioraffinaderier är mycket motiverad för att framtidssäkra den produktionskapacitet för biodrivmedel som byggs upp under de kommande åren. Den effektiva bioelektrobränsletekniken är inte allt ekonomiskt konkurrenskraftig jämfört med rena biodrivmedel med nuvarande marknadsförhållanden.

# CONTENTS

1 INTRODUCTION .....	11
1.1 BACKGROUND .....	11
1.2 PROJECT SCOPE AND OBJECTIVES .....	12
2 METHODOLOGY .....	13
2.1 OVERALL APPROACH .....	13
2.2 PROCESS MODELLING OF BIOFUEL PRODUCTION PATHWAYS .....	13
2.3 EFFICIENCY METRICS .....	14
2.4 TECHNO-ECONOMIC ANALYSIS .....	16
2.5 GREENHOUSE GAS FOOTPRINTS .....	18
3 THEORETICAL EFFICIENCIES OF BIOFUEL PRODUCTION .....	20
4 INITIAL TECHNOLOGY SCREENING .....	25
4.1 CARBON AND ENERGY EFFICIENCY OF BIOFUEL PRODUCTION.....	25
4.2 PRIORITIZED TRACKS AND ELECTRIFICATION OPTIONS.....	29
5 INTERMITTENT ELECTRIFICATION AND HYDROGEN STORAGE .....	30
5.1 INTERMITTENT ON/OFF ELECTROLYZER OPERATION.....	30
5.2 ELECTROLYZER OPERATION WITH FLEXIBILITY SERVICES.....	35
5.3 CONCLUSION .....	37
6 CARBON AND ENERGY EFFICIENCY OF BIO-ELECTRO FUELS PRODUCTION.....	38
6.1 ELECTROLYSIS .....	38
6.2 LIGNOCELLULOSIC ETHANOL.....	39
6.3 ETHANOL-TO-JET FUEL .....	43
6.4 HYDROTHERMAL LIQUEFACTION OF WOODY BIOMASS.....	46
6.5 FAST PYROLYSIS .....	49
6.6 BLACK LIQUOR GASIFICATION (BLG) .....	52
6.7 BLACK LIQUOR GASIFICATION FOR METHANOL PRODUCTION.....	55
6.8 BLACK LIQUOR GASIFICATION FOR FISCHER TROPSCH FUELS .....	59
6.9 DUAL FLUIDIZED BED (DFB) GASIFICATION .....	64
6.10 DFB GASIFICATION FOR SNG PRODUCTION .....	65
6.11 DFB GASIFICATION FOR FISCHER TROPSCH (FT) PRODUCTION.....	70
6.12 FLUIDIZED BED (FB) GASIFICATION .....	75
6.13 FB GASIFICATION FOR SNG PRODUCTION.....	76

6.14	FB GASIFICATION FOR FISCHER TROPSCH (FT) PRODUCTION .....	79
6.15	REFERENCE ELECTROFUEL TRACKS.....	82
6.16	SUMMARY AND CONCLUSIONS.....	83
6.17	EXCESS HEAT IN DITRICT HEATING NETWORKS .....	89
7	ECONOMIC PERFORMANCE .....	91
7.1	INVESTMENT COST ESTIMATES .....	91
7.2	PRODUCTION COST ESTIMATES .....	92
8	GREENHOUS GAS FOOTPRINTS .....	102
9	SCENARIOS FOR LARGE SCALE IMPLEMENTATION .....	105
9.1	BIOFUEL DEMAND SCENARIOS.....	105
9.2	NATIONAL SUSTAINABLE BIOMASS SUPPLY SCENARIOS.....	107
9.3	BIOFUEL PRODUCTION SCENARIOS.....	107
10	SUMMARY AND CONCLUSIONS .....	114
	REFERENCES .....	121
	APPENDIX 1. INTERMITTENT ELECTRIFICATION AND HYDROGEN STORAGE.....	126
	ELECTRICITY PRICE SCENARIOS .....	126
	METHODOLOGY FOR ELECTRICITY PRICE MINIMIZATION .....	129
	APPENDIX 2. EQUIPMENT COST FOR MAJOR PROCESS UNITS .....	130
	APPENDIX 3. CAPEX AND SPECIFIC INVESTMENT .....	132
	APPENDIX 4. MVR APPLICATION TO LIGNOCELLULOSIC ETHANOL PROCESS.....	134
	PRETREATMENT .....	134
	DISTILLATION .....	135
	DRYING.....	136
	APPENDIX 5. ADDITIONAL DATA FOR PROCESS MASS AND ENERGY BALANCE .....	137
	APPENDIX 6. PRODUCTION COST BUILD-UP .....	151

# 1 INTRODUCTION

## 1.1 BACKGROUND

Biofuels are an important component in the transition to a bio-based economy and a sustainable energy system, globally (International Energy Agency 2021) but more pronounced in a Nordic context (Hansson et al. 2019). Two important factors for a sustainable transition are good climate performance of the biofuels produced and efficient use of limited resources. The production processes for lignocellulosic biofuels that are commercially available today or are under commercial development often have relatively low resource efficiency in terms of the utilisation of biomass carbon. In a future where demand for the limited biomass resource is increasing, technologies that do not use the biogenic feedstocks in a resource-efficient way will not be competitive.

The hypothesis underpinning this project is that the integrated use of electricity in biofuel production can provide major benefits in terms of increased production potential, carbon efficiency and/or greenhouse gas performance, in biofuel production. The effects may be different depending on the type of biofuel process in which it is applied. The potential benefits of electrification come from a variety of specific challenges in biofuel production (Anton Larsson 2014; Wetterlund et al. 2022), contributing to increased costs and/or losses, which can be solved or mitigated by the use of electrical energy:

1. Biomass contains oxygen that (most often) must be removed as CO<sub>2</sub> or H<sub>2</sub>O, since most fuel products are hydrocarbons. In many process options, hydrogen is used, directly or indirectly, to remove oxygen.
2. Biomass typically has an (atomic) H/C ratio of 1-1.5 while hydrocarbon-based fuels have H/C $\approx$ 2. This means that carbon yield is necessarily lost unless hydrogen is added.
3. Many transformation processes, such as gasification and steam reforming, take place at high temperature with energy supply from the biogenic feedstock itself, which leads to losses.

Different technical solutions for electrification are relevant for different types of production processes and these can provide different benefits such as improved climate performance, increased production potential and improved carbon utilisation. This project studies the use of electrical energy through integrated measures. Examples of technologies for integrated use of electricity have been studied in the past and the European potential for the example of gasification-based production, as described by Hannula (Hannula 2016), has been found to be very significant. Flexibility is often highlighted for gasification applications, enabling the integration to a volatile electricity system (Poluzzi et al. 2022; Habermeyer et al. 2021). Other examples of electrification technologies with potential to improve resource efficiency are electrically heated steam reformers (Wismann et al. 2019a) and heat pumps to produce low temperature heat for evaporation or distillation (Fornell 2012).

Despite this, many aspects and technical possibilities for different production technologies have in previous work only been discussed in a general and fragmented way, which means that they cannot be compared. There is a lack of both an overall picture of the technical possibilities available for integrated electrification in biofuel production and a generic analysis of these possibilities. This

project aims to fill this particular gap and give a basis for decision-making for strategic decisions in policy development, technology development and development of commercial projects.

## 1.2 PROJECT SCOPE AND OBJECTIVES

The overall project objective is to provide a generic picture of the possibilities, advantages and disadvantages integrated electrification can provide in biofuel production.

Specifically, the project aimed to:

1. Report on the possibilities for integrated electrification that exist within different biofuel value chains with technical and commercial relevance at present and in the short and medium term
2. Report on the potential impact of integrated electrification on production potential, carbon efficiency and resource utilisation in biofuel production for different biofuel value chains
3. Report the potential impact of integrated electrification on production costs and greenhouse gas performance for different biofuel value chains and analyze which types of partial electrification provides the greatest benefit, including resource efficiency
4. Present scenarios for the implementation of the technology and their impact, e.g. in the form of electricity demand.

The biofuels production pathways to be included in the analysis are based on criteria determined in discussions in the project group. The following criteria for selection of biofuel production pathways were used:

- Production potential in the Nordic region
- Feedstocks: focus on lignocellulosic forest residues, but potentially also agricultural
- Product focus on road transport and jet fuels, drop-in and other. Not dedicated marine fuels.

## 2 METHODOLOGY

### 2.1 OVERALL APPROACH

The project approach is to a large extent based on process modelling using data from open literature. We used a staged approach

1. Initial screening of biofuel production technologies, commercial and under development, and mapping of their carbon and energy efficiency. Comparison to theoretical efficiencies estimated in a separate analysis.
2. Inventory of technologies, commercial and under development, allowing partial electrification of biofuel production. Mapping of these technologies towards biofuel processes and qualitative evaluation of their applicability and relevance.
3. Selection of biofuel production technologies to study in depth, based on relevance in a Nordic context and electrification potential. Conceptually designing a number of modified biofuel processes with partial electrification that will be evaluated in the rest of the project.
4. Calculating mass and energy balances for the base case and modified biofuel processes, to evaluate the effects of partial electrification on production potential, energy efficiency, carbon efficiency and resource utilization.
5. The energy and material balances are inputs to an evaluation of economy, resource efficiency and greenhouse gas performance under different scenarios. The economic analysis is based on traditional investment and cost analyses and include effects from integration with other industries.
6. Estimated efficiencies, production costs and GHG footprints are used in a scenario analysis that illustrates how the Swedish biofuel demand could be met by a combination of biofuels, bio-electrofuels and electrofuels under different technology options. The scenarios illustrate biomass and electricity demand as well as total cost and GHG emissions for the different options.

The studied system for efficiency and economic analysis ends at the plant gate, i.e. efficiency or cost effects in distribution or vehicle use of the fuels is not considered, which in practice means that it is assumed that the fuels behave as the current fossil fuels. In the GHG footprint analysis, the system boundaries and methodology is set by the Renewable Energy Directive, which for example prescribes how feedstock GHG is estimated and what the fossil comparator is, when calculating greenhouse gas savings.

The focus in terms of relevant feedstocks, processing technologies and products is set by the relevance for future Nordic conditions.

### 2.2 PROCESS MODELLING OF BIOFUEL PRODUCTION PATHWAYS

Process modelling of technology tracks was done in two steps. In the first step process mass and energy balances were developed using open literature data and knowledge in the participating organizations. The literature data used are describe below separately for each track. When required, different process technologies were combined in an appropriate manner to make a complete production track, e.g. gasification technologies were combined with gas cleaning and Fischer Tropsch

synthesis. As far as possible, the same technology options were used for different production technology tracks in order to make the results comparable and relevant, e.g. using the same Fischer Tropsch yields for different gasification technologies.

In this initial screening stage, detailed process including integrated electrification options were thus not developed. The focus was on understanding where carbon and energy losses occur in each of the production technology tracks and making a semi-quantitative estimate of how indirect electrification could improve carbon efficiency, including which electrification options would be most promising. Hence, the data sources were selected to be representative and “reasonable” implementation-wise rather than being heavily optimized for efficiency. Typical criteria for selection is that the balances have a base in empirical data of some type, process designs account for the compromise between efficiency and equipment cost and that other studies have reached similar efficiencies.

To make the reference technology tracks more comparable to the electrified options to be studied in the remainder of the project, we have chosen not to include any fossil feedstocks in the configurations studied. This is most relevant for processes using hydrogen (e.g. HVO) which is normally sourced from fossil gas (natural gas reforming or other fossil based H<sub>2</sub> in the refinery). In these cases, we have instead used biogas reforming, and included the biogas consumption in the energy and carbon balances. This means that greenhouse gas performance would be similar for the reference configurations and options that use electrolysis hydrogen from renewable electricity.

The mass and energy balances developed were combined with an assessment regarding which technologies has the most significant production potential in a Nordic context, which is the scope of the project. The result is a list of prioritized technology tracks and a list of electrification options for each of these that were carried further to a more detailed analysis.

Tracks selected for detailed analysis were modelled using tools available and fit for evaluation of a given track. An important pre-requisite in process model development was the possibility for quantitatively assessing the effect of the various relevant electrification options on the mass and energy balances, for example electricity consumption and yields of various products. The tools used were predominantly the flow-sheeting software Unisim Design (Honeywell), Python and Microsoft Excel.

To harmonize the results and allow an overall evaluation, high level mass and energy balances that enable evaluation of common Key Performance Indicators (KPI) were derived based on the models developed for the selected tracks, with and without electrification. Detailed description of modelling strategies and relevant assumptions are presented with the respective track documentation in chapter 6 below. Each technology track has a reference configuration assuming state-of-the-art performance (without indirect electrification) and one or multiple electrified configuration(s) depending on identified electrification solution(s).

## 2.3 EFFICIENCY METRICS

This section concerns mass and energy balances for biofuel production processes. The carbon and energy efficiency metrics used as key performance indicators to summarize these and compare different tracks are shown in Figure 1. There are no standards for process efficiency metrics but these are in agreement with what is generally used. The use of a carbon efficiency metric is much less

common than energy efficiency in this type of study, which reflects the fact that carbon efficiency has not been in the focus of biofuel process development, as noted in the Background section above.

In addition, exergy efficiency is calculated analogously to energy but using energy flows converted to electricity equivalents using the factors 0.40 for solid biomass, 0.55 for biogas and 0.05 for low-grade heat. Note that a net electricity flow is used, i.e. a biofuel production system can only have electricity either in or out, not both.

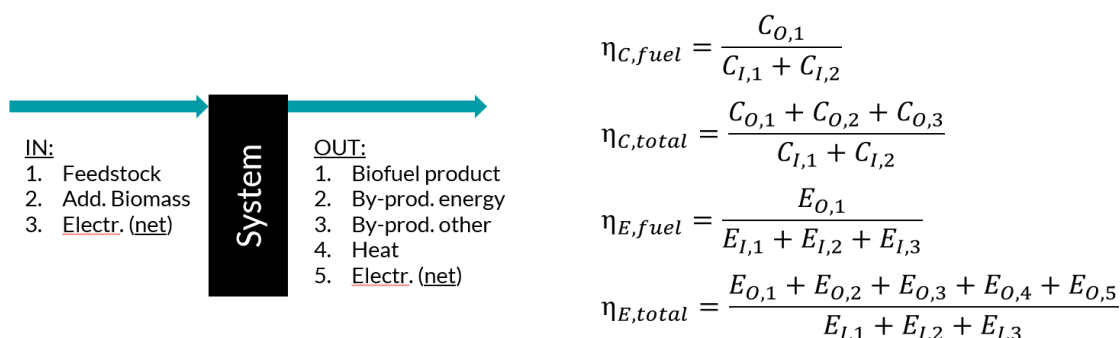


**Figure 1. Definition of carbon and energy efficiency metrics used as key performance indicators in this study.**

When evaluating the energy efficiency, we have used any electricity input as such, without any consideration of losses/efficiency when it was generated. This means that from a resource efficiency perspective, we have assumed a primary energy factor of one (1) for the electricity, which is typically used for solar and wind power.

Another aspect generated is the marginal efficiency of the added electricity in a bio-electrofuels plant. This metric attempts to measure how efficiently added electricity is converted to fuel product on energy basis. It does not include any carbon efficiency aspect. For each electrified configuration (denoted  $x$  in the equation below), the difference in biofuel production and electricity use to the base configuration (i.e. “non-electrified”) is used to calculate the marginal efficiency. It can be noted that all configurations are compared to the base configuration, so for configurations that include several electrification options (for example electrolysis and heating) the metric obtained is for the combination of options.

$$\eta_{el,marginal} = \frac{E_{biofuel,x} - E_{biofuel,base}}{E_{el\ input,x} - E_{el\ input,base}}$$

A separate, specific, efficiency evaluation is made of a case when excess heat from the bio-electrofuel production process replaces biomass-based heat. When this is the case, the avoided use of biomass fuels for heat production can be credited, giving a lower *net* biomass input to the bio-electrofuel production process and – as a consequence – a higher carbon efficiency, see Figure 2. In this calculation, we have simplistically assumed that biomass energy can be converted without significant losses, which is the case in a modern plant with flue gas condensation. Since it is very different if electricity is co-produced or not in a district heating plant, we have not included this aspect,

i.e. we account only for the part of the biomass that is used for heat production in a CHP. These simplifications, which are required, do not make the results less valid on the high level of analysis carried out in this study, rather the opposite since there is no generic bio-CHP plant. A specific analysis needs to be done when looking at implementing bio-electrofuels technology integrated with a specific bio-CHP plant.

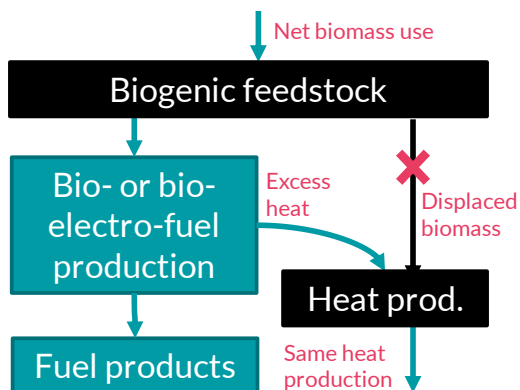


**Figure 2. Principle for evaluation of carbon efficiency when excess heat from the bio-electrofuel production process replaces biomass-based heat production.**

## 2.4 TECHNO-ECONOMIC ANALYSIS

### 2.4.1 Methodology and assumptions for estimating total fixed capital expenditure (CAPEX)

Total equipment procurement cost, EPC, is derived by applying the following procedure, which is typical for this type of study (Smith 2005; Brown 2007):

1. List major process units for each technology track and identify relevant sizing parameter
2. Estimate base cost for the identified major process units, based on published data, inhouse information or by consultation with experts and technology developers. The base cost and reference capacity are documented in appendix 2. Equipment cost for major process units.
3. Adjust costs to Euro value 2020 (annual average) using Chemical Engineering Plant Cost Index (CEPCI). For base cost currencies other than Euro, the cost is converted to Euro equivalent of the reference year using annual average exchange rate of the reference year before applying CEPCI adjustment
4. Adjust equipment costs to correspond sizes evaluated in this work using cost-to-capacity scaling law
5. Apply relevant installation cost factor for base costs that doesn't include installation costs
6. Estimate total EPC using factors to account for balance of plant (BOP). BOP accounts for direct costs (equipment erection, piping, instrumentation & controls, electrical, utilities, offsites, buildings and site prep)

7. Estimate total CAPEX by applying factors to account for other direct costs (civil work, slab and ground prep) and indirect costs (engineering and supervision, construction risk insurance, environmental permitting, recruitment and staff training, contingencies)

The major process units are identified and sized based on the detailed mass and energy balance evaluation carried out in WP2 of the project.

#### 2.4.2 Economic performance indicators

Production cost (PC) is evaluated as the main economic indicator of the reference cases and electrified versions of the technology tracks studied. PC (SEK/MWh or €/MWh) is calculated according to the following expression, see e.g., (Holmgren et al. 2016):

$$PC = \frac{CRF \cdot CAPEX + O\&M + \sum_{i=1}^n Input_i \cdot Cost_i - \sum_{co=1}^m coprod_{co} \cdot Cost_{co}}{\text{Total biofuel products (TBP)}}$$

Where:

- CRF – capital recovery factor (annuity) evaluated assuming 8% interest (i) and 20 years (y) economic lifetime

$$CRF = \frac{(1+i)^y \cdot i}{(1+i)^y - 1}$$

- CAPEX – total fixed investment cost derived according to the process configurations, capacities and system boundaries established in this study
- O&M – annual fixed operating and maintenance cost evaluated as 3% of the CAPEX
- Input and Cost<sub>i</sub> – cost of feedstock, electricity, and other chemicals and utilities with process as listed in Table 1.
- Coprod. and Cost<sub>co</sub> – revenue generated by non-biofuel coproducts, such as solid fuels, lignin, and char with process as listed in Table 1.
- TBP – total biofuel production on energy basis (e.g. MWh/y). For pathways with multiple biofuel outputs, the products are aggregated according to their energy equivalency.

Table 1 presents the cost of parameters used in the economic evaluations. Electricity price is critical to the economic feasibility of the electrified tracks. PC cost is evaluated under electricity prices 30 and 40 €/MWh, representative prices in line with the results of the long-term market analysis carried out by the Swedish electricity grid operators (Svenska Kraftnät 2021) and a high-level analysis of potential for intermittent operation, see chapter 5 for more details.

**Table 1 Cost of parameters.**

Parameter	Unit	Value	Remark and references
Biomass	€/MWh	17.25	Average for woodchips, sawdust, and forest residue (“Wood Fuel and Peat Prices” 2018)
Electricity	€/MWh	30/40	Based on electricity system scenarios from Svenska Kraftnät (Svenska Kraftnät 2021), see further section 5.
Oxygen	€/ton	60	Electrolysis configurations, SOEC or PEM (assumed the same as over-the-fence industrial oxygen price)
Scrubber oil	€/MWh	106	DFB configurations, Rapeseed oil methyl ester (RME) (BioShare)
Biogas	€/MWh	90	HTL, Pyrolysis tracks
Lignin pellets	€/MWh	20	Lignocellulosic ethanol, pellet 12% moisture. Recalculated from (Thunman et al. 2019), i.e., 25 €/MWh for 10% moisture.
Char by-product	€/MWh	20	HTL byproduct, price assumed same as for lignin pellets.

## 2.5 GREENHOUSE GAS FOOTPRINTS

Carbon neutrality is considered of high importance in this study; thus, all base case tracks avoid fossil-based energy sources or utilities. Base case designs that require external heat or hydrogen for upgrading are assumed to use biogas. However, emissions related to biomass supply chain and electricity generation are inevitable. GHG performance of the bio-electrofuel tracks are evaluated using emission factors presented in Table 2, which are very similar to those used in the Renewable Energy Directive.

The emission factor of biomass supply chain is taken from de la Fuente et al., (de la Fuente et al. 2017) for logging residue. The emission factor for logging residue accounts for emissions related to transportation to roadside, loading/unloading machinery, chipping at roadside, transport to terminal including loading/ unloading, and transport to industry (5 km). The factor is an average value for the three geographic locations studied in Northern Sweden (Umeå, Örnsköldsvik and Storuman). Each location considers 120 km radius harvesting area. The obtained GHG footprint is close to published generic values for forestry residues (Gode et al. 2011).

Emissions related to electricity generation are specific for Sweden and refer to the Swedish Energy Agency recommendation for emission factor of the Swedish electricity mix, about 13.1 gCO<sub>2</sub>eq/MJ (Jafri et al. 2020). This figure is believed to be high for the current and future Swedish electricity mix and will likely be halved according to discussions we had with knowledgeable project partners. Therefore, the GHG footprints of all the tracks are evaluated assuming 13.1 and 7 gCO<sub>2</sub>eq/MJ emission factors for electricity. A zero-emission electricity scenario is also evaluated in order visualize the effect it has.

The emission factors of fossil counterparts are taken from Jafri et al., (Jafri et al. 2020). The fossil factors reported in the reference publication are converted to HHV basis to match the units used in this study. Table 2 also indicates which of the fossil fuel products that are the relevant comparison for each bio-electrofuel track. The indicated relationship is used as basis for calculating GHG emissions reduction potential of the bio-electrofuel tracks.

**Table 2 GHG emission factors.**

Parameter	Emissions factor	Unit	Bio-electrofuel tracks compared	References
Biomass	45	kg CO <sub>2</sub> -eq/ODt		(de la Fuente et al. 2017)
Electricity	7–13	kg CO <sub>2</sub> -eq/GJ		(Jafri et al. 2020)
Natural gas	67.0 60.9	kg CO <sub>2</sub> -eq/GJ LHV kg CO <sub>2</sub> -eq/GJ HHV	SNG	(Jafri et al. 2020)
Diesel	95.5 89.4	kg CO <sub>2</sub> -eq/GJ LHV kg CO <sub>2</sub> -eq/GJ HHV	HTL, FP, FT, ATJ	(Jafri et al. 2020)
Petrol	93.5 87.4	kg CO <sub>2</sub> -eq/GJ LHV kg CO <sub>2</sub> -eq/GJ HHV	EtOH, MeOH	(Jafri et al. 2020)

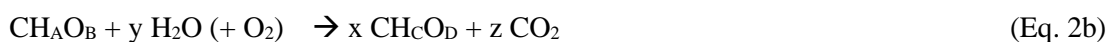
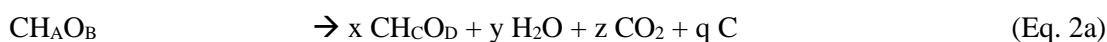
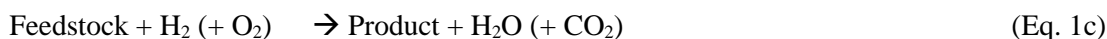
### 3 THEORETICAL EFFICIENCIES OF BIOFUEL PRODUCTION

A major aspect that can explain why carbon efficiencies are often low for biofuel production technologies is that the yield of biofuel production can be limited by stoichiometry, i.e. by the relation of the elemental composition of the feedstock and the product. In order to give a basis of comparison for the carbon and energy efficiencies presented in chapters 4 and 6, this chapter presents theoretical efficiencies for various cases from a stoichiometric point of view. It is very important to note that these do not include any consideration of energy self-sufficiency or side reactions/by-products. This means that to realize the efficiencies presented below it would be necessary to have a “perfect” process without by-products and access to energy input that would be required (which could in practice be by heat and/or electricity).

We define three types of theoretical efficiency using different assumptions:

1. Assuming that the biomass feedstock is the only material input to the process. This implies that the process is a so-called disproportionation, where biomass is decomposed into the biofuel product and, potentially, carbon dioxide, solid carbon, and water (Eq. 1a and 2a).
2. Assuming that water (steam) is used as to convert biomass (somewhere in the process), which is for example the case in gasification-based processes and in tracks including steam reforming and water gas shift (Eq. 1b and 2b)
3. Assuming that elemental hydrogen (for example from water electrolysis) can be added and utilized in the process (Eq. 1c and 2c)

Eq. 1a-1c and 2a-2c show representations of the overall chemical reactions occurring under the three assumptions, with the chemical compositions of the various biomass feedstocks and products being represented by the molecular formulas  $\text{CH}_A\text{O}_B$  and  $\text{CH}_C\text{O}_D$  respectively. The occurrence of elements such as nitrogen and metals (ash) is neglected in these simplified reactions. Addition of oxygen is shown in parenthesis as in practice (for realistic feedstocks and products) it will never improve the theoretical efficiency, i.e. should not be used in this theoretical perspective.



The theoretical carbon and energy efficiency will be dependent on the elemental composition of the feedstock and desired product. Expressions for this were derived based on Eq. 2a-2c. Typical elemental compositions for some feedstocks and products that are relevant are shown in Table 3 and Table 4. The different elemental compositions are visualized in Figure 3.

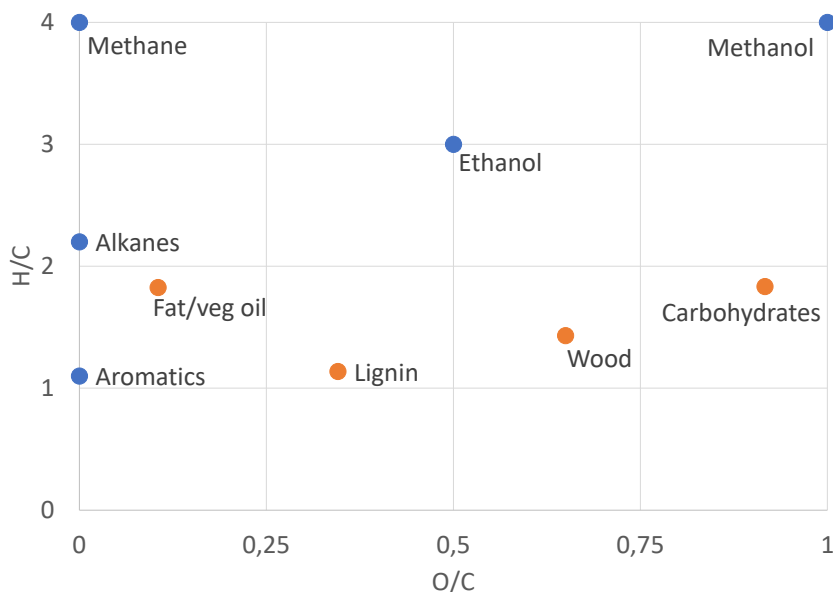


**Figure 3. Van Krevelen diagram of products (blue) and feedstocks (orange), visualizing the differences in elemental composition.**

Carbon efficiencies were also converted to energy efficiencies using the carbon-basis heating values listed in the tables. This means that theoretical energy efficiency as derived in this chapter is not an overall energy efficiency of the process but just the energy in the product compared to the energy in the feedstock, irrespective of other inputs that may be needed. Hence:

- Carbon efficiency is a measure of how efficiently carbon in the feedstock is utilized by conversion into the product (in the range 0-100%)
- Energy efficiency is a measure of how much energy in a (fuel) product that can be produced from a unit energy of feedstock without considering energy self-sufficiency (can be >100% for high carbon efficiency, since the overall energy balance is not considered).

**Table 3. Typical elemental composition and higher heating value (HHV) for relevant feedstocks.**

	C	H	O	HHV [MJ/kg]	HHV/C [MJ/kg C]
Wood	1	1.43	0.65	20.4	40.5
Carbohydrates	1	1.83	0.92	17.4	41.3
Lignin	1	1.14	0.35	27	42.0
Fat/veg oil	1	1.82	0.11	40	51.7

**Table 4. Typical elemental composition and higher heating value (HHV) for relevant products**

Products	C	H	O	HHV [MJ/kg]	HHV/C [MJ/kg C]
Methane	1	4	0	55.5	74
Alkanes*	1	2.2	0	46	54.4
Aromatics*	1	1.1	0	42	45.8
Methanol	1	4	1	22.7	60.5
Ethanol	1	3	0.5	29.7	56.9

\* Alkanes assumed as  $\text{CH}_{2.2}$  (corresponding to for example decane) and aromatics as  $\text{CH}_{1.1}$  (corresponding to for example a benzene/toluene mix).

Results for wood feedstock are shown in Figure 4 (as stacked bars, since the theoretical efficiency increases stepwise for assumptions 1-3 above). When hydrogen is added (Eq. 1c och 2c), theoretical carbon efficiency is always 100%, since all oxygen can be removed as water and any missing H/C ratio can be compensated. For the cases without hydrogen addition (Eq. 1a-b, 2a-b) the efficiency is higher for products with lower H/C ratio, since the yield is limited by hydrogen deficiency.

Typical theoretical carbon efficiencies without hydrogen addition, i.e. without electrification for most tracks, is just above 50% for methane and 65-70% for the other products (excluding aromatics at 80%). Methane has the highest product H/C ratio and thus the lowest theoretical carbon yield. Hydrogen addition can theoretically improve carbon efficiency by 50-100% relative compared to cases using only water/steam. This indicates a good potential for electrification to improve carbon efficiency.

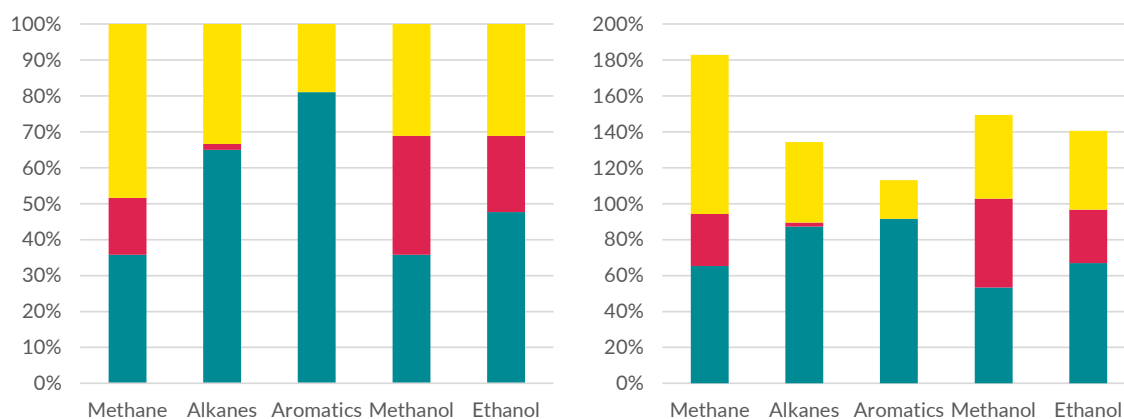


**Figure 4. Theoretical carbon (left) and energy (right) efficiency for “typical” wood feedstock to different products for disproportionation (blue, eq. 1a and 2a), with addition of water (red, eq. 1b and 2b), and with addition of hydrogen (yellow, eq. 1c and 2c).**

The theoretical energy efficiency, displayed for wood feedstock in Figure 4 (right), is markedly different from the carbon efficiency due to the different energy content per carbon for the products, see Table 4. Without hydrogen addition (Figure 4 right, blue and red bars), theoretical energy yield is typically 90-100% (but note the somewhat uncommon definition of theoretical energy efficiency used here, see above). With hydrogen addition, it is possible to get more energy in the product than

in the feedstock for all cases. Methane has the highest value with 180% theoretical energy efficiency, which of course means that a lot of hydrogen needs to be added to this type of process and that the hydrogen energy can be captured in the methane product.

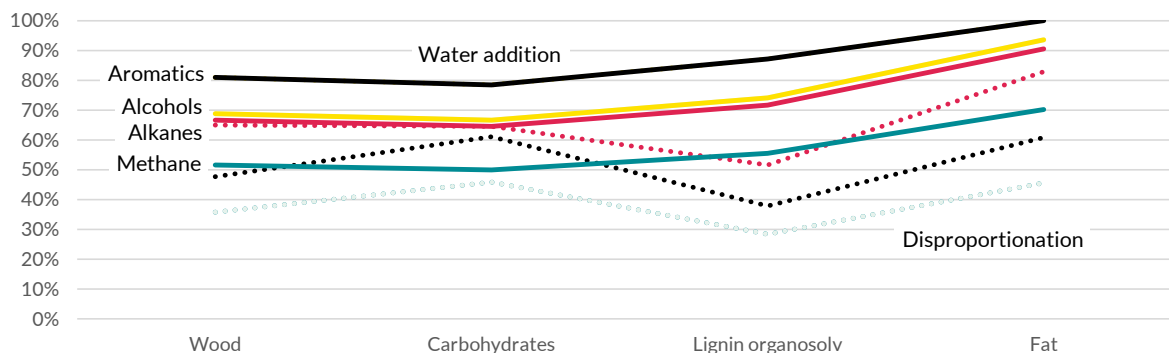


**Figure 5.** Theoretical carbon efficiency with water addition (solid lines) and for disproportionation (dotted lines, same coloring, methane and methanol lines coincide) for different feedstocks. Theoretical carbon efficiency for hydrogen addition is always 100% (not shown).

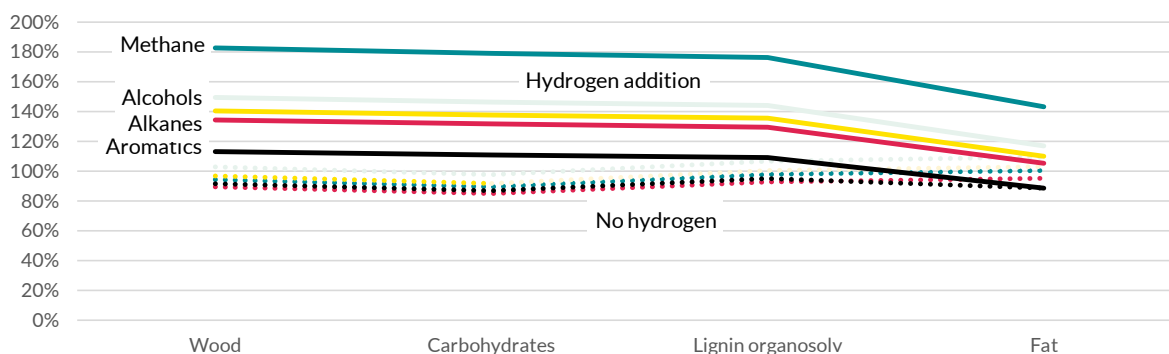


**Figure 6.** Theoretical energy efficiency for hydrogen addition (solid lines) and water addition (dotted lines, same coloring) for different feedstocks. Theoretical carbon efficiency for disproportionation is not shown.

Figure 5 shows the influence of using different feedstocks on theoretical carbon efficiency (excluding hydrogen addition). As expected, theoretical yields are higher for feedstock with higher H/C ratios and lower feedstock oxygen content. This is simply explained by the fact that the theoretical yield is higher the more similar the feedstock is to the desired product. Typically, the theoretical carbon yield increases by 20 percentage points for fat/oil compared to wood (lignocellulose) or cellulose.

Figure 6 shows that the theoretical energy efficiency is rather constant for a given product, for all lignocellulosic components (cellulose, lignin or the combination wood) as feedstock. Without hydrogen addition, fat/oil also has a similar theoretical energy efficiency but the benefit of adding hydrogen is much less than for the other feedstocks, which is of course due to the high hydrogen content of this feedstock to start with.

The results of this analysis of theoretical efficiencies can be summarized in a few points:

- Theoretical carbon efficiency without hydrogen addition is 50-80% for lignocellulosic feedstock and highly dependent on the desired product molecule, especially its elemental composition. Carbon efficiency is in general lower for products that have high H/C ratio, with methane being the extreme.
- This 50-80% carbon efficiency translates to 90-100% theoretical energy efficiency, when only limited by stoichiometry (i.e. looking at energy in product compared to energy in feedstock, without requiring energy self-sufficiency of the conversion process).
- Hydrogen addition can dramatically change the picture and always gives 100% theoretical carbon efficiency.
- Energy yields with hydrogen addition (on biomass feedstock basis) is >100% and as high as 180% for methane from lignocellulose. This means that a large amount of hydrogen needs to be added and that this energy can be stored on the methane product.
- For fat/oil feedstock, theoretical carbon efficiency is higher, due to the greater similarity between the feedstock and the product. But this also means that the benefits that can be achieved from hydrogen addition is smaller.

## 4 STUDIED BIOFUEL PRODUCTION TECHNOLOGIES

This chapter describes the results from the initial screening of biofuel production technologies and electrification options that was used to prioritize technologies for a more detailed study of the effect of integrated electrification, described in the next chapter.

The biofuels production pathways to be included in the screening were determined based on relevance for the Nordic region, presently and future. This resulted in inclusion of the biofuel production pathways listed Table 5.

**Table 5. Biofuel production pathways included in the screening stage of the project.**

Category	Technology	Product	Feedstock
<b>Anaerobic digestion</b>	Anaerobic digestion	Biogas	Sludge
	Anaerobic digestion	Biogas	Manure + food waste
<b>Gasification</b>	EFG	FT crude*	Black liquor
	EFG	MeOH	Black liquor
	DFBG	SNG	Forest residues, bark
	DFBG	FT crude*	Forest residues, bark
	DFBG	MeOH	Forest residues, bark
	O2-FBG	SNG	Forest residues, bark
	O2-FBG	FT crude*	Forest residues, bark
	O2-FBG	MeOH	Forest residues, bark
<b>Biodiesel and HVO</b>	HVO	HVO	Tall oil
	HVO	HVO	Slaughterhouse waste
	HEFA	HEFA	Tall oil
	HEFA	HEFA	Slaughterhouse waste
	RME	RME	Rapeseed oil
<b>Lignin sep.+upgrad.</b>	HDO	Diesel + gasoline	Kraft lignin
<b>Liquefaction + upgrad.</b>	FP + HDO	Diesel + gasoline	Forest residues
	IH2	Diesel + gasoline	Forest residues
	HTL + HDO	Diesel + gasoline	Forest residues
<b>Fermentation</b>	LC ethanol	Ethanol	Saw dust
	starch ethanol	Ethanol	Wheat
	Ethanol-to-jet	Biojet	Ethanol

\* Gasification and FT-based pathways are analyzed up to the production of FT crude without inclusion of an upgrading step from FT crude to fuel products at this screening stage.

### 4.1 CARBON AND ENERGY EFFICIENCY OF BIOFUEL PRODUCTION

The individual production track mass and energy balances that were developed in the screening stage (as described in 2.2) is not shown, since more detailed and accurate balances were developed for the prioritized tracks and are shown below (chapter 6). Instead, an overview of the screening

results with conclusion are presented. Figure 7 gives a summary of the carbon yields of the different processes that have been assessed, grouped per conversion technology. Figure 8 shows the same data but grouped according to product type.

Anaerobic digestion (AD), starch ethanol and HVO/HEFE/FAME technology tracks do not use lignocellulosic biomass as feedstock. The AD tracks studied here gives a rather low carbon efficiency to biogas and a large digestate stream (denoted solid residue in the figures). Some concentrated CO<sub>2</sub> comes from the biogas upgrading process. Starch ethanol has a 40+% efficiency, counting from grain (but excluding the straw, which is not included in the feedstock definition used here, somewhat arbitrarily).

RME production has high carbon efficiency, which is explained by the relative similarity of the feedstock (fat/oil) to the product (fatty acid ester) as discussed in chapter 3. HVO and HEFA tracks have high carbon efficiency from fat/oil to hydrocarbon for the same reason, but the efficiencies calculated in this report are based on the full original feedstocks crude tall oil and slaughterhouse residues, which contain a substantial fraction of non-fat components that are transformed into what is here defined as residues, since they are not transport fuel products (tall oil pitch and meat and bone meal, respectively). This calculation approach gives around 50-55% carbon efficiency for the HVO tracks.

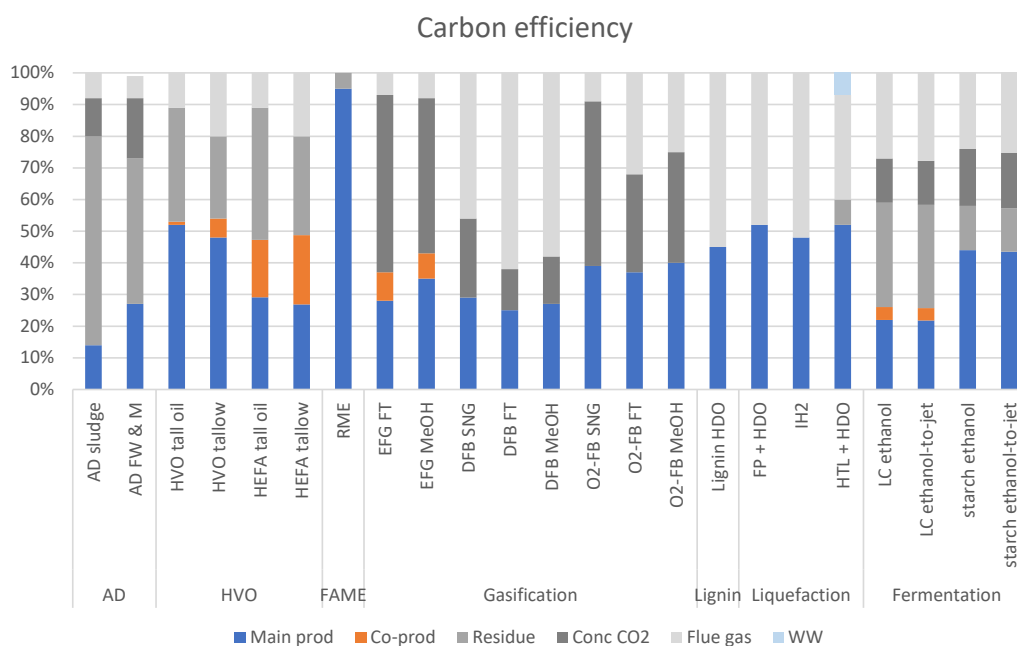


**Figure 7. Carbon yields of the different processes that have been mapped in this report, grouped per conversion technology (WW is waste water).**

The reminder of the discussion here is related to the tracks that use lignocellulosic feedstocks. Based on Figure 7, gasification technologies seem to give a little bit lower carbon efficiency than the hydrotreatment-based tracks (“lignin” and “liquefaction”). For the two direct gasification technologies, EFG and O2-FB, most of the carbon that does not end up in the product ends up in a concentrated CO<sub>2</sub> stream that can be captured or, better, utilized without separation. This gives a main

electrification opportunity, since using hydrogen addition to the syngas this enables converting also this carbon to biofuel product. Electrolysis can also give a synergy by using oxygen from the electrolyzer in the gasification process.

Another opportunity for gasification-based technologies is to use an electrically heated reformer, which is especially relevant for DFB and O<sub>2</sub>-FB-based production of methanol and FT products, since the syngas from these gasification technologies contain a fairly large fraction of methane that needs to be converted to hydrogen and carbon monoxide using a reformer. This reformer, in the base case, uses partial combustion of the gas for heat supply, leading to losses that can be removed by electric heating.

The indirect gasification technology, DFB, as implemented here, is not optimized for fuel product yield. The DFB process is tightly integrated with a CHP plant and optimized for total yield of electricity, heat and fuel product. This integration is also the reason for the relatively large amount of carbon that ends up as flue gas CO<sub>2</sub> using this technology<sup>1</sup>.

Carbon efficiency is generally around 50% for the refinery-integrated technologies (“lignin”, “liquefaction”). In these cases, by-products are combusted or reformed making the rest of the carbon end up in a flue gas stream. Electrically heated reforming is an option to increase carbon efficiency, but the potential impact is smaller than for gasification.

Lignocellulosic ethanol has the lowest carbon efficiency, mainly because lignin is not converted to a primary product but instead produces a solid by-product, lignin fuel pellets, which is used for internal heat demands. Replacing this use with electric heating could potentially free more lignin for export but technical development is currently needed in order to be able to convert this stream to biofuels. i.e. what is considered a primary product in this study. Another interesting option for this track is conversion of the CO<sub>2</sub> streams from fermentation and biogas upgrading, using electrolytic hydrogen and catalytic synthesis, for example CO<sub>2</sub> methanation.

Looking at carbon and energy efficiencies grouped by product, Figure 8 and Figure 9, there is no clear trend. The discussion about the different theoretical efficiencies in chapter 3 concluded that methane had lower theoretical efficiency but it seems that other factors than the feedstock-product stoichiometry limit carbon efficiency. The tracks that come closest to the theoretical efficiency are

- Methane (SNG) from oxygen-blown fluidized bed gasification (O<sub>2</sub>-FB) with 39% carbon efficiency compared to the theoretical 52% (without hydrogen addition).
- Liquefaction and hydrotreatment-based tracks (FP + HDO, HTL + HDO, IH<sub>2</sub>) with 45-52% carbon efficiency. This can be compared to the theoretical 67% (without external hydrogen addition) from lignocellulose feedstock. The fast pyrolysis track (FP+HDO) as

---

<sup>1</sup> An alternative approach for the calculation of balances and yields is used in the detailed analysis of selected tracks below, to include this aspect. For biofuel production plants that are tightly integrated with an existing plant, which is the case for CHP integrated DFB gasification and pulp mill integrated EFG of black liquor, an alternative approach using system boundaries that surrounds both plants can be used. This approach includes a differential analysis looking at total biomass supply to the CHP/pulp mill, at constant heat/pulp production, with and without biofuel plant integration.

modelled here also use some biogas for hydrogen generation, so the theoretical 67% is not completely relevant.

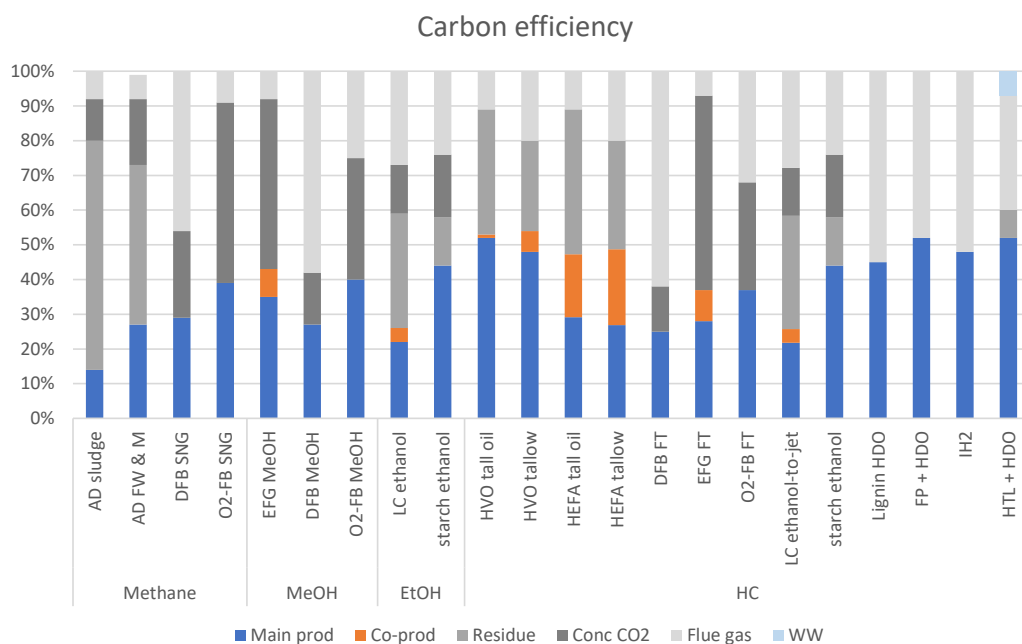


**Figure 8. Carbon yields of the different processes that have been mapped in this report, grouped per product type**

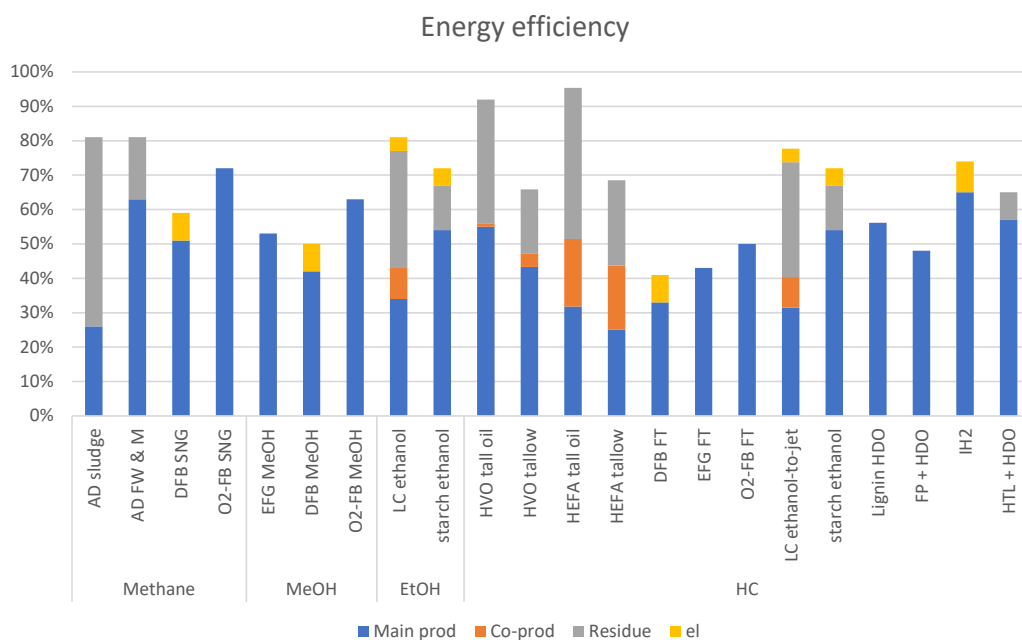


**Figure 9. Energy yields of the different processes that have been mapped in this report, grouped per product type**

## 4.2 PRIORITIZED TRACKS AND ELECTRIFICATION OPTIONS

Based on the work described above, the most promising production technologies and electrification options were identified according to the list below. These options formed the basis for the more detailed work with process design and modelling described further below.

- Lignocellulosic ethanol (EtOH)
  - Electrolysis hydrogen for fermentation CO<sub>2</sub> upgrading to methane
  - Electrolysis hydrogen for biogas CO<sub>2</sub> upgrading to methane
  - (Electric heating, low temperature, to increase lignin export)
- Lignocellulosic ethanol combined with ethanol to jet (ATJ)
  - Electrolysis hydrogen for fermentation CO<sub>2</sub> upgrading to methane or methanol
  - Electrolysis hydrogen for biogas CO<sub>2</sub> upgrading to methane
  - Electrolysis hydrogen for ethanol to jet
- Hydrothermal liquefaction and upgrading (HTL)
  - Electric heating of HTL reactor, high temperature, to increase biogas production
  - Electrolysis hydrogen for hydrotreatment, enabling biogas production from process off gases (HTL and HDT)
- Fast pyrolysis and upgrading (Pyro)
  - Electrolysis hydrogen for hydrotreatment, eliminating biogas use
  - Electrolysis hydrogen for NCG upgrading, for example through biological methanization
- Black liquor gasification-based methanol production (BLG-MeOH)
  - Electrolysis hydrogen for elimination of water gas shift
  - Electrolysis hydrogen for full utilization of syngas CO<sub>2</sub> (requires reverse shift reactor or modification of methanol reactor design)
- Black liquor gasification-based Ft liquids production (BLG-FT)
  - Electrolysis hydrogen for elimination of water gas shift
  - Electrolysis hydrogen for full utilization of syngas CO<sub>2</sub> (requires reverse shift)
  - Electric heating of the SMR reactor, high temperature, to increase FT production
- Dual fluidized bed gasification-based methane production (DFB-SNG)
  - Electrolysis hydrogen for full utilization of syngas CO<sub>2</sub>
  - Electric pre-heating of gasification steam
- Dual fluidized bed gasification-based FT liquids production (DFB-FT)
  - Electrolysis hydrogen for full utilization of syngas CO<sub>2</sub> (requires reverse shift)
  - Electric heating of the SMR reactor, high temperature, to increase FT production
  - Electric pre-heating of gasification steam
- Direct fluidized bed gasification-based methane production (O2FB-SNG)
  - Electrolysis hydrogen for full utilization of syngas CO<sub>2</sub>
  - Electric pre-heating of gasification steam
- Direct fluidized bed gasification-based FT liquids production (O2FB-FT)
  - Electrolysis hydrogen for full utilization of syngas CO<sub>2</sub> (requires reverse shift)
  - Electric heating of the SMR reactor, high temperature, to increase FT production
  - Electric pre-heating of gasification steam

## 5 INTERMITTENT ELECTRIFICATION AND HYDROGEN STORAGE

The role of renewable hydrogen production with hydrogen storage is often highlighted as a link between intermittent electricity production and decarbonization of continuous industrial processes. A future electricity system based on a large fraction of wind and solar power will have highly fluctuating electricity prices and likely a demand for electricity user flexibility.

Electricity demand flexibility in connection with water electrolysis can take different forms depending on the time scale looked at.

- Intermittent on/off type operation of the electrolyzer on a time scale of hours-days, in order to avoid peak electricity prices
- Electricity system frequency control by allowing automatic used power alterations and selling services to the grid operator Svenska Kraftnät on a second-minute time scale

These two are discussed separately below. It is important to note that some of the biorefinery processes in which hydrogen from electrolyzers are used, are typically difficult to make flexible in terms of load/production. In addition, full load operation is typically desired in order to make full use of the equipment investments. Hence, in this project it has been assumed that in order to operate an electrolyzer flexibly, there has to exist a buffer, in form of a hydrogen storage, in order to “absorb” the varying hydrogen production. There could be potential to develop the flexibility of the fuel production processes, but that is not something that has been considered in this project.

### 5.1 INTERMITTENT ON/OFF ELECTROLYZER OPERATION

A water electrolyzer can be operated intermittently with a hydrogen storage as a buffer towards continuous use in for example electrified biofuels production. The lower average electricity price obtained by avoiding electrolyzer operation in high-cost periods could then compensate for hydrogen storage costs if these are not too high. The purpose of the work described in this section was to make a high-level analysis of the potential profitability of hydrogen storage in connection with a bio-electrofuels production process.

#### 5.1.1 Methodology and electricity system scenarios

Electricity system scenarios from Svenska Kraftnät (Svenska Kraftnät 2021) was used as the basis for the electricity price levels and variability. Of the four scenarios available, only the two scenarios with high future electricity demand were used, since these were considered more relevant and more in line with other scenarios for electricity demand (Svenskt Näringsliv 2019). These scenarios are (see (Svenska Kraftnät 2021) and Appendix A for more details):

- EP (“elektrifiering planerbar”) – this scenario has an electricity production of 181 TWh 2030 and 260 TWh 2045 of which 64 TWh is used for hydrogen production.

In this scenario electricity will become the primary energy carrier in Sweden and will be used within the chemistry, steel and cement industry in order to export emission-free prod-

ucts and fuels. This will lead to a great increase in electricity demand, which will be provided by intermittent renewables along with already existing and new nuclear power and CHP.

- EF (“elektrifiering förnybart”) – this scenario has an electricity production of 187 TWh 2030 and 285 TWh 2045 of which 84 TWh is used for hydrogen production.

Even greater increase in electricity demand is anticipated in this scenario as sector coupling, the hydrogen economy, export of emission-free products and fossil-free fuels becomes more significant. Off-shore wind power will constitute the main part of the increased capacity together with solar power and on-shore wind, whereas nuclear power will be fully decommissioned by 2045

Average electricity prices for the scenarios for SE1 (north Sweden) and SE3 (mid-south Sweden) are shown in Figure 10. It can be noted that these are not dramatically different between the scenarios or between 2035 and 2045. The price variability is larger for EF than EP in 2045, both on a short and long time scale, but there is no significant difference between scenarios in 2035<sup>2</sup>.

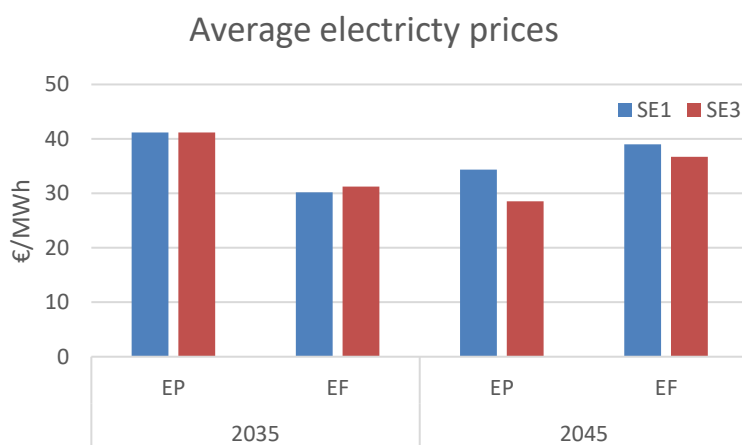


**Figure 10.** Average electricity prices for SE1 and SE3 in the studied scenarios.

The methodology used to study the potential benefits of hydrogen storage consisted of two steps

1. Investigate the potential for a decreased average electricity purchase price depending on hydrogen storage volume (controls maximum time without electrolyzer running) and electrolyzer over-capacity (controls time required for re-filling storage after use).
2. Investigate the cost for investment in the hydrogen storage and electrolyzer over-capacity and adding this to the decreased electricity purchase price to see if there is a net economic benefit.

The methodology for step 1 involves setting up a series of optimization problems, where the aim was to minimize the total cost of electricity purchase for each scenario, storage size and trading

<sup>2</sup> See figures 17-19 of the Svenska Kraftnät report for more information on price variability.

zone. When the optimization was successful the values were saved and the iteration process continued for another storage size, over capacity or weather year. This was repeated for the selected trading zones (SE1 and SE3), scenarios (EF and EP) and years (2035 and 2045).

This optimization was performed with a one-year foresight horizon over 35 weather years for the scenarios EP and EF at years 2035 and 2045 for trading zones SE1 and SE3 with a storage size of 2 and 5 days respectively resulting in a total of 560 successful optimizations. The main result achieved for each optimization was the total electricity cost for operating the electrolyzer. The results were averaged over the 35 weather years for each scenario, trading zone and storage size.

The methodology for step 2 involves using the following assumptions for investment costs:

- Hydrogen storage options: high-pressure tanks or rock caverns
  - High-pressure tank investment 500 €/kg H<sub>2</sub> with no economies of scale (Reuß et al. 2017)
  - Rock cavern investment is 23 €/kg H<sub>2</sub> @100 GWh<sup>3</sup> storage but with significant economies of scale (scaling exponent 0.28) (Reuß et al. 2017)
- PEM electrolyzer over-capacity with installed system cost of 800 €/kW<sub>el</sub> (corresponding to 2030 scenario in (Schmidt et al. 2017) with no economies of scale)
- Yearly capital cost is estimated by an annuity of 10% (corresponding to 8% interest and 20 years economic lifetime)
- Operation O&M is estimated as 3% of investment per year

The investment costs were annualized and divided by the total amount of electricity purchased, so that a “storage cost” per MWh of electricity was arrived at, which could then be added to the average electricity price.

This two-step procedure then gives an indication of whether the construction of hydrogen storage is profitable for the range of parameters studied, i.e., 2- or 5-days hydrogen storage and 10-100% electrolyzer over-capacity.

### 5.1.2 Results

We chose two scales of hydrogen storage, leading to two different investment cost scenarios for hydrogen storage. In the small scale we assume pressurized hydrogen tanks which are estimated at 500€/kg H<sub>2</sub> as specified above. For the large scale, rock caverns storing 1 Mton (35 GWh) of hydrogen were assumed, which corresponds to 5 days storage for 300 MW hydrogen (roughly 500 MW electricity) which is approximately the largest case in this study (most electrified O2FB and BLG cases, see chapter 6).

Figure 11 and Figure 12 show average electricity purchase costs, both *uncorrected*, i.e., only accounting for the potential decrease in electricity purchase price if hydrogen storage can help avoid-ing purchase during high process periods, and *corrected*, i.e., including the costs associated with

---

<sup>3</sup> 100 GWh corresponds roughly to 1 GW for 4 days, 1 GWh is roughly 10 MW for 4 days

construction and operation of the storage and electrolyzer over-capacity. We have chosen to show data for scenario EF 2035, which has the lowest price variability, and EF 2045, which has the highest price variability. The scenarios EP 2035 and 2045 would be somewhere in between these.

It is clear from both figures that there is a clear potential to decrease the electricity purchase costs (dashed lines). For the high price variability scenario EF 2045 and 5 day storage and 100% electrolyzer, the potential is almost 50% average price decrease from ~40 €/MWh to ~20 €/MWh. For 2035 EF the potential is up to 30%. However, from Figure 11 (solid lines) it is clear that when accounting for the high storage investment cost scenario (500 €/kg H<sub>2</sub>, tanks or small caverns), the corrected cost is increased as soon as hydrogen storage is implemented, and that the situation becomes worse with larger storage (5 days).

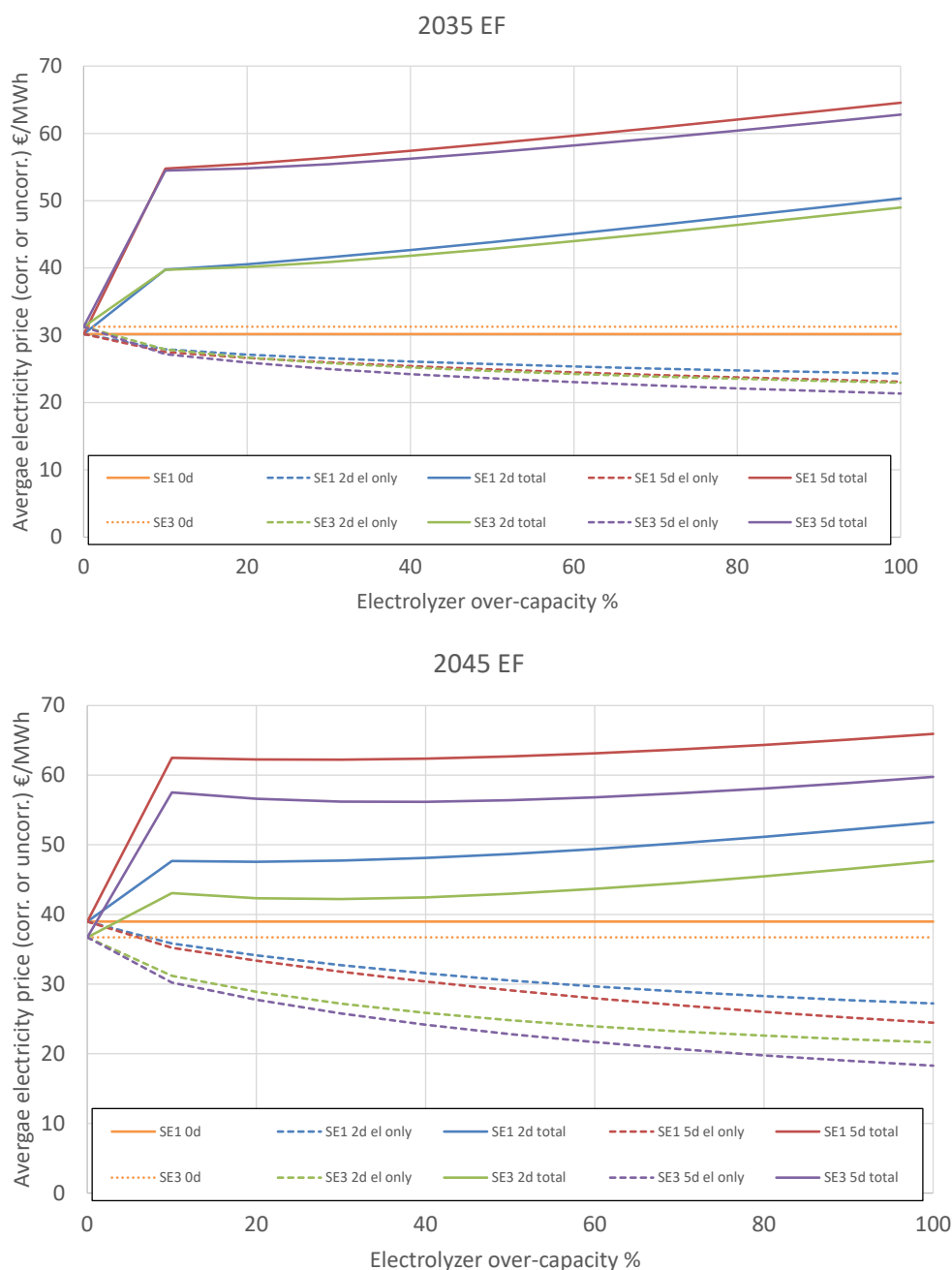


**Figure 11. Average electricity prices for scenarios EF 2035 (top) and 2045 (bottom) for case hydrogen tank storage (500 €/kg H<sub>2</sub>) investment. Average prices without hydrogen storage (orange). Dashed lines show (red, purple, blue, green) decreases in electricity purchase costs with increasing storage and electrolyzer capacity. Solid lines show corrected electricity prices incl. additional investments.**

Figure 12 instead shows results from a scenario where hydrogen storage can be built for the 55 €/kg H<sub>2</sub>, i.e. 35 GWh hydrogen rock caverns. In that optimistic case, there is potential for hydrogen storage implementation to be profitable in SE3 for the high price variability scenario 2045 EF. The electricity cost can be reduced by up to 3 €/MWh (approx.. 10%) for 20-40% electrolyzer over-capacity. However, for SE1 in the 2045 EF and for both SE1 and SE3 in the lower price variability scenario 2035 EF, the analysis does not show any potential benefits.

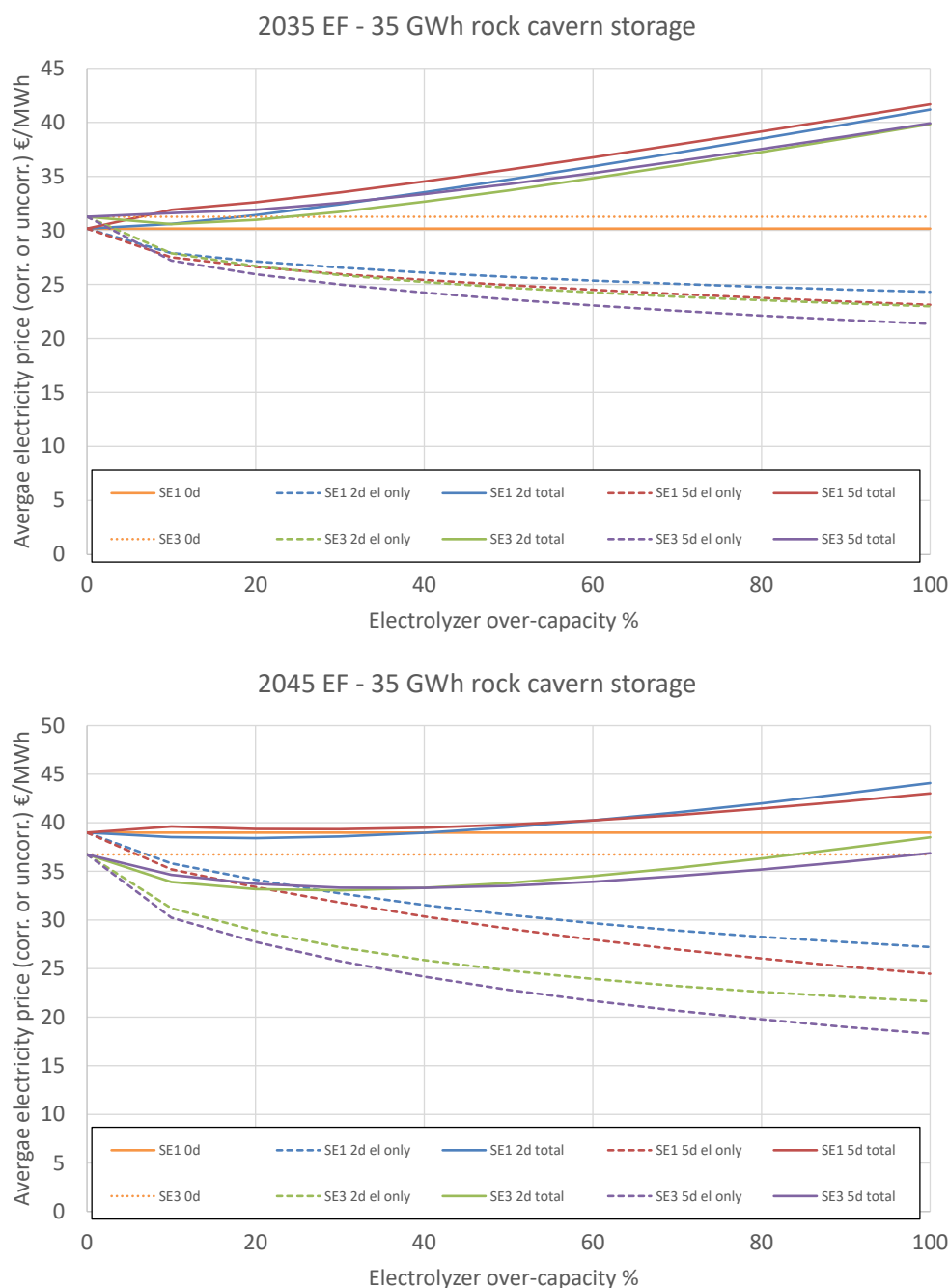


**Figure 12. Average electricity prices for scenarios EF 2035 (top) and 2045 (bottom) for rock cavern storage (55 €/kg) investment. Average prices without hydrogen storage (orange). Dashed lines show (red, purple, blue, green) decreases in electricity purchase costs with increasing storage and electrolyzer capacity. Solid lines show corrected electricity prices incl. additional investments.**

## 5.2 ELECTROLYZER OPERATION WITH FLEXIBILITY SERVICES

In addition to the on/off type of response to electricity market prices discussed above, it is often proposed that electrolyzers can offer grid balancing services, which would generate a revenue

stream that can decrease overall hydrogen production cost. It has been shown that PEM electrolyzers can be controlled with a response time short enough to be useful for grid frequency control (Hovsapian 2017; Eichman et al. 2014).

### 5.2.1 Methodology

The electricity market scenarios used in the previous section do not contain any future estimates of prices for grid services. It has shown very difficult to predict historical market prices for grid services based on empirical grid data and it is considered even more difficult to make any predictions of future prices. In this section, we still try to make a rough scenario of a potential revenue stream from grid services, based on historical price data. We use the frequency control service FCR-N as an example since the time scale of this service (seconds-minutes) is markedly different from the price-controlled operation discussed above (hours-days) and because it has been discussed as promising for hydrogen production.

FCR-N is a service where a local controller is installed at an electricity consumer, which can then be used to regulate the power used, up or down in order to improve the grid frequency stability. Svenska Kraftnät continuously purchases FCR-N service so that 230 MW is available in Sweden. Power consumers that are approved and have installed controllers are allowed to make bids. The average prices for FCR-N have been varying according to Table 6. As noted above, the future development of these is difficult to predict.

**Table 6. Average FCR-N market prices 2017-2020 (SvenskKraftnät 2022)**

	FCR-N average market price
2017	23,5 €/MW/h
2018	38,5 €/MW/h
2019	30,9 €/MW/h
2020	15, 7 €/MW/h
Average 2017-2020	27 €/MW/h

In order to be able to offer FCR-N services continuously, it is required to have

1. Electrolyzer over-capacity corresponding to the amount of services needed.
2. Hydrogen storage capacity according to the hydrogen production over-capacity and the time frame in which up- and down-regulation can be expected to cancel out.

For item 1, we use the same assumption as in the previous section, i.e. that electrolyzer over-capacity is associated with an investment of 800 €/kW<sub>el</sub> (see 5.1).

For item 2, to understand the maximum storage capacity needed, we looked at historical data from April 2020. Those data indicates that the accumulated net deviation from the nominal power consumption is within ±2MWh per MW of flexibility offered for FCR-N and hence that you would need approximately a 2 h storage capacity. To have margin, we have used a 5 h storage capacity, corresponding to 3 MWh of hydrogen storage (approximately 60% el-to-hydrogen efficiency) per MW FCR-N offered. Compared to the on/off operation (see 5.1), the storage capacity required for FCR-N flexibility services is small (4 h compared to 2-5 days). Hence, only the high-pressure tank

option with an investment of 500 €/kg H<sub>2</sub> (Reuß et al. 2017), corresponding to 15000 €/MWh H<sub>2</sub> is used.

### 5.2.2 Results

With the assumptions from the previous section, the investment required for offering 1 MW of FCR-N is 800 k€ for electrolyzer and 45 k€ for storage tanks. Using an annuity of 10% to calculate capital cost (corresponding to 10 years straight pay-back or 8% interest over 20 years) and 2% O&M per year, the cost of the equipment required for the FCR-N services is 101 k€/MW/y or 12 €/MW/h (assuming 8500 h/y operation).

This tentative cost of 12 €/MW/h can be compared to the 2017-2020 average for FCR-N services, which is 27 €/MW/h. It is clear that if you manage to get the average price for a full year of FCR-N services, you can make a profit of 15 €/MW/h, with MW corresponding to the amount of electrolyzer overcapacity. This means that if a bio-electrofuels plant, as a reasonable example, installs 50% electrolyzer over-capacity (i.e. 0.5 MW of FCR-N is offered per MW of average electrolyzer power consumption), there is a potential to save 7.5 €/MWh of electricity purchased. If you assume that you can get the average price of 27 €/MW/h 50% of the time, or equivalently that you can get 50% of the average price 100% of the time, there is a potential to save 3,75 €/MWh of electricity purchased.

In summary, based on historical prices of FCR-N services and 50% installed electrolyzer over-capacity, the potential net revenue from selling FCR-N services can be 4-7 €/MWh of electricity consumption. This is significantly better than the cost savings discussed above but the future potential revenue for flexibility services, such as FCR-N, is highly uncertain.

## 5.3 CONCLUSION

A conclusion from these results is that intermittent on/off operation and hydrogen storage to decrease average electricity purchase price does not seem to show a significant potential to decrease production costs for bio-electrofuels production. Only one of the studied cases showed potential for corrected electricity cost decrease and in that case less than 10%. Of course, scenarios with higher electricity price variability may change that conclusion.

The potential to offer flexibility services to the grid operator was studied using the FCR-N instrument as example. Historical prices indicate that it can be possible to decrease the net electricity cost by 4-7 €/MWh, i.e. 10-20% of the average electricity price in the electricity system scenarios used. But these results are very uncertain due to the uncertainty of future revenues from flexibility services. Ant the 10-20% potential cost decrease is much smaller than the uncertainty in the electricity prices in the scenarios used.

We have therefore chosen not to explicitly include intermittent operation, hydrogen storage and flexibility services in the techno-economic calculations. However, by using different average electricity prices, hydrogen storage can be said to be implicitly included. Based on the results of this section, we have used 30 €/MWh and 40 €/MWh as electricity prices in the techno-economic analysis, see 2.4 and chapter 7. In the techno-economic analysis, we have note differentiated electricity use for hydrogen production and other purposes (such as compression, heating).

## 6 CARBON AND ENERGY EFFICIENCY OF BIO-ELECTRO FUELS PRODUCTION

In this chapter, the results of the modelling of the selected tracks (see 4.2) are presented in separate sub-chapters. The results are presented with the scale/production capacity considered realistic for a commercial implementation of the technology, but efficiencies are in most cases largely scale independent. The results are summarized at the end of the chapter, using the efficiency metrics described in 2.3.

### 6.1 ELECTROLYSIS

Electrolysis is not a separate production track, but is described here in a separate sub-chapter, since it is a technology used as an electrification option in many of the production tracks. Two different electrolysis technology, proton exchange membrane (PEMEC) and high-temperature solid oxide (SOEC) are considered for integration to the production process.

Figure 13 illustrates the simplified system schematic of both electrolyzer systems. All systems presented in this report use the same system configuration, while the size of the electrolysis is set to match the given hydrogen requirement. The required heat for increasing the water feed temperature to operating temperature is provided firstly from internal heat integration in the electrolysis system, or with the biofuel production plant where possible. Electricity is used for the final high-temperature heating for SOEC. Internal heat integration is indeed more vital for SOEC as this system operates at higher temperatures.

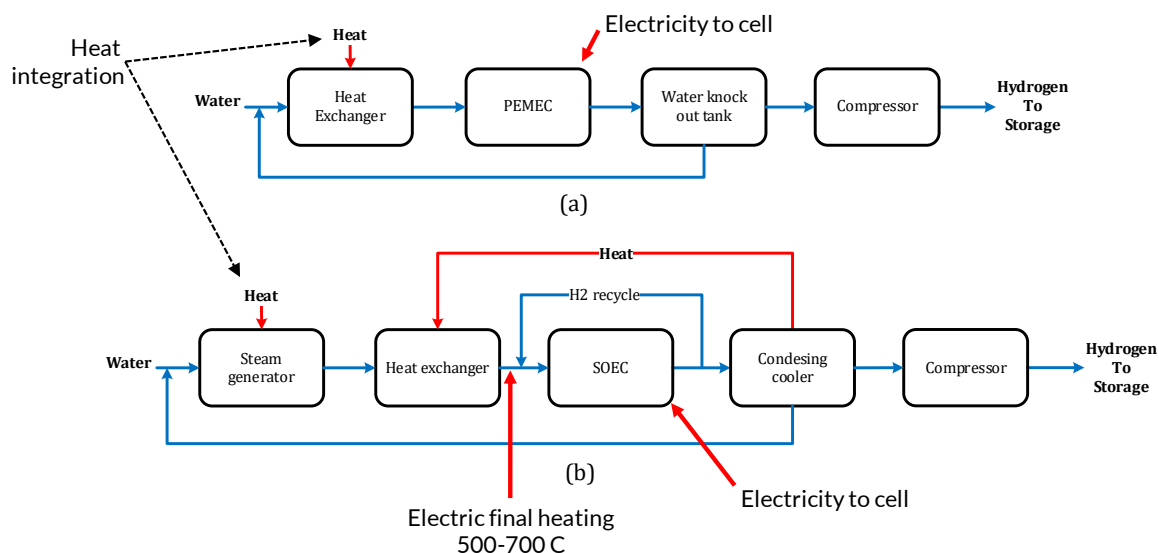


**Figure 13** Simplified system schematic of a) PEMEC and b) SOEC

Electrolyzer systems are modeled using Aspen Plus. Built in blocks from the Aspen Plus library was used to model heat exchangers as well as compressors. However, there is no readily available block to represent electrolyzer unit itself. In this case, a stoichiometric reactor linked to user defined calculator blocks was used to introduce the electrochemical reactions as well as electrical power requirement and other operational parameters such as voltage. The table below shows the

input parameters used in the model development and few of key results based on kg H<sub>2</sub> that is produced by each system.

**Table 7 Electrolysis system assumptions and key results**

Parameter	Unit	Value	
		SOEC	PEMEC
Temperature	C	700*	70**
Pressure	atm.	1	1
Voltage	V	1.6	2**
Utilization Factor	---	0.7	0.7
Sweep Air***	---	None	None
Hydrogen Recirculation	%	14	None
<b>Results</b>			
Water Consumption	kg/kg <sub>H2</sub>	8.97	8.97
Oxygen Production	kg/kg <sub>H2</sub>	7.94	7.94
Electrolysis Electrical Demand	GWh/kg <sub>H2</sub>	43	53
Hydrogen Compression 40 bar	GWh/kg <sub>H2</sub>	2.9	2.4
Heat Input	GWh/kg <sub>H2</sub>	9	0.5
Electrical Efficiency	%	77.4	62.7
System Efficiency	%	60.4	59.3
* <a href="https://elcogen.com">https://elcogen.com</a>			
** <a href="https://www.hiat.de">https://www.hiat.de</a>			
*** Anode side in case of no immediate use of produced oxygen			

## 6.2 LIGNOCELLULOSIC ETHANOL

### 6.2.1 Process description and modelling methodology

The base case (EtOH) ethanol plant description and capacity are based on simultaneous saccharification and fermentation SSF pathway (Frankó, Galbe, and Wallberg 2016). The plant produces 48 MW HHV (5.8 ton/h) ethanol from 137 MW HHV (56 ton/h at 55% moisture content) sawdust. In addition to ethanol, the process produces biogas (via anaerobic digestion AD distillation stillage) and solid fuel in form of pellets (primarily derived from lignin). In the pretreatment process 20 and 4 bar saturated steam are consumed by directly mixing with the feedstock. Additional 4 and 20 bar steam are required for heating in the upgrading (distillation reboiler) and for preheating drying air in the pellet dryer (required to reduce moisture content of pellets to 12%), respectively. In the base case, steam requirements are satisfied internally by combusting solid residuals of the AD and part of lignin in an integrated CHP plant operated in a Rankine cycle with maximum cycle pressure and temperature of 90 bar and 470°C. The plant has internal electricity consumption of 3.6 MW<sub>el</sub> which in the base case was supplied by the CHP.

A process block diagram of lignocellulosic ethanol pathway with indication for electrification options is shown in Figure 14. Electricity can contribute to improve the yield of pellets by reducing solid residues combusted in the base case and that of biogas by utilizing concentrated CO<sub>2</sub> produced in the fermentation and AD upgrading steps using electrolysis-derived hydrogen. Thus, two

electrification options are evaluated for this pathway. In the first option (EtOH\_MVR), mechanical vapor recompression (MVR) heat pumps are considered to take advantage of available low-pressure vapor and hot water for producing process steam at required pressure levels. Description of the MVR configurations and the process sections involved are presented in Appendix 3. In the second option (EtOH\_MVR\_H2), in addition to the MVR the process is enhanced with electrolysis that produces hydrogen to convert the CO<sub>2</sub> from fermentation and AD into biomethane via catalytic methanation and upgrading.

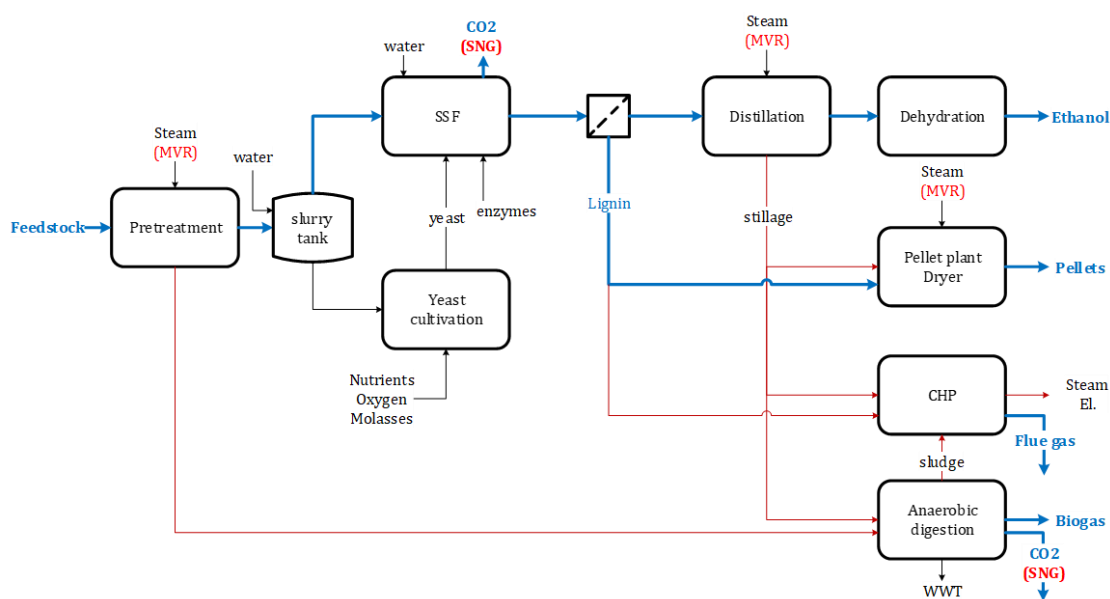


**Figure 14. Schematics of lignocellulosic ethanol (electrification options indicated in brackets)**

The process modelling of the three configurations are implemented in UniSim Design® flowsheeting software. Thermodynamic property model NRTL was selected due to the polar mixture of ethanol and water. Detailed modelling approach is summarized in Table 8.

**Table 8 Lignocellulosic ethanol modelling methodology including electrified options**

Pretreatment	Pressurized mixing to 4 bar, 95°C and to 20 bar, 205°C successively. Yield reactor to decompose feedstock to fermentable sugars and water insoluble solids (WIS)
Depressurizing pretreated feedstock	Flash tanks at 4 bar and 1 bar
Fermentation	Conversion reactor at 35°C
Ethanol upgrading	Beer column at 3 bar, 15 stages, 93% vol. ethanol, reboiler run on external heat. Rectifier column – shortcut column, reboiler run on energy recovered from beer column condenser. Molecular sieve – component splitter
Anaerobic digestion (AD)	Conversion reactor
Biogas upgrading	Amine wash – component splitter
CO <sub>2</sub> compressor (electrified option)	Two stage compressors with intercooler to 40°C, polytropic efficiency 79%
Reverse water gas shift (electrified option)	Equilibrium reactor, 750°C, 30 bar
SNG synthesis	Three equilibrium reactors in series with cooling between reactors and a final condensing cooler to 40°C

### 6.2.2 Mass and energy balances

Carbon and energy balances are shown by the Sankey diagrams Figure 15 and Figure 16, respectively. Table 26 in Appendix 4 details the carbon and energy balance for lignocellulosic ethanol under base case (EtOH) and electrification options.

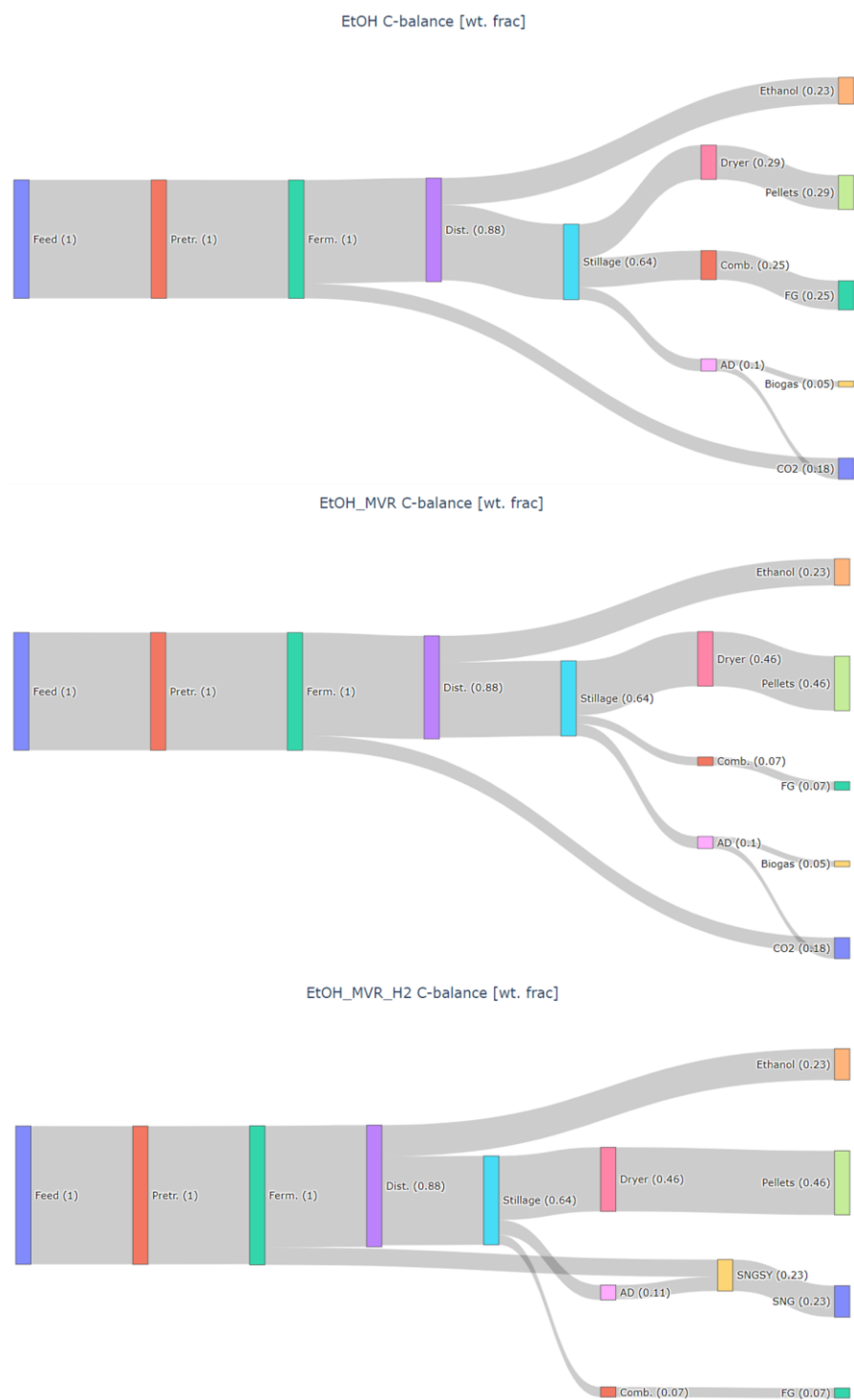


Figure 15 Carbon Sankey diagrams – lignocellulosic ethanol.

It should be noted that electrification does not increase ethanol yield, but pellets and biogas. Accordingly, when MVR heat pumps (EtOH\_MVR) were considered for lifting flash vapors to process steam pressure levels pellet production increased by about 60% while the system shifts from net electricity exporter to importer. Furthermore, adding electrolysis (EtOH\_MVR\_H2) raises electricity deficit from about 9 MW<sub>el</sub> under MVR option to about 90 MW<sub>el</sub>. The corresponding production of biomethane (synthetic natural gas, SNG) increases by about 450% from 14 MW<sub>HHV</sub> biogas in the base case.

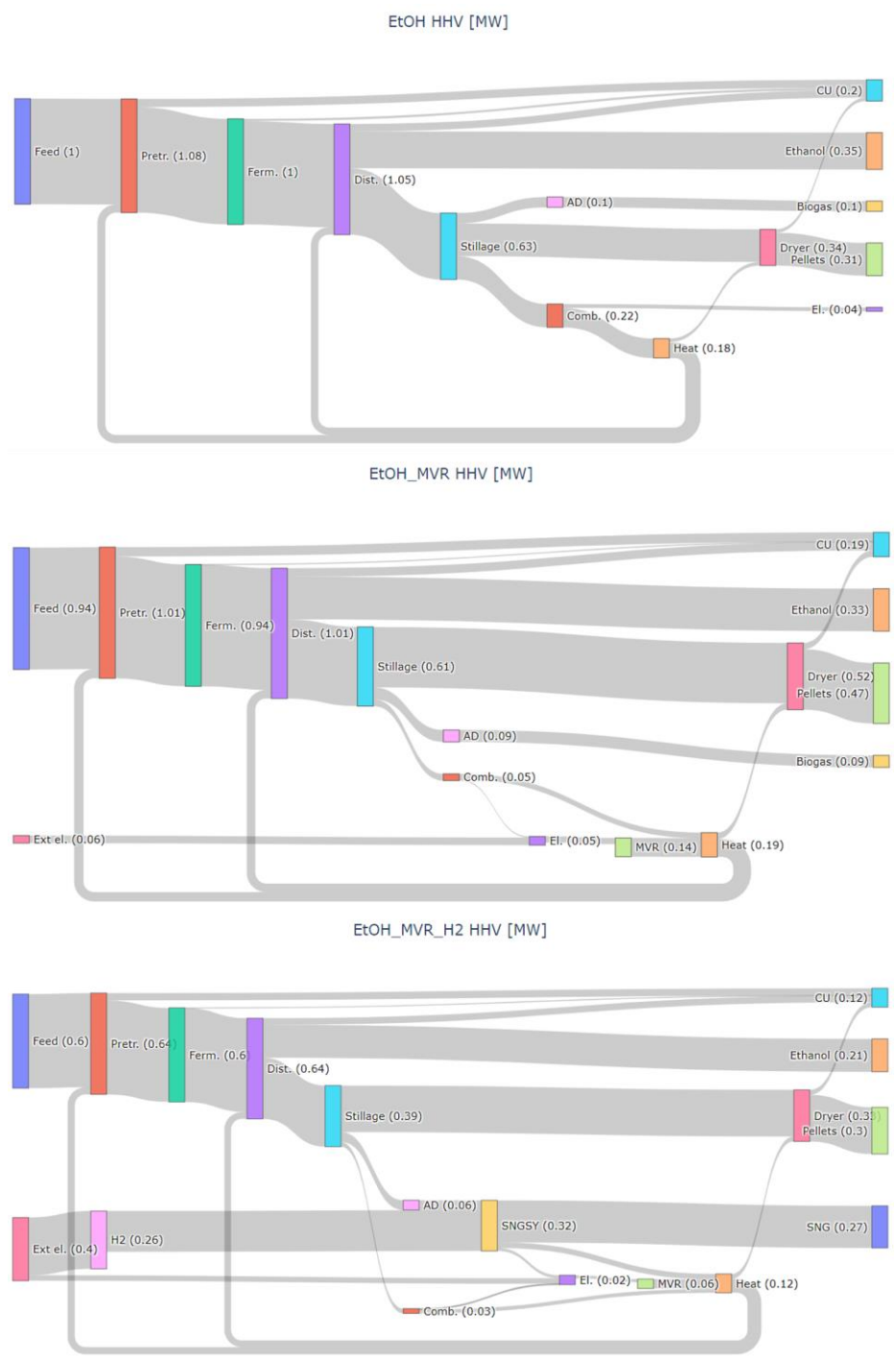


Figure 16 Energy Sankey diagrams – lignocellulosic ethanol

### 6.2.3 Summary of electrification potential

Electrification contributes both as source of heat and hydrogen to boost carbon conversion efficiency of lignocellulosic ethanol production process. With the help MVR heat pumps the thermal loads of pretreatment (100%), distillation (100%) and pellet drying (50%) can be satisfied with electricity. The results show that MVR heat pumps increase carbon in products to 75% (EtOH\_MVR) from 57% in the base case (EtOH). Adding electrolysis further increased the carbon efficiency to 93% (EtOH\_MVR\_H2) by enabling co-production of synthetic natural gas.

## 6.3 ETHANOL-TO-JET FUEL

### 6.3.1 Process description and modelling methodology

Sustainable aviation fuel (SAF) is becoming a priority among liquid renewable fuels. Alcohols-to-Jet (ATJ) pathways for SAF production have been recognized as short-term strategy to reduce CO<sub>2</sub> emissions from aviation (Geleynse et al. 2018). This pathway was first certified in 2016 (using isobutanol) and 2018 (using ethanol) (Susan van Dyk and Jack Saddler 2021). IEA predicts that this pathway could reach commercialization by 2025 (Susan van Dyk and Jack Saddler 2021). To elaborate ATJ pathway, the lignocellulosic ethanol plant presented in previous section was expanded to include ethanol-to-jet conversion steps shown in Figure 17. In practice, the ATJ steps can utilize ethanol sourced from multiple plants allowing production volumes that exploit economy-of-scale benefits. The reference case has a capacity of 104 MW HHV total hydrocarbons, 92 MW HHV jet and 12 MW HHV diesel fraction. This would require ethanol feed 113 MW HHV, equivalent to about 2.5 times the ethanol plant capacity and configuration presented above (Figure 14).

Figure 17 illustrates a simplified schematic of ATJ process consisting of three main steps, namely: dehydration, oligomerization, and hydrogenation. Ethanol is first dehydrated into ethylene where hydroxy group is removed in the form of water vapor resulting in about 45% mass reduction. Depending on the temperatures, pressures, and performance of the design, a combination of distillation, liquid-liquid separation, and molecular sieves might be used to remove water. If there is low conversion in the dehydration reactor, unreacted alcohols may be recycled by feeding this stream to the prior alcohol/water separation unit (if the alcohol is produced through fermentation). The oligomerization of ethylene into higher hydrocarbon chain lengths, typical for jet range 9 to 16, is commercially available technology in the petrochemical industry. Ethylene oligomerization for ATJ achieves carbon range distribution C<sub>4</sub> to C<sub>20+</sub> centered around C<sub>10</sub> and C<sub>12</sub>. In the final stage, the olefins must undergo hydrogenation step to saturate the double bonds formed during oligomerization. Sufficiently saturated product is critical to ensure desired fuel properties, such as low reactivity (Geleynse et al. 2018). Hydrogen required in the process can be partly sourced by recycling unreacted hydrogen gas from the product stream.

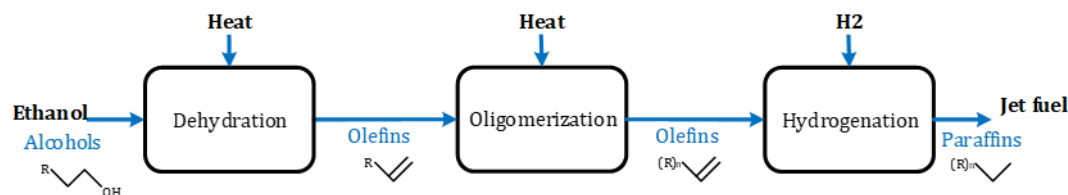


**Figure 17 Process block diagram – ATJ pathway**

Electricity can contribute both as heat source (dehydration and oligomerization) and hydrogen source (hydrogenation) in the ATJ configuration evaluated in this work. In the reference case (EtOH2Jet), heat and hydrogen were assumed to be sourced from biogas produced at the background ethanol sites, which assume base case configuration (EtOH) described in section 4.1. Under electrified option (EtOHJet\_H2), heat and hydrogen were derived from electricity and the corresponding background ethanol plants assume electrified configuration (EtOH\_MRV\_H2). Moreover, EtOHJet\_H2 was evaluated assuming SOEC and PEM electrolysis options.

### 6.3.2 Mass and energy balances

Figure 18 in combination with Table 27 and Figure 66 in Appendix 3 summarizes carbon and energy balance for the ethanol-to-jet process, including aggregated indicative balances for the background lignocellulosic ethanol plants. The EtOH2Jet base configuration consumes about 55% of biogas produced at ethanol production sites. Two-third of the biogas is used for heating and the rest for hydrogen production. Under EtOH2Jet\_H2 case, about 13 MW<sub>el</sub> is required for heating and 5.1 MW<sub>e</sub> SOEC or 5.6 MW<sub>e</sub> PEM for hydrogen production.

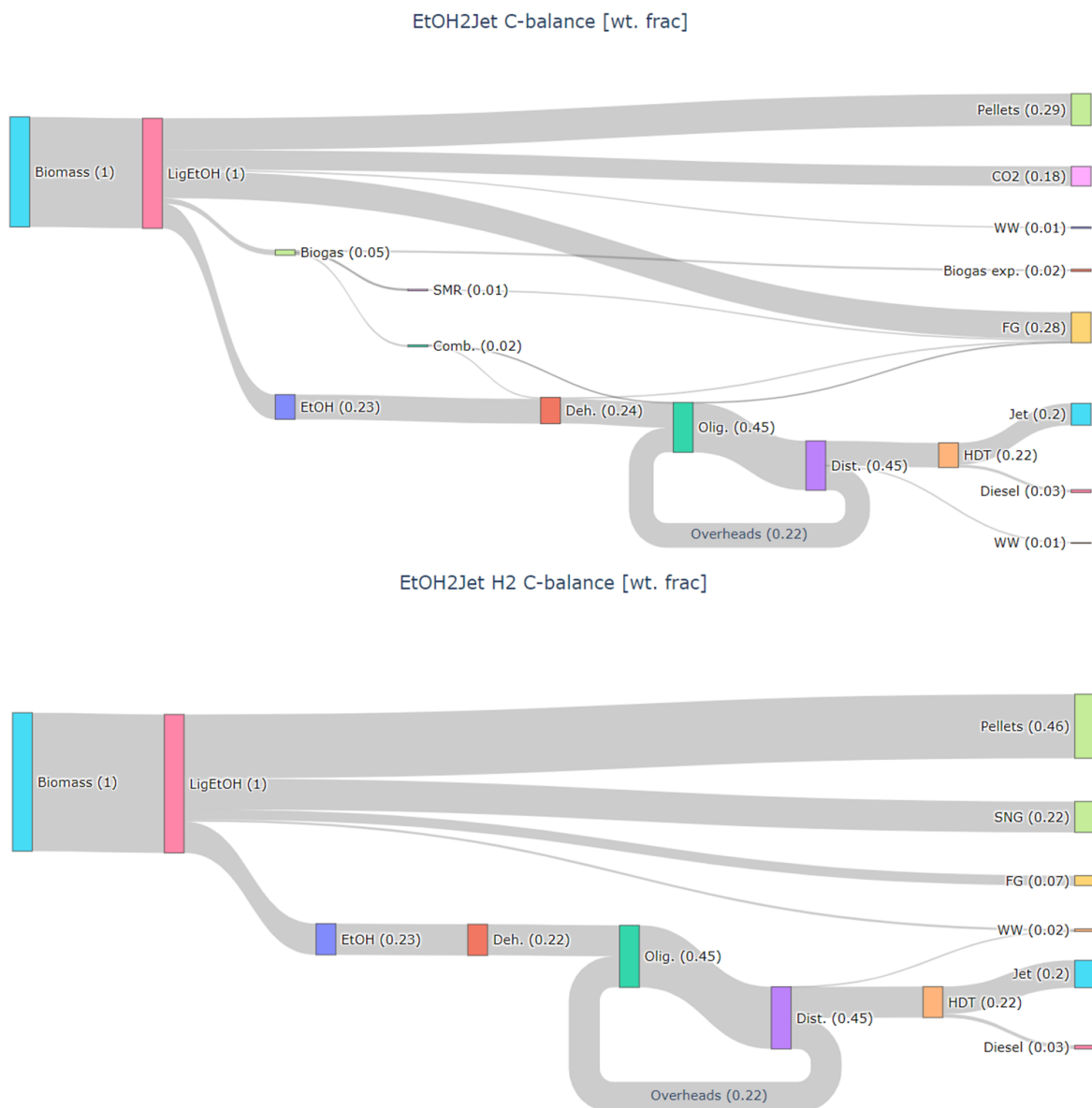


**Figure 18 Carbon Sankey diagrams – lignocellulosic ethanol to jet fuel (including indicative balances for the background ethanol plants).**

### 6.3.3 Summary of electrification potential

Ethanol-to-jet process consumes about 10% and 3.5% ethanol energy equivalent (HHV basis) in form of heat and hydrogen, respectively. In the EtOH2Jet case 12 and 6 MW HHV biogas is used to supply heat and hydrogen requirements, respectively. Hydrogen is assumed to be produced in an integrated SMR as depicted in Figure 66 (EtOH2Jet). EtOH2Jet\_H2 configuration consumes 13 MW<sub>e</sub> for heating and 5.6 MW<sub>e</sub> for electrolysis PEM configurations, Figure 66 (EtOH2Jet\_H2). From a systems perspective that include generation of ethanol for ATJ, electrification increases carbon conversion by increasing pellets and biogas/SNG yield, see Table 9. Jet fuel or diesel productivity is not impacted by electrification.

## 6.4 HYDROTHERMAL LIQUEFACTION OF WOODY BIOMASS

### 6.4.1 Process description and modelling methodology

The hydrothermal liquefaction (HTL) process data, description and flow diagram were as presented in WP1 which were taken from Tews et al. (Tews et al. 2014a). In this work, 94 MW HHV feedstock is pretreated into pumpable slurry and liquefied in water media under subcritical conditions, 204 bara and 300°C. Biooil, aqueous, gas and solid phases are separated in subsequent stages. The biooil phase is hydrotreated and upgraded into 68 MW HHV energy equivalent products, namely gasoline (49), diesel (11) and heavy hydrocarbons (8) components.

The HTL models used to derive mass and energy balances are implemented in UniSim Design. To enable reasonable estimation of missing parameters, appropriate thermodynamic property models were selected for the different process sections, HTL (SRK), hydrogen plant (PRSV) and upgrading (NRTL). Detailed description of modelling of the HTL pathway is summarized in Table 9.

**Table 9 HTL of forest residue modelling approach.**

Slurry prep	Mixing tank, atmospheric
Slurry pump	Rotary pump exit pressure 208 bar, 300°C
HTL	Yield reactor at 207 bar, 300°C, fed preheated slurry at 300°C using heat recovered from HTL product effluents
H <sub>2</sub> plant	Steam reformer, exit temp. 950°C, 30 bar, modelled as eq. reactor Additional steam injection at 400°C, to favor equilibrium towards H <sub>2</sub> PSA – modelled as component splitter
HDT	Yield reactor, H <sub>2</sub> demand 0.05kg/kg biocrude
Upgrading	Distillation based on boiling point, gasoline <155°C, diesel <365°C and heavies >365°C
Anaerobic digestion (AD)	Conversion reactor
Biogas upgrading	Amine wash – component splitter
Biogas combustor	Gibb's reactor, with spec. control on flue gas O <sub>2</sub> concentration

In the base case (HTL\_biogas) configuration biogas is used both as source of energy for the liquefaction reactor and as source of hydrogen for upgrading biooil into transport grade biofuels. Part of the biogas requirement is supplied from AD of the HTL aqueous phase. Part of the hydrogen requirement derives from the non-condensable gases produced in the HTL reactor and upgrading off-gases.

A process block diagram for forest residue based HTL and upgrading to biofuels including electrification options is shown in Figure 19. Two electrification options are evaluated depending on the extent of biogas replaced with electricity. In the first option (HTL\_H2) only biogas used to produce hydrogen is replaced with electrolysis-based hydrogen. In the second option (HTL\_xH2), in addition to electrolysis the energy demand of the HTL reactor is supplied with electricity. In the latter option biogas derived from AD of the HTL aqueous phase is exported as main product.

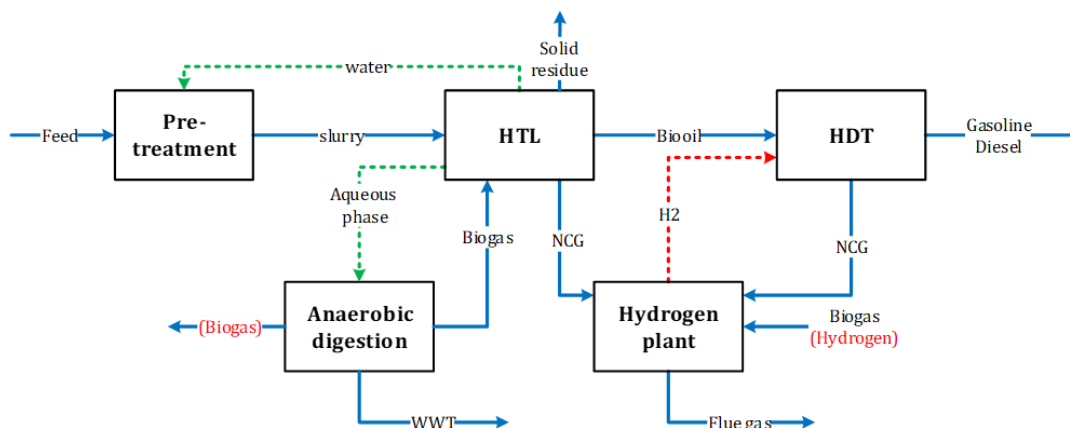


Figure 19 Schematics of HTL of forest residue to biofuels (electrification options indicated in brackets)

#### 6.4.2 Mass and energy balances

Figure 20 in combination with Appendix 4 (Figure 67 and Table 28) summarizes carbon and energy balance of the base case and electrified options. In the base case (HTL\_biogas) configuration the process barely requires external electricity ( $0.67 \text{ MW}_{el}$ ) but consumes about 38 MW HHV biogas. Under the electrified options, the share of external electricity increases to about 21 and 38  $\text{MW}_{el}$  for HTL\_H2 (biogas for hydrogen replacement) and HTL\_xH2 (total external biogas replacement) scenarios with PEM electrolysis technology, respectively. The corresponding biogas demands drop to 20 and 0 MW HHV for HTL\_H2 and HTL\_xH2, respectively.

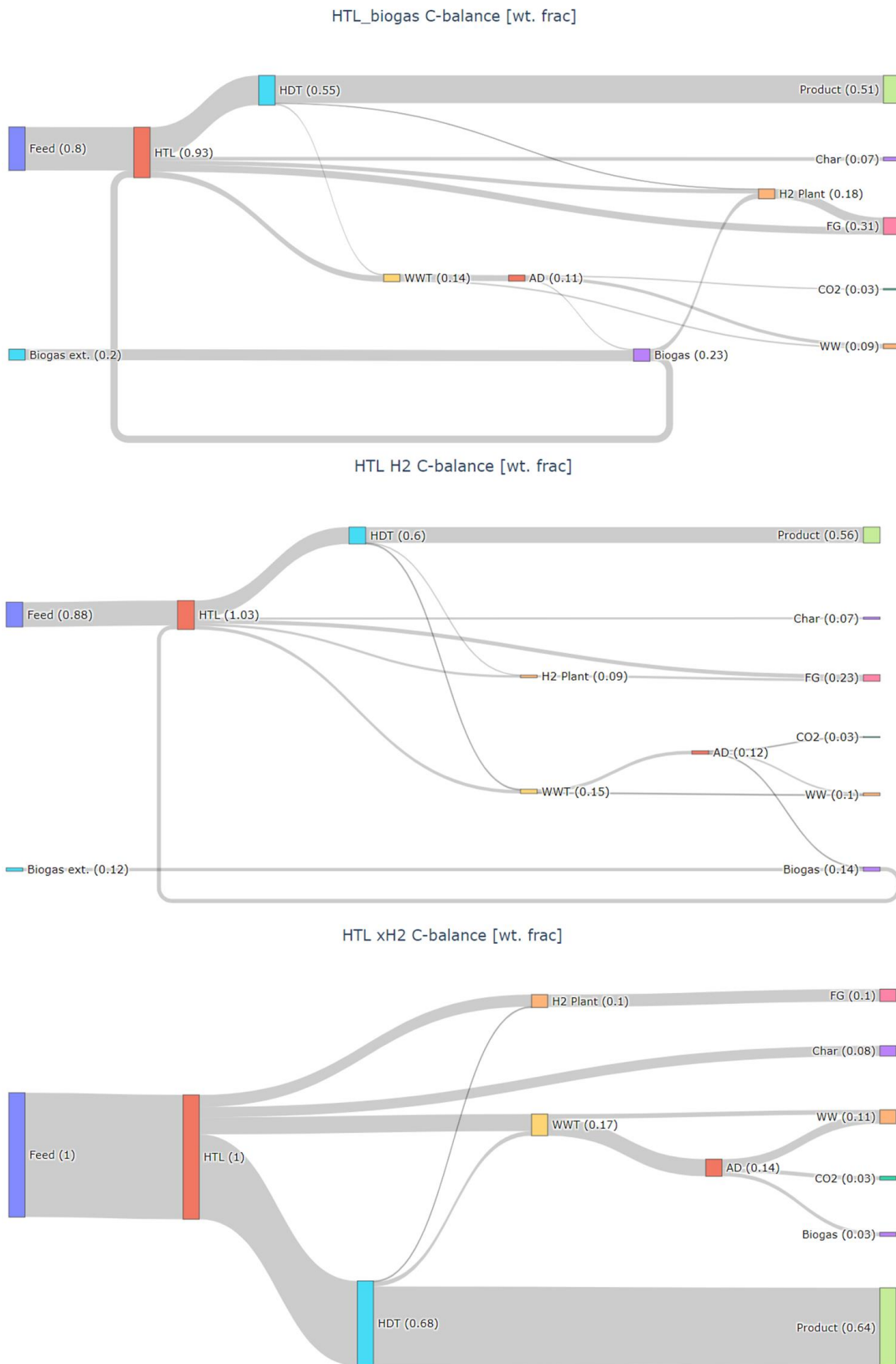


Figure 20 Carbon Sankey diagrams – HTL and upgrading

### 6.4.3 Summary of electrification potential

The electrification potential for HTL and upgrading track is limited to replacing biogas consumed in the base case for heating the HTL reactor and as feed to the H<sub>2</sub>-plant onsite. Thus, electrification does not directly increase HTL product yield but reduces carbon loss of the process by as much as 20% when electricity replaces external biogas. Under the HTL\_xH<sub>2</sub> case 5 MW HHV biogas is exported in addition to drop-in biofuels.

## 6.5 FAST PYROLYSIS

### 6.5.1 Process description and modelling methodology

Process configuration, description, data and flow diagram (Figure 21) were as presented in WP1 which were taken from Carrasco et al (Carrasco et al. 2017). The plant capacity considered in this study was however scaled to reflect the commercial pyrolysis configuration developed by BTG bioliquids® which so far has operational installations in the Netherlands (Empyro Hengelo), Finland (Green Fuel Nordic) and Sweden (Pyrocell)<sup>4</sup>. The pyrolysis plant has feedstock capacity 27 MW HHV which after pyrolysis and subsequent oil hydrotreatment upgrading is converted into 20 MW HHV energy equivalent hydrocarbon products, namely gasoline (10), diesel (7) and heavy fraction (3).

The mass and energy balances were derived from a model developed in UniSim Design, as documented Table 10. To enable reasonable estimation of missing parameters, appropriate thermodynamic property models were selected for the different process sections, pyrolysis, condensation, and hydrogen plant (PRSV) and upgrading (NRTL).

**Table 10 Fast pyrolysis and upgrading modelling approach**

Pretreatment	Conveyor dryer, to 8% moisture content
Fast pyrolysis	Yield reactor, 520°C, 1.013 barg
Separation	Cyclone, separate char & bed material
Quench tower	Flash tank at 75°C cooled with recycled pyrolysis oil
H <sub>2</sub> plant	Steam reformer, exit temp. 950°C, 30 bar, modelled as eq. reactor Additional steam injection at 400°C to favor equilibrium towards H <sub>2</sub> PSA – component splitter
HDT	Yield reactor, H <sub>2</sub> demand 0.05kg/kg biocrude
Upgrading	Distillation based on boiling point, gasoline <155°C, diesel <365°C and heavies >365°C
CHP	Char combustor modelled as conversion reactor with spec. control on flue gas O <sub>2</sub> concentration. Preheated sand to pyrolysis reactor. Steam Rankine cycle, HPS at 540°C and 120 bar

<sup>4</sup> These commercial plants do not use hydrotreatment processes to upgrade pyrolysis oils to fuels currently. Empyro and Green Fuel Nordic produces fuel oil (for heating) and Pyrocell upgrades the oil by catalytic cracking in the Preem Refinery. Thus, the oxygen will be removed as CO<sub>2</sub>, not as H<sub>2</sub>O as it would with hydrotreatment. Pyrolysis oil hydrotreatment is not yet a commercial process.

In the base case (Pyro\_biogas), the intermediate product biooil is hydrotreated and upgraded onsite using hydrogen derived from steam reforming of externally supplied biogas. Part of the hydrogen requirement is produced by reforming the non-condensable gases generated during pyrolysis reaction. The pyrolysis reactor is heated with hot sand from a combustor that burns pyrolysis char. In addition, the combustor produces HPS at 120 bar and 540°C which is expanded to generate electricity in a condensing steam turbine operated in a Rankine cycle.

The potential for electrification in this case is limited to replacement of the external biogas with electrolysis derived hydrogen (Pyro\_H2). The option to use an electrically heated pyrolysis reactor, which could potentially have avoided combustion of pyrolysis char, was evaluated but it was considered technically uncertain how it would be implemented. Hence, this electrification option was not included.

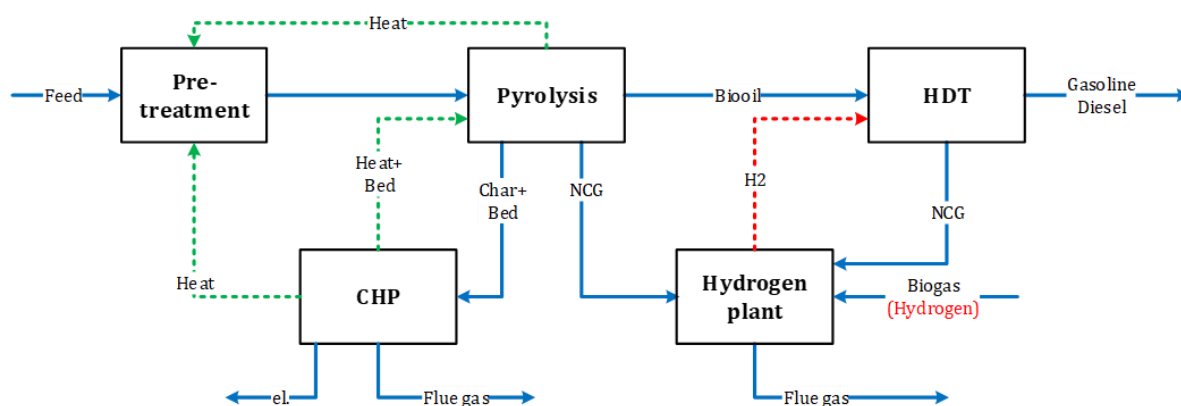


**Figure 21 Schematics of fast pyrolysis of forest residue to biofuels (electrification option indicated in bracket)**

### 6.5.2 Mass and energy balances

Figure 22 and Appendix 4 (Figure 68, Table 29) summarizes carbon and energy balance of major process streams under the base case (Pyro\_biogas) and electrified option (Pyro\_H2). The Pyro\_biogas configuration resulted in a net electricity export 1.7 MW<sub>el</sub> whereas the Pyro\_H2 configuration resulted in net electricity deficits of 7 and 9 MW<sub>el</sub> for SOEC and PEM electrolysis processes, respectively. Figure 22 and Figure 68 show Sankey diagrams for carbon and energy flows, respectively.

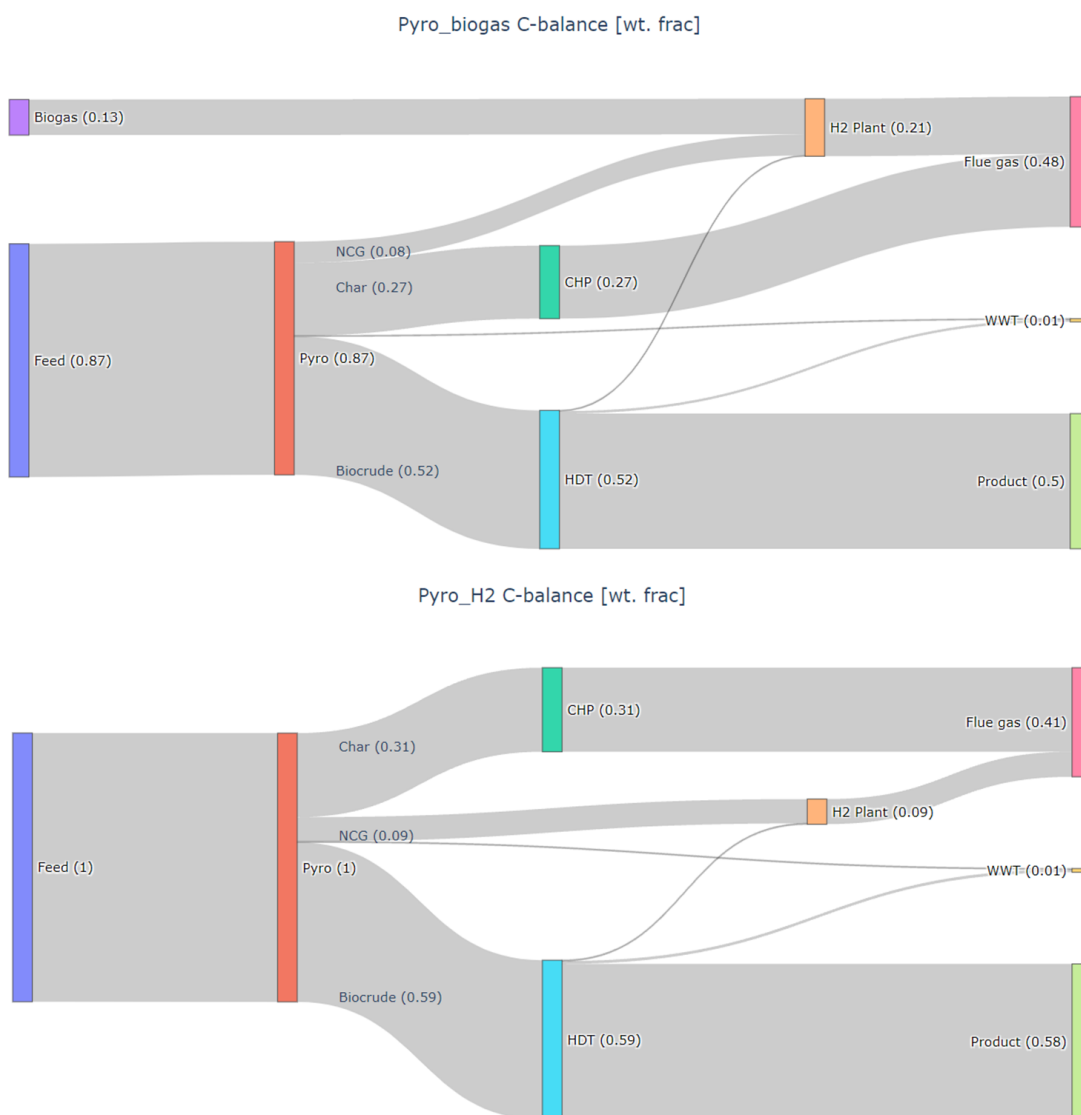


**Figure 22 Carbon Sankey diagrams – fast pyrolysis.**

### 6.5.3 Summary of electrification potential

When it comes to pyrolysis the application of electricity to improve process performance is limited to replacing hydrogen source for upgrading pyrolysis oil to biofuels. The overall carbon efficiency sees 8% increase from 50% under Pyro\_biogas case to 58% in the Pyro\_H2, and the corresponding change in energy performance is even smaller about 4%, from 57% in Pyro\_biogas to 61%. About 31% of the carbon in feedstock ends up as char, which is combusted to regenerate the bed material for pyrolysis. Thus, it is difficult to achieve significant improvement in carbon conversion without recovering char somehow and exporting it as product.

## 6.6 BLACK LIQUOR GASIFICATION (BLG)

This sub-chapter describes the black liquor gasification (BLG) process and its integration with a pulp mill. This process is common to the two biofuel production pathways, producing methanol and drop-in fuels, described in the following sub-chapters.

Black liquor (BL) is a byproduct of chemical pulping process containing inorganic (pulping chemicals), organic (lignin, small fractions of cellulose and hemicellulose) fractions and water. Entrained flow gasification (EFG) of black liquor has been successfully demonstrated at pilot scale (3 MW<sub>th</sub>) for over 25 000 h in Piteå, Sweden (Jafri et al. 2016). The BLG reactor is oxygen-blown operated at 30 barg and 1050°C. The raw gas generated in the reactor is quenched with water to recover pulping chemicals in the form of green liquor which is sent back to the chemical recovery loop of the pulp mill. Thus, the raw gas exits the BLG unit saturated at about 210°C. The raw gas is then cooled in a counter-current condenser to 40°C, while low-pressure steam (LPS, 3-5 bar) and hot water are produced from the recovered heat. In the reference case, oxygen is assumed to be delivered from an air separation unit (ASU) onsite which has electricity consumption about 0.5 kWh/kg-O<sub>2</sub> (Zhang et al. 2014). Under electrified configurations involving electrolysis, part or total oxygen requirement is covered from the electrolysis unit. The BLG mass and energy balance used for the reference case derives from data measured at the pilot plant (Jafri et al. 2016), and scaled-up techno-economic evaluations (Ekbom et al. 2003; Carvalho et al. 2018). Process block diagram for EFG of BL including syngas handling to achieve high quality syngas ready for biofuel synthesis is shown in Figure 23, and Table 11 documents the corresponding modelling strategies implemented.

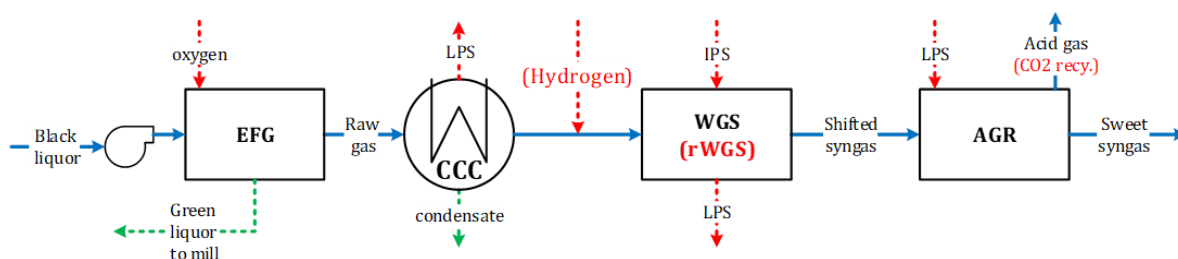


**Figure 23** Schematics of EFG of BL up to sweet syngas (electrification options indicated in brackets).

**Table 11** BLG modeling methodology up to sweet syngas.

BL pump	Centrifugal pump with outlet pressure 31 barg. Adiabatic efficiency: 75%
BLG (EFG)	Equilibrium reactor, 1050°C, 31 barg. Empirical correlation for components with poor equilibrium prediction, e.g., H <sub>2</sub> S, CH <sub>4</sub>
Counter current condenser (CCC)	Multiple heat exchangers . Flash at 80°C and 40°C
WGS reactor	Saturator 190-200°C. Equilibrium reactor ~400°C
AGR (amine wash)	Component splitter. Steam demand for reboiler duty calculated externally

The BLG cases were evaluated under integrated configurations in which the system boundary included steam system of the pulping process, as illustrated in Figure 24, in a similar way as many other studies of BLG (Carvalho et al. 2018; Jafri et al. 2020; 2019). In a conventional pulp mill, us-

ing the Kraft pulping process, BL is combusted in a recovery boiler to generate HPS which expands in steam turbine that allows extraction of process steam at required pressure levels. The cooking chemicals are recovered in smelt form at the bottom of the recovery boiler. Process steam deficit is complemented from a biomass boiler fueled with falling bark. When part of the BL is utilized for biofuel production, the steam produced in the recovery boiler is significantly reduced. Additional biomass must be supplied to the biomass boiler which was assumed to have capacity enough to ramp-up steam production. As depicted in Figure 24, part of pulping process steam is satisfied by excess heat from the subprocess of the biofuel plant, leading to a lower fuel make-up demand in the biomass boiler.

From a systems perspective BL becomes internal stream and its consequence is reflected on the changes in biomass intake and net power generation as well as on the produced biofuels, all of which cross the system boundary shown in Figure 24.

The mass and energy balance of the BLG cases were derived from models implemented in UniSim Design using PRSV thermodynamic property package. The steam balances from UniSim Design models were aggregated with a reference pulp mill model CHP system (described in the next section) to derive integrated process streams.

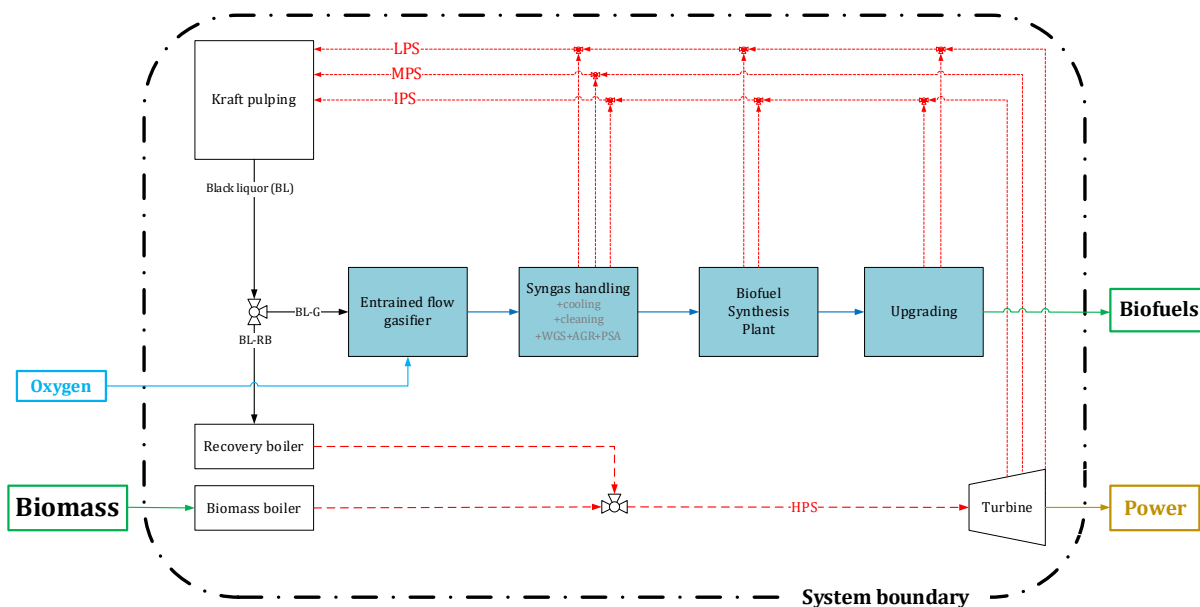


Figure 24 Integrated BLG based biofuels process system boundary.

### 6.6.1 Reference pulp mill

The pulp mill in which the BLG process is integrated have been simulated as a state-of-the-art pulp mill using softwood as feedstock (Berglin et al. 2011). The production was set to 2 000 ADt pulp per day, corresponding to about the size of the largest pulp mill in operation in Scandinavia today. The softwood raw material used in the pulp mill consists of 50% pine and 50% spruce. This generates about 3 760 tBLS (BL solids) per day.

Under business-as-usual (BAU) operation, the reference pulp mill has steam surplus from the combustion of black liquor in the recovery boiler. The falling bark generated during the debarking of incoming biomass was partly used to fuel the lime kiln. The remainder can be combusted in a bark boiler, generating additional high-pressure steam (HPS), but in the reference case of this work that was not implemented, meaning that excess bark is exported from the mill. Still, the mill has large steam surplus which is used for power generation in a condensing turbine.

Some key features of the energy system of the reference mill are:

- Recovery boiler with steam data 100 bar(g), 505°C.
- Feed water preheating to 175°C to increase HP steam generation.
- Recovery boiler flue gas cooler to reduce LP steam consumed in air preheating.
- Medium pressure (MP) steam preheating of all recovery boiler combustion air to 205°C.
- Recovery boiler soot blowing steam is extracted at 25 bar(g) from the turbine instead of using HP steam.
- MP steam is extracted from the steam turbine at 9 bar(g) and 12 bar(g)
- Low pressure steam is extracted at 3.5 bar(g)
- Pressurized condensate system
- Temperature of the hot water (85°C) and maximum use of hot water for boiler feed water heating.

The power consumption for the mill is estimated to 727 kWh/ADt and the resulting power balance is presented in Table 12. To reflect actual mill Kraft pulp mill operation the steam generated from the biomass boiler of the reference mill is excluded. Excluding the HPS from the biomass boiler, about 614 kWh/ADt is sold to the grid. This corresponds to 51 MW electricity exported to the grid. The net-power to the grid with the bark boiler in operation would have been about 993 kWh/ADt.

**Table 12. Power balance for the reference mill BAU excluding biomass boiler, kWh/ADt.**

Power balance	kWh/ADt	MW
Back-pressure part of the turbine	841	70
Condensing part of the turbine	500	42
Sum	1341	112
Consumption	kWh/ADt	MW
Process	727	61
Sold	614	51

## 6.7 BLACK LIQUOR GASIFICATION FOR METHANOL PRODUCTION

### 6.7.1 Process description and modelling methodology

The BLG methanol pathways assume about 60% of available BL corresponding to 338 MW HHV (2 220 tBLS/day) is gasified into raw gas. The carbon content of BL sets the upper limit for biofuel production. The total BL carbon flow in this case was estimated 34 ton/h (about 10% of BL carbon is inevitably returned to the mill as part of green liquor). Multiple syngas conditioning steps are required to achieve a gas composition optimal for methanol synthesis (MSY), e.g. measured by the so-called synthesis gas Module (M),  $[H_2-CO_2]/[CO+CO_2]$ . Sweet syngas at MSY reactor entry has an optimal M value 2.07 from a raw gas value 0.05. Thus, in the base case the raw gas undergoes water gas shift (WGS) to enrich its  $H_2$  composition and acid gas removal (AGR) to reduce impurities and  $CO_2$  prior to entering the MSY reactor. Figure 25 shows process block diagram from sweet syngas to methanol, and Table 13 documents the corresponding modelling assumptions.

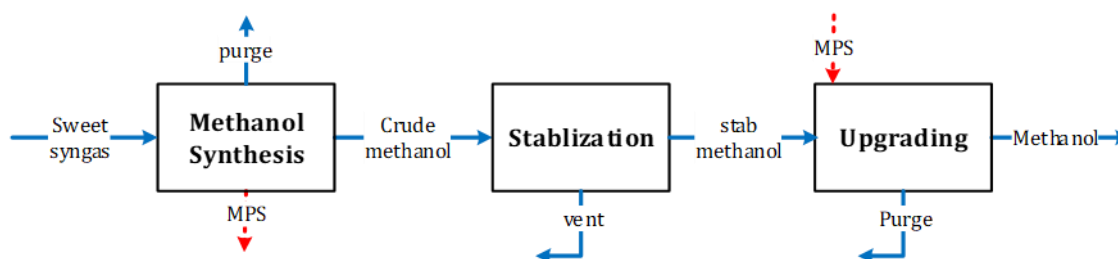


Figure 25 Schematics of methanol synthesis from sweet syngas.

Table 13 Methanol synthesis modelling.

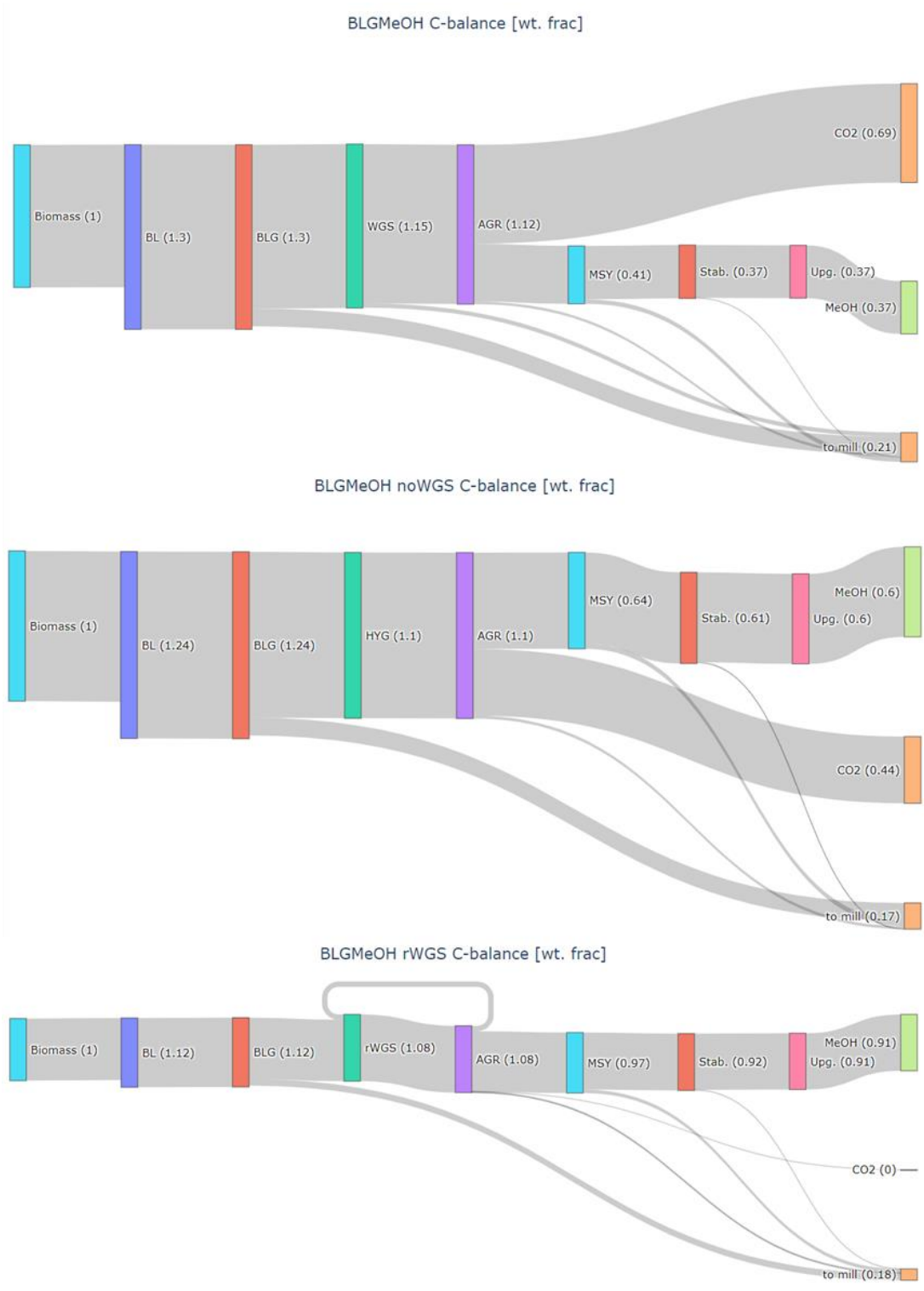
Gas compressor	Centrifugal compressor with aftercooler to 125°C, outlet pressure 80 barg, polytropic efficiency 79%
Methanol Synthesis (MSY)	Equilibrium reactor, 233°C, 80 barg
Methanol stabilization (MST)	Multiple stage column
Methanol purification (MPU)	Distillation column, product spec 99.99 vol. % methanol

To increase carbon conversion and yield of methanol, two electrification options were evaluated based on the extent of utilization of electrolysis-based hydrogen. The first option (BLGMeOH\_noWGS) aims at removing the need for WGS by adding hydrogen enough to adjust the gas Module without sacrificing CO, but still with AGR removal of  $CO_2$  formed in the gasifier. In the second option (BLGMeOH\_rWGS), additional hydrogen is made available to convert all  $CO_2$  into CO in a reverse WGS (rWGS) process. SOEC and PEM electrolysis technologies were considered for each electrification option. A total of five cases were evaluated for the methanol pathway.

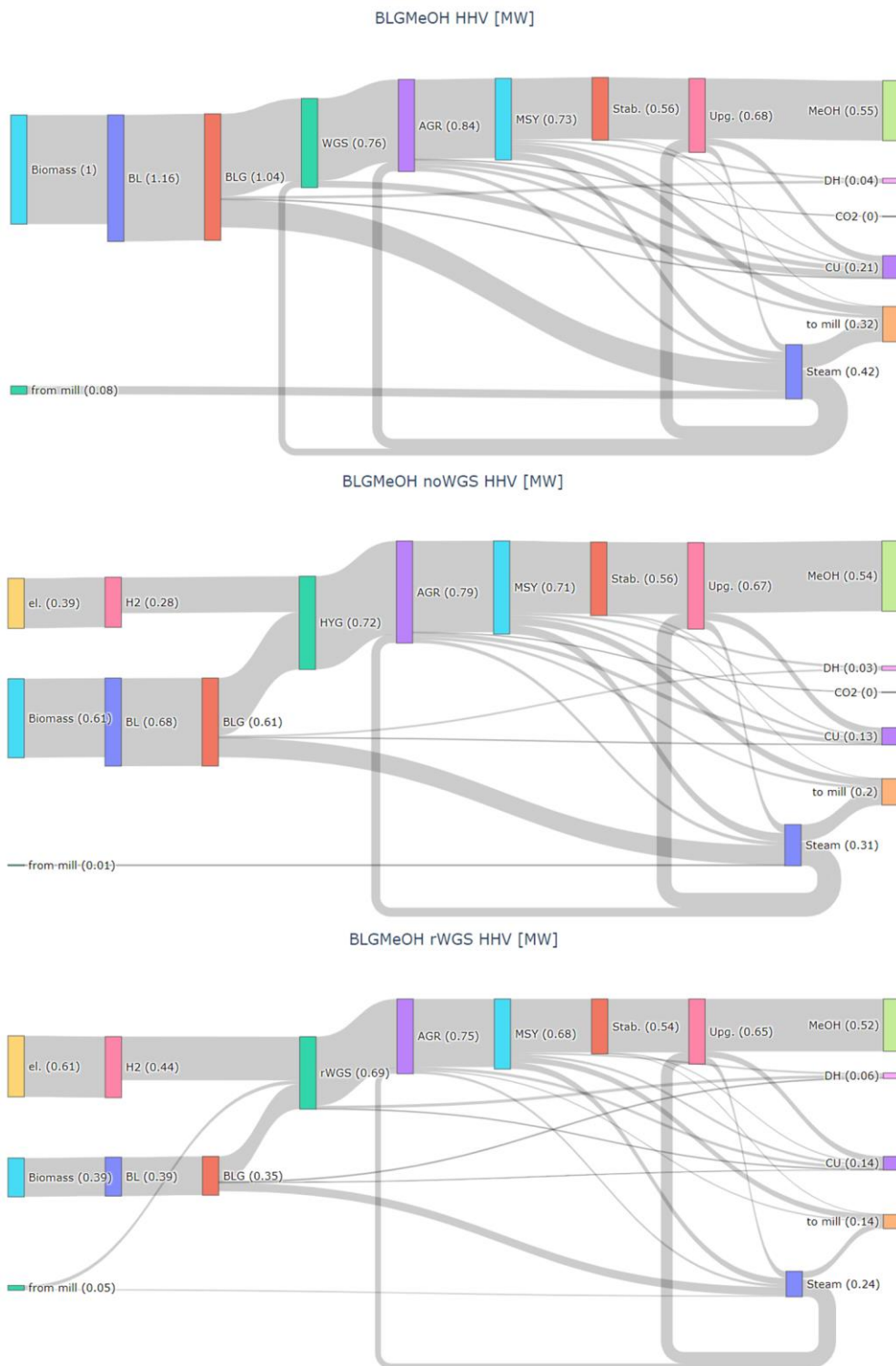
### 6.7.2 Mass and energy balances

Figure 26 and Figure 27 and Table 30 (Appendix 4) summarizes carbon and energy balance of BLGMeOH cases. In the BLGMeOH case, about 291 MW HHV additional biomass must be

supplied to the mill to maintain steam balance of the mill, while net electricity is reduced by 16 MW<sub>el</sub> (electricity export reduces from 51 to 35 MW<sub>el</sub>). The corresponding methanol production was 160 MW HHV. For the BLGMeOH\_noWGS case, the additional biomass increases to 304 MW HHV and net electricity reduction to 173 MW<sub>el</sub> (SOEC) or 192 MW<sub>el</sub> (PEM). The corresponding methanol production increases by about 170% to 270 MW HHV compared to BLGMeOH. The BLGMeOH\_rWGS cases resulted in methanol production 456 MW HHV from additional biomass input 338 MW HHV and net electricity reduction 481 MW<sub>el</sub> (SOEC) or 533 MW<sub>el</sub> (PEM).



**Figure 26 Carbon Sankey diagrams – BLG methanol. Note that the pulp mill energy integration is simplified by showing a smaller make-up biomass demand than BL flow.**



**Figure 27 Energy Sankey diagrams – BLG methanol. Note that the pulp mill energy integration is simplified by showing a heat flow “to mill” and a smaller make-up biomass demand than BL flow.**

### 6.7.3 Summary of electrification potential

The results show electrolysis-based hydrogen significantly contributes to improving the carbon conversion performance of BLG methanol pathway. The part of carbon in BL that exits the biofuel plant as concentrated CO<sub>2</sub> stream reduces progressively from 53% to 35% to 0.6 PPM under BLGMeOH, BLGMeOH\_noWGS and BLGMeOH\_rWGS cases, respectively, Figure 26. Nearly all this carbon becomes methanol and increases the productivity of the corresponding cases by the same margin, from 29% (BLGMeOH) to 48% (BLGMeOH\_noWGS) to 81% (BLGMeOH\_rWGS). Compared to the replacement biomass, the carbon conversion efficiency to methanol increases from 37% BLGMeOH to 60% BLGMeOH\_noWGS to 91% BLGMeOH\_rWGS, Figure 26. The marginal electricity share in input increases from 0% to 39% to 61% for BLGMeOH, BLGMeOH\_noWGS and BLGMeOH\_rWGS cases, respectively, Figure 27. The combined effect of increased methanol productivity and increased share of electricity is that the overall energy performance of the systems remain in the same range, 0.53–0.58.

## 6.8 BLACK LIQUOR GASIFICATION FOR FISCHER TROPSCH FUELS

### 6.8.1 Process description and modelling methodology

The BLG Fischer Tropsch (FT) pathways assume about 60% of available BL corresponding to 338 MW HHV is gasified into raw syngas (same as for BLG to methanol). Like the methanol pathway, multiple syngas conditioning steps are required to achieve optimal FT Synthesis (FTS) which is achieved at H<sub>2</sub>/CO molar ratio 2. In addition, impurities and CO<sub>2</sub> must reduce to specified levels. Thus, the raw syngas which initially has H<sub>2</sub>/CO molar ratio about 1 and CO<sub>2</sub> composition about 30% vol. successively goes through a WGS to boost its H<sub>2</sub> composition and an amine wash to remove CO<sub>2</sub> and impurities. To improve productivity, FT tail gas and upgrading off-gases may be reformed and recycled to the FTS reactor as depicted in Figure 28. Table 14 presents the modelling assumption for BLG based FT track.

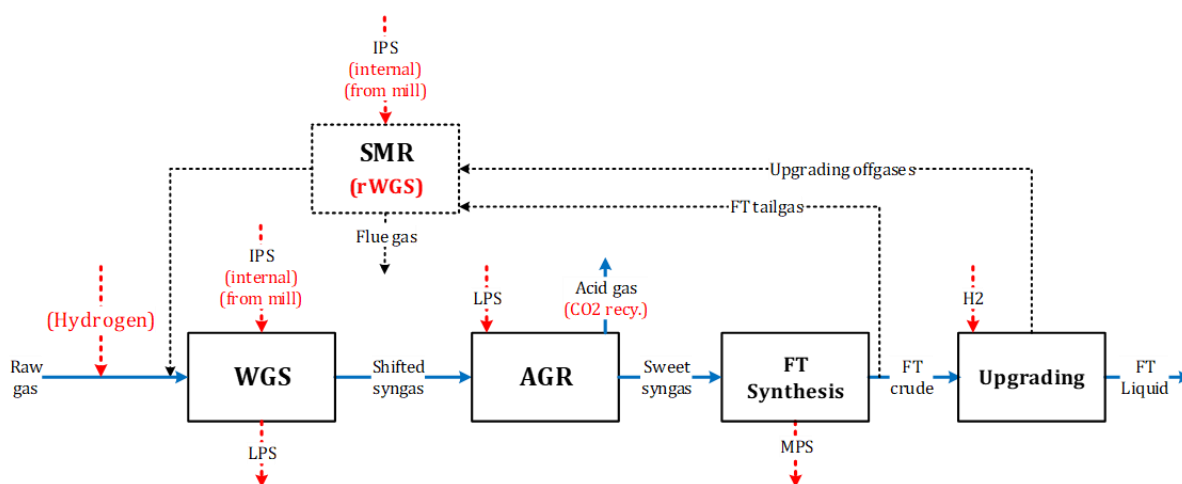


Figure 28 Schematics of BLG for FT fuels – gas conditioning (electrification options indicated in bracket), synthesis and upgrading.

**Table 14 FT fuels synthesis and upgrading modelling.**

FT tail gas compressor	Centrifugal compressor, outlet pressure 21 barg polytropic efficiency 79%
FT Synthesis (FTS)	Synthesis – yield reactor, maintained at 240°C, 80% internal recycle Water cooled reactor, produce 12barg saturated steam Separation – 3-phase decanter at 40°C to FTL, FT water and gases
Upgrading	Upgrading was not explicitly modelled but H <sub>2</sub> demand for upgrading is internally produced PSA modelled as component splitter
Steam reformer	Equilibrium reactor, exit temperature 950°C C1 to C4 assumed to be reformed

Two electrification options were evaluated based on the extent of utilization of electrolysis-based hydrogen to increase overall carbon conversion, thereby the yield of FT products. The first option aims at removing the need for WGS by adding hydrogen enough to adjust the FTS feed H<sub>2</sub>/CO ratio without sacrificing CO. In the second option, additional hydrogen is made available to convert all CO<sub>2</sub> into CO in a reverse WGS process. SOEC and PEM electrolysis technologies were considered for each electrification option.

FTS generates a wide range of hydrocarbon chain lengths including light components C<sub>1</sub> to C<sub>4</sub>, which are assumed to be reformed into H<sub>2</sub> and CO components and recycled to boost overall carbon conversion. Two types of steam reformers (SR) were considered to utilize the light FTS products, a conventional side-fired steam reformer (SMR) and an electric resistance-heated steam reformer (eSMR), which is under development but not yet commercial. The SMR configuration sacrifices part of the incoming gas in an integrated combustor to deliver the heat required to drive the reformer. The eSMR acquires the heat requirement for reforming through reactor surfaces which are heated with electric resistance (Wismann et al. 2019b).

IPS is consumed in both the WGS and SR. Two alternatives were evaluated depending on how the IPS demand was satisfied. In the first alternative, the gas sacrificed in the SR combustor is controlled to satisfy the IPS making the biofuel process self-sufficient with IPS. In the second alternative, the control on fuel consumption of the SR combustor was removed and any IPS deficit was assumed to be sourced from the pulp mill, influencing the mill energy balance and the need for make-up fuel.

A total of 12 cases were evaluated combining different options for gas conditioning (WGS, no WGS or rWGS), reforming (SMR or eSMR), IPS self-sufficiency and electrolysis technology (SOEC or PEM). The abbreviations used and definition of the cases are summarized in Table 15.

**Table 15 BLG FT cases evaluated.**

Abbreviation	Steam reformer	Conditioning	IPS self-sufficiency	Electrolysis
BLGFT SMR	SMR	WGS	Yes	
BLGFT xSMR	SMR	WGS	No	
BLGFT xSMR noWGS	SMR	No WGS	No	SOEC
BLGFT xSMR noWGS	SMR	No WGS	No	PEM
BLGFT xSMR rWGS	SMR	rWGS	No	SOEC
BLGFT xSMR rWGS	SMR	rWGS	No	PEM
BLGFT eSMR	eSMR	WGS	Yes	
BLGFT xeSMR	eSMR	WGS	No	
BLGFT xeSMR noWGS	eSMR	No WGS	No	SOEC
BLGFT xeSMR noWGS	eSMR	No WGS	No	PEM
BLGFT xeSMR rWGS	eSMR	rWGS	No	SOEC
BLGFT xeSMR rWGS	eSMR	rWGS	No	PEM

### 6.8.2 Mass and energy balances

Detailed carbon and energy balances of the BLGFT cases are presented in Appendix 4 (Table 31 and Table 32) for SMR and eSMR configurations, respectively. Figure 29 and Figure 30 show carbon and energy Sankey diagrams for BLGFT SMR configurations, Figure 69 and Figure 70 (appendix 4) show the corresponding eSMR configuration.

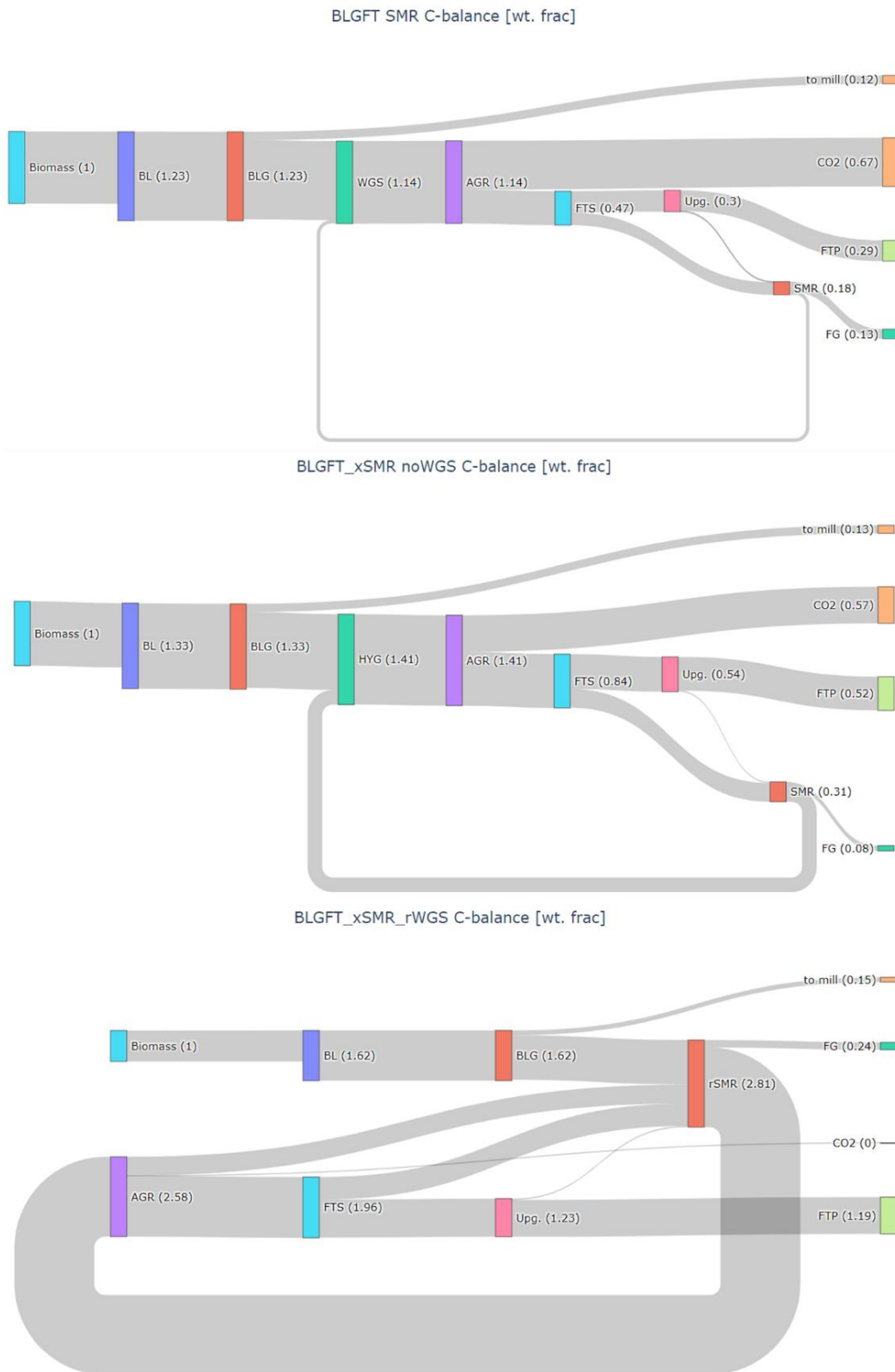


Figure 29 Carbon Sankey diagrams – BLG FT under SMR configuration.

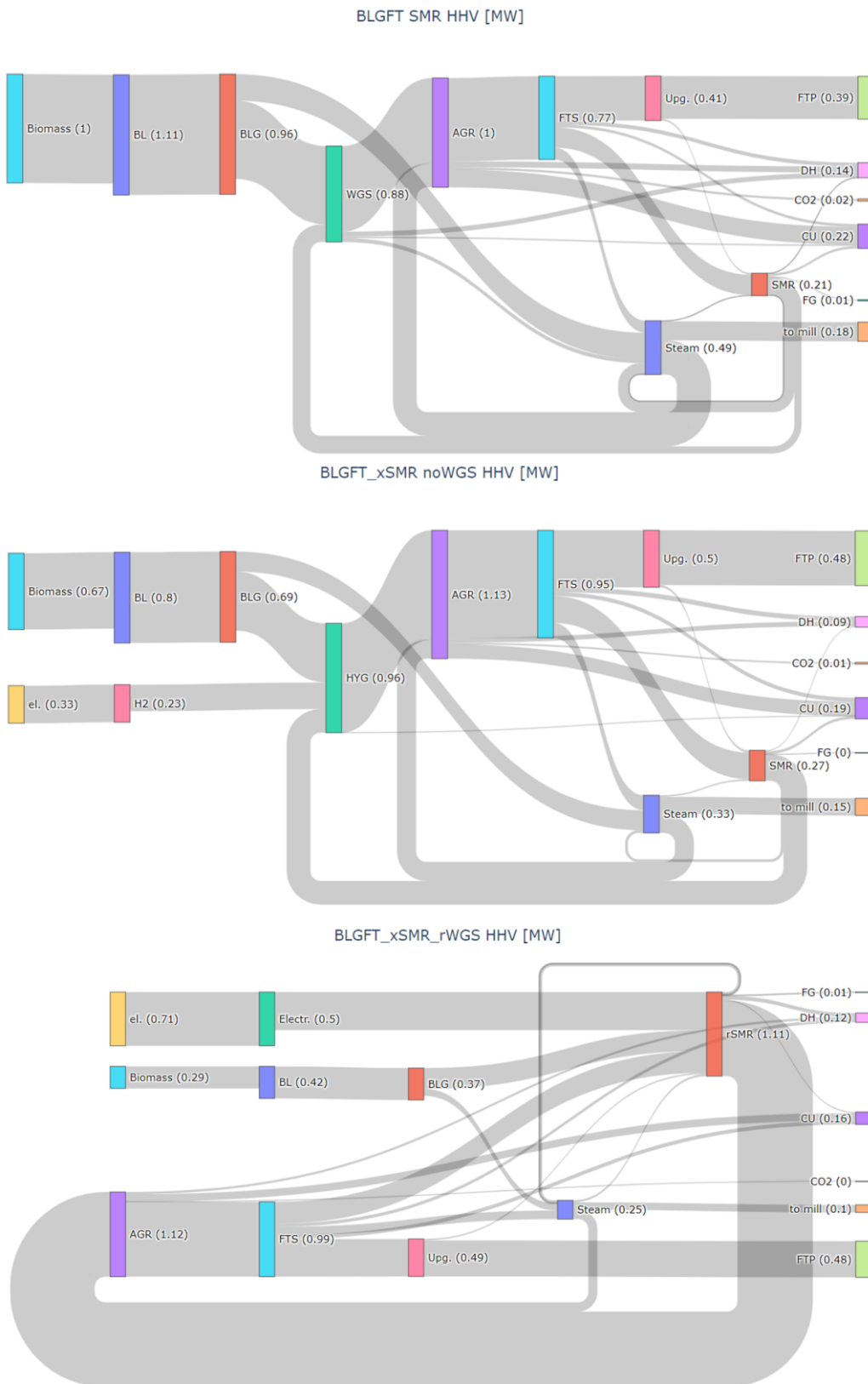


Figure 30 Energy Sankey diagrams – BLG FT cases under SMR configuration.

### 6.8.3 Summary of electrification potential

Depending on the reformer configuration, SMR or eSMR, two sets of scenarios were evaluated for the BLGFT pathway. The main difference between SMR and eSMR is that the eSMR cases use electricity to drive the reforming reactions whereas the SMR counterparts scarily part of the incoming gas. From a steam perspective, the SMR configurations generate entirely or part of the IPS process steam required by the biofuel process whereas the eSMR cases import it from the mill increasing the need for replacement feedstock. The combined effect is that the eSMR cases consume more feedstock (101%, 107% and 136%) and produce more FT fuel (104%, 110% and 116%) for BLGFT, BLGFT\_noWGS and BLGFT\_rWGS configurations, respectively, Table 31 (SMR) and Table 32 (eSMR).

The carbon exiting the biofuel plant as concentrated CO<sub>2</sub> reduces from (numbers in brackets for eSMR) 55% (55%) to 43% (44%) to 0.04% (4.2%) for BLGFT, BLGFT\_noWGS and BLGFT\_rWGS, respectively, see Figure 29 (SMR) and Figure 69 (eSMR). The corresponding share of marginal electricity in input increases from (numbers in brackets for eSMR) 0 (0) to 33% (34%) to 71% (63%) for BLGFT, BLGFT\_noWGS and BLGFT\_rWGS, respectively, see Figure 30 (SMR) and Figure 70 (eSMR). When evaluated at systems level, i.e., relative to carbon in replacement biomass fuel to the pulp mill, carbon conversion efficiency to FT products could exceed 100% which was the case for BLGFT\_rWGS, at about 120% (SMR) and 105% (eSMR).

## 6.9 DUAL FLUIDIZED BED (DFB) GASIFICATION

This sub-chapter describes the dual fluidized bed (DFB) gasification (BLG) process and its integration with a combined heat and power (CHP) plant. This process is common to the two biofuel production pathways, producing methane and drop-in fuels, described in the following sub-chapters.

The principle of a DFB gasification process is based on splitting the gasification process into two interconnected fluidized bed reactors as illustrated in Figure 31. Biomass is fed to the gasification reactor where it is partially converted by the heat from the combustion reactor into a raw gas. Heat is transported with the bed material that is circulated between the reactors. Unconverted fuel in the form of char is transported from the gasifier to the combustor with the bed material where it is burnt to produce heat. In addition to the char, off-streams such as tar and combustible off-gases can be burnt in the combustion reactor. Additional fuel to the combustor is also required to cover the heat demand of the process. In a stand-alone unit some of the cleaned raw gas, referred to as product gas, is recirculated to control the temperature of the process, while in a co-production unit additional biomass can be used instead.

Major contaminants such as particles, tar and steam are removed from the gas by cooling and scrubbing the gas. The bulk of H<sub>2</sub>S can be removed together with some of the CO<sub>2</sub> through amine scrubbing before final polishing using guard beds to produce a sulfur free fresh gas for the synthesis process.

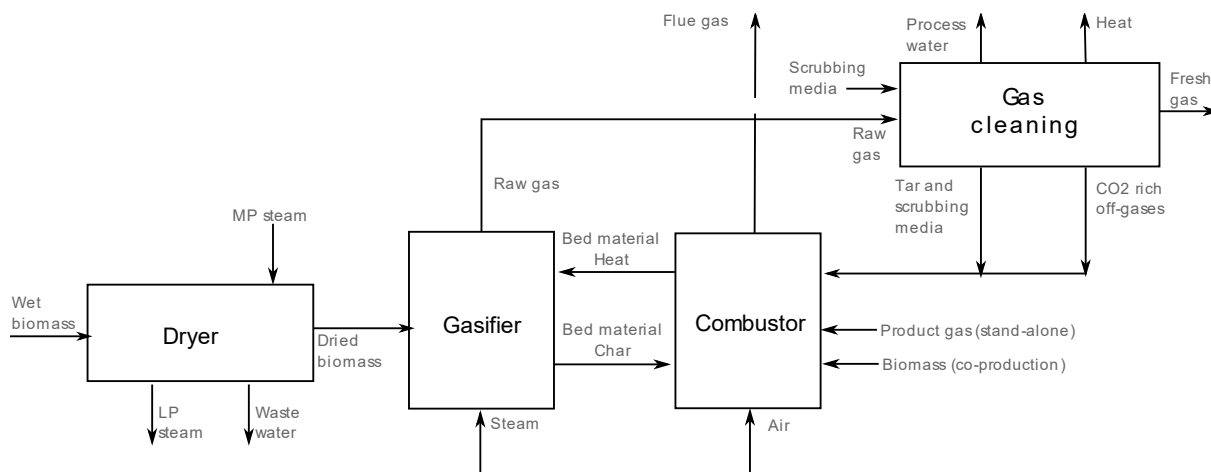


**Figure 31: Schematics of a DFB gasification system including the primary gas cleaning.**

In a stand-alone DFB-gasifier the process is optimized for producing as much product gas as possible from the fuel fed to the gasification reactor while the combustion reactor is operated only to generate the heat required for the gasification process. This technology has been used for commercial production of heat and power in several plants e.g. Senden, Oberwart and Güssing with up to about 16 MW (LHV) of biomass feed. It has also been used in a demonstration plant for production of SNG, the GoBiGas plant, with a thermal input of about 32 MW (LHV) and 20 MW biogas production (Anton Larsson, Gunnarsson, and Tengberg 2018; Thunman et al. 2019). To optimize the yield of product gas, an activated bed material was used in these plants (olivine sand activated with calcium and potassium), which also impose the need of a post combustion chamber. As biomass is fed only to the gasification reactor, it is required to recirculate some of the cleaned product gas during operation and to use an additional fuel such as natural gas during start-up.

In a co-production DFB gasification unit, the combustion process is operated to produce more heat than required by the gasification to enable steam, heat and power, or district heating production. This is possible by having a larger combustion reactor with dedicated fuel feeding to the combustor as well as to the gasifier. The co-production concept can be applied to existing boilers through retrofitting it with an additional gasification reactor, which has been demonstrated with the Chalmers gasifier (2-4 MW thermal input). Retrofitting an existing plant reduces the investment cost significantly but also enables simplification of the process whereas it is not as crucial to optimize the yield of gas. For example, regular silica sand can be utilized, and the temperature can be slightly reduced. BioShare is looking to commercialize a cost-efficient co-production concept and it is therefore this concept that is analyzed in this report.

## 6.10 DFB GASIFICATION FOR SNG PRODUCTION

Figure 32 shows the main process steps required to produce SNG from fresh gas. The composition of the gas is adjusted before the synthesis mainly through water gas shift (WGS), pre-methanation and CO<sub>2</sub> removal (AGR).

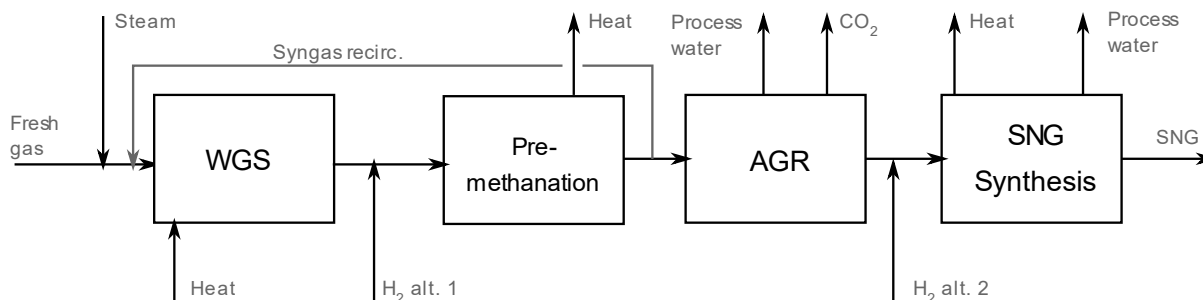


**Figure 32: Simplified process for DFB SNG production including indications of how H<sub>2</sub> can be introduced to the system.**

Electricity can be introduced to the DFB-SNG process to improve the carbon utilization and increased the marginal efficiency of biomass to SNG. The electricity can be added as heat or as H<sub>2</sub> produced through electrolysis. Adding electricity for heating is only considered for applications where it is not possible or impractical to cover the heat demand through process integration and heat recovery. Adding H<sub>2</sub> to the process will decrease the amount of CO<sub>2</sub> from the process which instead can be utilized in the process to produce additional SNG. Hydrogen can be added to replace the need for the WGS reactor where hydrogen would be produced by converting CO and H<sub>2</sub>O to CO<sub>2</sub> and H<sub>2</sub>. The water gas shift reaction will also occur in the pre-methanation reactor and therefore adding the hydrogen up-stream of the pre-methanation will have a different impact than adding down-stream, therefore to alternatives for the addition of H<sub>2</sub> was considered here and are indicated as *H<sub>2</sub> alt. 1* and *H<sub>2</sub> alt. 2* in Figure 32. Even more hydrogen can be added to the process up to a point where there is no need to extract CO<sub>2</sub> from the syngas as it instead can be utilized in the process to maximize the carbon utilization.

### 6.10.1 Modelling methodology

Four main scenarios have been simulated and are listed in Table 16. Scenarios involving electrolysis has been divided into sub scenarios based on different technologies used for the electrolysis a) PEM, and b) SOEC.

**Table 16: List of bio-electro fuel production cases simulated.**

Notation	Case description
DFB-SNG Base	Base case
DFB-SNG 1	Electricity can be used to reduce the heat demand of the gasification process by preheating the fluidization medias (air and steam, see Figure 30)
DFB-SNG 2a	Addition of H <sub>2</sub> produced with PEM to remove the need of the WGS reactor. Added downstream of the pre-methanation (H <sub>2</sub> alt. 2 in Figure 31)
DFB-SNG 2b	Addition of H <sub>2</sub> produced with SOEC to remove the need of the WGS reactor. Added downstream of the pre-methanation (H <sub>2</sub> alt. 2 in Figure 31)
DFB-SNG 3a	Addition of H <sub>2</sub> produced with PEM to remove the need of the WGS reactor. Added up-stream of the pre-methanation (H <sub>2</sub> alt. 1 in Figure 31). Recirculation of syngas is required to limit the temperature in the pre-methanation reactor.
DFB-SNG 3b	Addition of H <sub>2</sub> produced with SOEC to remove the need of the WGS reactor. Added up-stream of the pre-methanation (H <sub>2</sub> alt. 1 in Figure 31). Recirculation of syngas is required to limit the temperature in the pre-methanation reactor.
DFB-SNG 4a	Maximum carbon utilization through addition of H <sub>2</sub> produced with PEM. Added up-stream of the pre-methanation (H <sub>2</sub> alt. 1 in Figure 31). Recirculation of syngas is required to limit the temperature in the pre-methanation reactor.
DFB-SNG 4b	Maximum carbon utilization through addition of H <sub>2</sub> produced with SOEC. Added up-stream of the pre-methanation (H <sub>2</sub> alt. 1 in Figure 31). Recirculation of syngas is required to limit the temperature in the pre-methanation reactor.

The gasifier performance is estimated based on empirical data and experience from previous industrial scale DFB gasifiers. The subsequent cleaning, handling and SNG synthesis is based on the work by Alamia et al, modelling the GoBiGas demo plant (Alamia et al. 2017). Table 17 below highlights the main definitions and assumptions used in the modelling work.

**Table 17: The main assumptions used when modelling the Bio-SNG process.**

Main compressor	Outlet pressure 30 bar, 3 stage compressor. Interstage cooling down to 55 °C. Assumed isentropic efficiency: 78%
Gas cleaning	Tar removed by scrubbing with RME, tar enriched RME sent to CHP furnace for destruction. MDEA Reboiler duty : 2.24 MW/kg Acid Gas (Alamia et al. 2017). Fraction of CO <sub>2</sub> in stream co-absorbed when removing H <sub>2</sub> S: 0.1 Assumed “complete” removal of H <sub>2</sub> S in gas, probably with help of guard beds. BTX separated out using activated carbon and sent to furnace. Heat losses currently neglected.
WGS reactor - Low temperature catalyst	Gibbs minimization reactor. Inlet temp: 200 C.
Pre-methanator	Irreversible decomposition of higher hydrocarbons to syngas followed by equilibrium reactors. Inlet temp: given by WGS reactor and olefin content. Max allowed outlet temp 700 °C, regulated by recirculation if necessary. Subsequent cooling by raising HP steam
CO <sub>2</sub> removal – Activated MDEA Amine scrubber	Reboiler duty : 0.83 MW/kg Acid Gas (Alamia et al. 2017).
SNG synthesis - 4 staged adiabatic reactors with interstage cooling	Equilibrium reactors. Inlet temp 250 °C. The 2 last reactors are polishing steps, i.e. water is condensed out before to push the equilibrium to the necessary CH <sub>4</sub> concentration for pipeline specifications. Interstage cooling by HP steam raising in the first 2 reactors. LP and district heating in the polishing steps.

### 6.10.2 Mass and energy balances

Mass- and energy flows for the simulated cases are summarized in Figure 33 and Table 33 of Appendix 4. The values are marginal flows meaning that it is the increased amount of each flow required of a retrofitted DFB-gasifier compared to a reference CHP-plant with equivalent high pressure steam production.

Results shows that introducing electricity to the process has very little effect on the energy efficiency, but it increases the carbon efficiency from 0.39 in the base case to up to 0.95 in an optimized case, Figure 33. The marginal amount of biomass decrease as more electricity is added. When electricity is introduced to the process more heat is also produced that can be used for high-pressure steam production and therefore the amount biomass can be reduced while maintaining the same amount of high-pressure steam as the reference CHP-plant. In Figure 33, this reduced biomass has been considered while normalizing the flows, making the biomass input exceed 1.0.

The marginal efficiency for the electricity introduced is 55% while using a PEM and 64% when using a SOEC for the H<sub>2</sub> production. As this efficiency is constant for all the cases it stipulates that the production capacity of the plant will increase linearly with the amount of electricity added to the process via electrolysis. Using electricity to pre-heat the process streams (case DFB-SNG 1) however have a neglectable impact on the production in this type of CHP-integrated process. For a stand-alone process it has a better potential as has previously been shown (Anton Larsson, Gunnarsson, and Tengberg 2018).

Adding hydrogen from electrolysis to this type of SNG production plant will decrease the amount of CO<sub>2</sub> produced and instead increase the production of SNG as illustrated by the Sankey diagram

in Figure 33. Note that the carbon in the input flow exceeds 1 as they are normalized with the amount of carbon in the marginal increase of biomass required for the integrated SNG production compared to a reference CHP-plant with equivalent high pressure steam production. Part of the carbon in the fuel is transported to the combustion section and will end-up as diluted CO<sub>2</sub> in the flue gas while of the carbon will also end-up as an almost pure CO<sub>2</sub> stream. The fraction in the flue gas is not affected by the analyzed addition of H<sub>2</sub> and would require separation from the flue gas in order to increase the carbon utilization further.

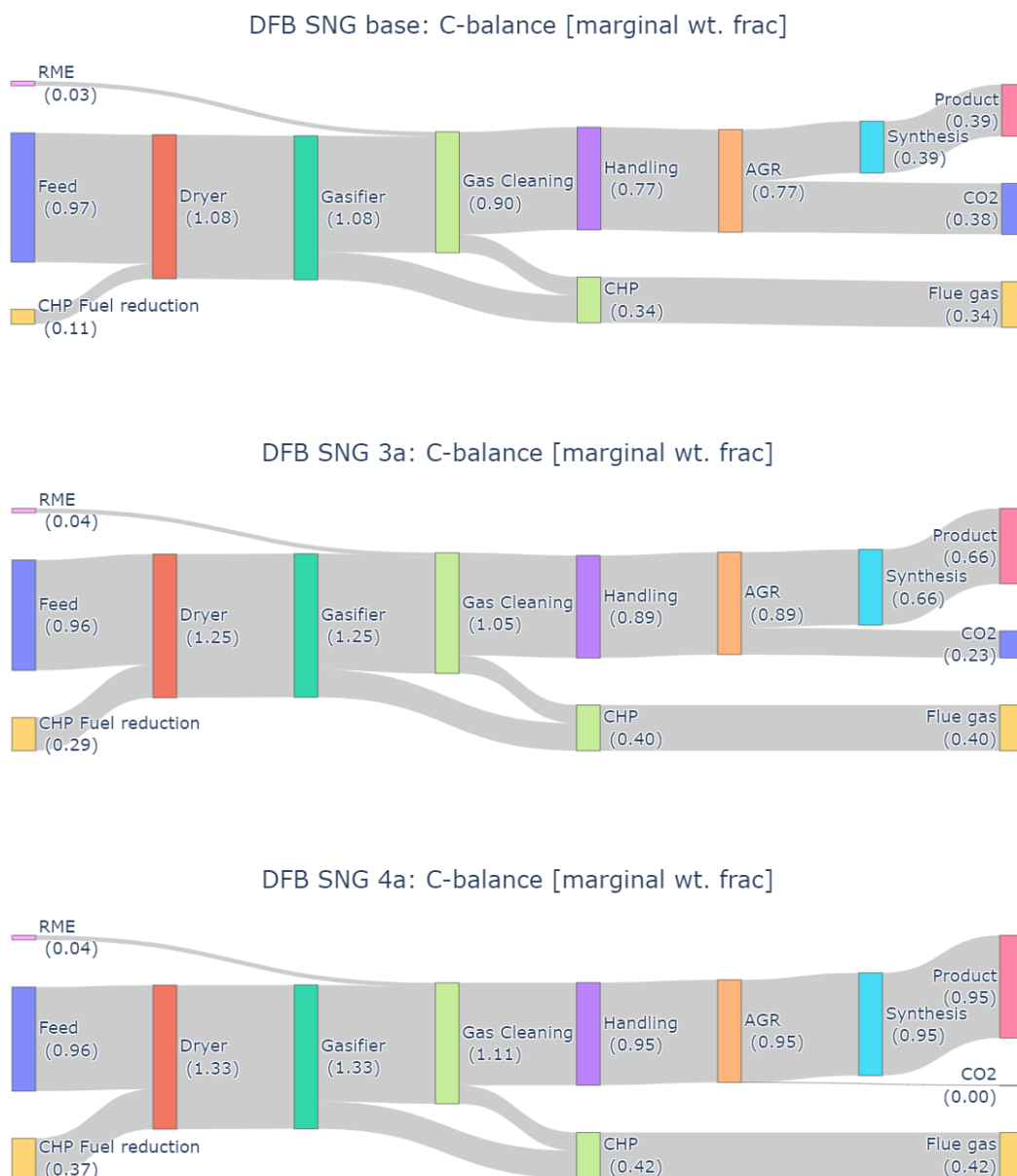


**Figure 33 Carbon Sankey diagrams – DFB-SNG Base (no electrification), DFB-SNG 3a, and DFB-SNG 4a. Note that the flows are normalized with the marginal biomass input, i.e. taking into account the reduced biomass in the connected CHP unit.**

### 6.10.3 Summary of electrification potential

Introduction of hydrogen produced through electrolysis can improve the utilization of the carbon from the biomass from 39% carbon utilization without electricity to up to 95% carbon utilization in the extreme case. The marginal efficiency of electricity to SNG depends on the type of hydrogen production and is 55% using PEM and 64% using SOEC. In a CHP integrated process PEM offers bigger savings in the amount of biomass used for steam production while SOEC offers the most efficient utilization of the electricity.

Introducing electricity is an efficient way to increase the capacity of the process without increasing the capacity of the gasifier. Results shows that the production capacity can be roughly doubled if the electrical input is maximized. The increase in production per MW of electricity added to the process is linear and its therefore just as effective to add 30 MW of electricity as adding 80 MW.

### 6.11 DFB GASIFICATION FOR FISCHER TROPSCH (FT) PRODUCTION

There is a significant difference between the production of SNG, discussed in the previous sub-chapter, and FT liquids in the sense that when producing SNG, methane in the gasifier syngas is part of the product while for FT it needs to be reformed. Figure 34 process block diagram of the DFB based FT track, and the corresponding modelling assumptions are documented in Table 19. The gas from a DFB-gasifier contains a significant concentration of CH<sub>4</sub>, typically 7-15%<sub>vol</sub>, and it would be a significant loss of efficiency not to reform and utilize the methane in the process.

A conventional technology for methane reforming is the steam methane reformer (SMR) where light hydrocarbons are heated and catalytically reformed together with steam into syngas. This process requires a high temperature which is sustained by burning some of the fresh gas to indirectly heat the process. Down-stream the SMR the composition of the syngas needs to be adjusted through WGS and AGR before it is synthesized into FT-crude and separated from the tail-gas. The FT-synthesis has a limited single pass efficiency and produce some undesired light hydrocarbons and therefore requires recirculation of the tail gas to the reformer. The FT-crude is assumed to up-graded in a final hydrotreating step onsite into drop-in biofuels.

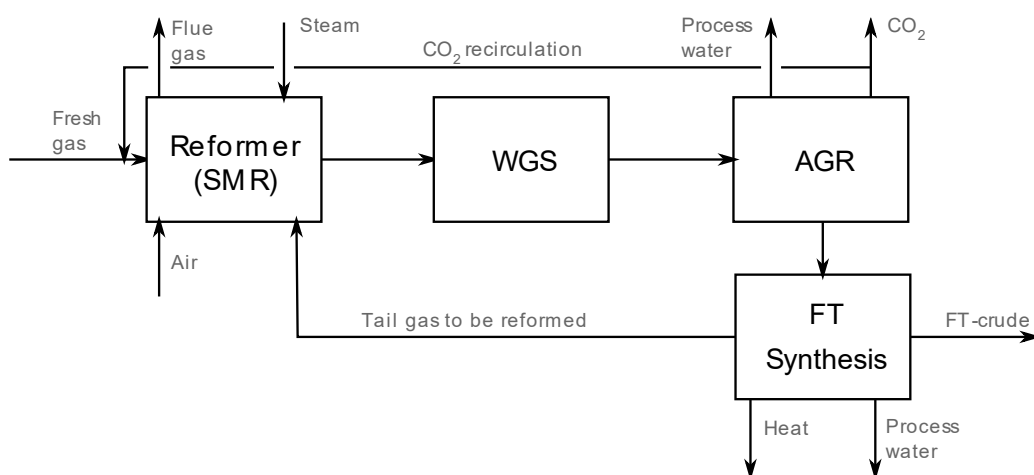


Figure 34 Simplified process for DFB Fischer Tropsch production.

Electricity can be introduced to the DFB-FT process to improve the carbon utilization and increased the marginal efficiency of biomass to FT-crude. The electricity can be added as heat or as H<sub>2</sub> produced through electrolysis. Adding electricity for heating is only considered for applications where it is not possible or impractical to cover the heat demand through process integration and heat recovery. Two such scenarios were identified, 1) additional pre-heating of the air and air used for fluidization this was simulated for the SNG case but gave an insignificant impact and are therefore excluded here, and 2) using an electrically heated SMR process (eSMR) instead of burning part of the fresh gas.

Adding H<sub>2</sub> to the process will decrease the amount of CO<sub>2</sub> from the process which instead can be utilized in the process to produce additional SNG. Hydrogen can be added to replace the need for the WGS reactor where hydrogen would be produced by converting CO and H<sub>2</sub>O to CO<sub>2</sub> and H<sub>2</sub>. The water gas shift reaction will also occur in the SMR and hydrogen is here added up-stream of the SMR. The SMR includes a pre-reformer where reactions are exothermic, and the temperature should not surpass 650 °C. Recirculation of CO<sub>2</sub> can be used to control this temperature but it can also be used to maximize the carbon yield

Three main scenarios have been simulated and are listed in Table 18. Scenarios involving electrolysis has been divided into sub scenarios based on different technologies used for the electrolysis a) PEM, and b) SOEC.

**Table 18: List of bio-electro fuel production cases simulated.**

Notation	Case description
DFB-FT Base	Base case
DFB-FT 1	eSMR
DFB-FT 2a	eSMR and addition of H <sub>2</sub> produced with PEM to remove the need of a WGS-reactor.
DFB-FT 2b	eSMR and addition of H <sub>2</sub> produced with SOEC to remove the need of a WGS-reactor.
DFB-FT 3a	eSMR and addition of H <sub>2</sub> produced with PEM to maximize the carbon utilization.
DFB-FT 3b	eSMR and addition of H <sub>2</sub> produced with SOEC to maximize the carbon utilization.

For the DFB part of the process the model is the same as for the DFB-SNG track. For the FT part the layout and methodology follow that outlined in the Energiforsk report “*Co-Generation of Bio Jet in CHP Plants*” (A. Larsson, Gustavsson, and Gustafsson 2020). The only difference in this work is that the CO<sub>2</sub> content in the reformer section is regulated by its own recirculation loop rather than by leaving the CO<sub>2</sub> in the tail gas recirculation loop. Table 5 below list the major assumptions used:

**Table 19: The main assumptions used in the DFB-FT modelling work.**

Main compressor	Outlet pressure 30 bar, 3 stage compressor. Interstage cooling down to 55 C. Assumed is-entropic efficiency: 78%
Gas cleaning	Tar removed by scrubbing with RME, tar enriched RME sent to CHP furnace for destruction. MDEA Reboiler duty : 2.24 MW/kg Acid Gas (Alamia et al. 2017). Fraction of CO <sub>2</sub> in stream co-absorbed when removing H <sub>2</sub> S: 0.1 Assumed “complete” removal of H <sub>2</sub> S in gas, probably with help of guard beds. BTX separated out using activated carbon and sent to furnace. Heat losses currently neglected.
Pre-reformer	Adiabatic. Irreversible decomposition of higher hydrocarbons to syngas followed by Gibbs minimization. Inlet temp: 380 °C. Max allowed outlet temp 650 °C, regulated by CO <sub>2</sub> recirculation as thermal ballast. Steam ratio chosen as to give 1.8 mol H <sub>2</sub> O/mol C in hydrocarbons entering the reformer
Reformer	Assumed to be heated tubes with outlet at equilibrium, T <sub>out</sub> = 950°C Reformer heating = reaction enthalpy + heating from 800 °C to 950 °C. Uses part of fresh gas as fuel if fired, electricity in case of eSMR. Hydrogen added before reformer gives rise to reverse WGS and thus increased CO <sub>2</sub> utilization. Effluent cooled by Feed-Effluent exchange and HP steam raising
WGS Reactor	Adiabatic Gibbs minimization. Inlet temp 300 °C. High temperature catalyst
CO <sub>2</sub> removal	Activated MDEA Amine scrubber. Reboiler duty : 0.83 MW/kg Acid Gas (Alamia et al. 2017). Recirculated CO <sub>2</sub> recompressed from 9 to 29 bar.
FT synthesis	“Low temperature” operation at 220 °C. Alpha value at 0.9, thought to correspond to a Co-based catalyst. Production of oxygenates assumed negligible. Internal recirculation ratio of 0.7 Partial phase separation of waxes in the reactor vessel. – flash calculation. Reactor cooled to maintain 220 °C by boiling water on the shell side.
Phase separation	3 phase flash operating at 50 °C. Stabilizer column separating out C <sub>5</sub> and lighter, to ensure the crude holds a vapor pressure suitable for transport. Stabilizer column not rigorously calculated, just a sharp cut.
Bleed flow	Set to 1% of the tail gas stream, to avoid N <sub>2</sub> accumulation.
Recirculation compressor	Recompressing the FT tail gas from 22 to 28 bar to allow recirculating it back to the reformer. Assumed isentropic efficiency: 78 %

### 6.11.1 Mass and energy balances

Mass- and energy flows for the simulated cases are summarized in Figure 35 Appendix 4 Table 34. The values are marginal flows meaning that it is the increased amount of each flow required of a retrofitted DFB-gasifier compared to a reference CHP-plant with equivalent high pressure steam production. Results shows that introducing electricity to the process has very little effect on the energy efficiency, but it increases the carbon efficiency from 0.38 in the base case to 0.81 in an optimized case.

The marginal efficiency for the electricity introduced is 53-54% when using a PEM and 59-60% when using a SOEC for the H<sub>2</sub> production. As this efficiency is almost constant for all the cases it stipulates that the production capacity of the plant will increase almost linearly with the amount of

electricity added to the process via electrolysis. In the DFB-SNG case there was an excess of high-pressure steam from the synthesis section of the plant and the choice between PEM and SOEC therefore indirectly affected the amount of biomass to the process. However, this is not the case for the FT-synthesis process, which mainly enables medium pressure steam. In current analysis the medium pressure steam is used to produce DH and therefore the choice between PEM and SOEC affects the DH production rather than the amount of biomass to the process.

Electricity was also used to heat the reforming process in case DFB-FT 1 and results shows a marginal efficiency for the electricity addition of over 70% indicating that this is a very efficient way of introducing electricity to the process.

Adding hydrogen from electrolysis to this type of FT-crude production plant will decrease the amount of CO<sub>2</sub> produced and instead increase the production of FT-crude as illustrated by the Sankey diagram in Figure 35. Note that the carbon in the input flow exceeds 1 as they are normalized with the amount of carbon in the marginal increase of biomass required for the integrated FT-crude production compared to a reference CHP-plant with equivalent high pressure steam production. The figure illustrates how part of the carbon in the fuel is transported to the combustion section and will end-up as diluted CO<sub>2</sub> in the flue gas while of the carbon will also end-up as an almost pure CO<sub>2</sub> stream. In the base case part of the gas is also burnt for heat production in the SMR and more flue gas is generated there, however this loss is avoided by using an eSMR instead. The fraction in the flue gas is not affected by the analyzed addition of H<sub>2</sub> and would require separation from the flue gas in order to increase the carbon utilization further. Figure 35 also illustrates the recirculation required for the FT-process with recirculation downstream of the AGR as well as the FT-synthesis.

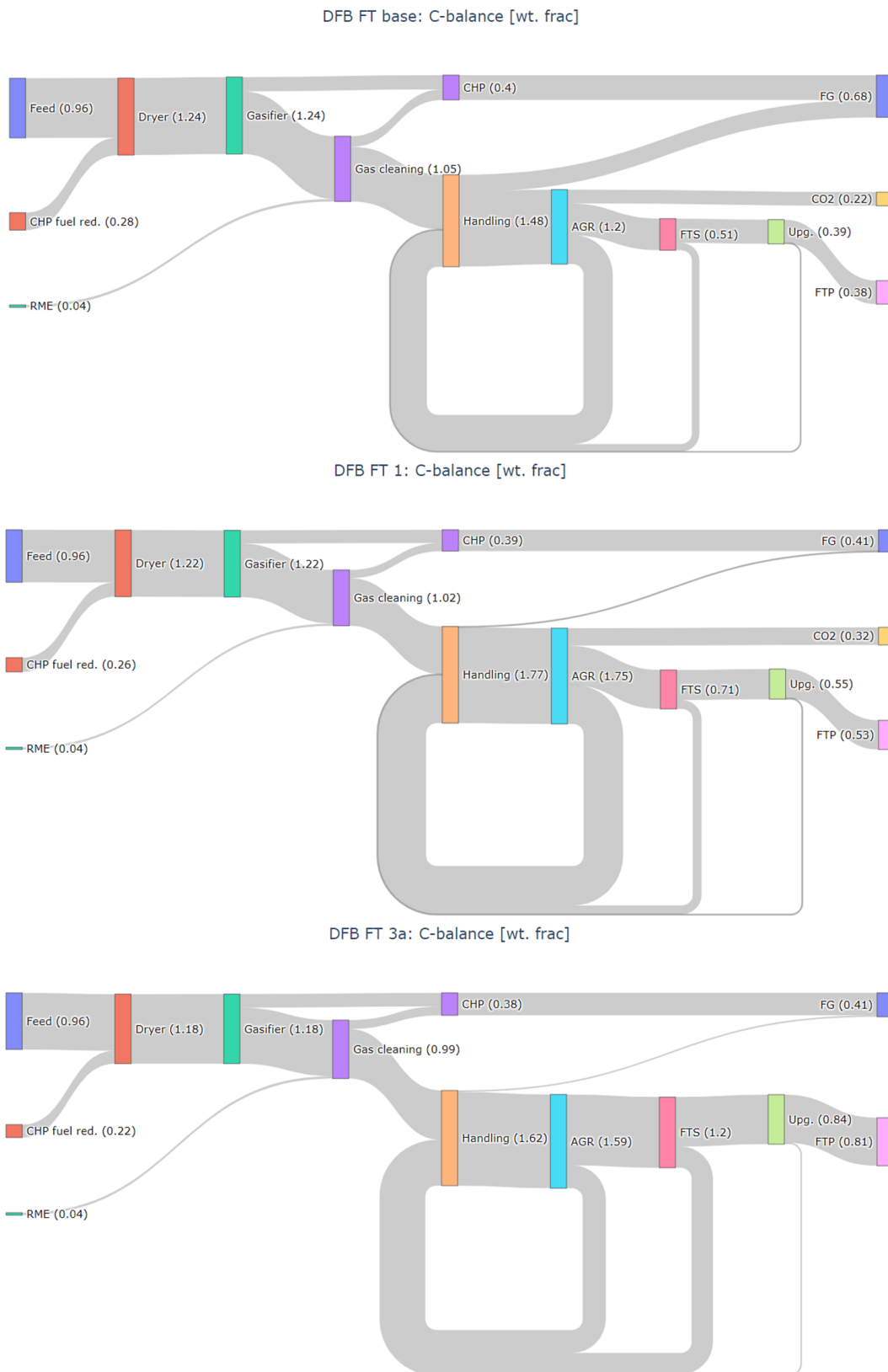


**Figure 35 Carbon Sankey diagrams – DFB-FT Base (no electrification), DFB-FT 1 (eSMR), and DFB-FT 3a (max H2 addition). Note that the flows are normalized with the marginal biomass input, i.e. taking into account the reduced biomass in the connected CHP unit.**

### 6.11.2 Summary of electrification potential

FT fuels can be produced with a marginal energy efficiency of about 50% and this is affected significantly by the amount of electricity added to the process. The carbon utilization and production capacity can however be increased significantly by adding electricity to the process. The marginal carbon utilization can be increased from 38% to up 81% and the capacity can be more than doubled.

The most efficient way of introducing electricity that was identified was to go from a classical gas fired SMR to an eSMR, which offers a marginal electricity of 72%. Combining the eSMR with addition of hydrogen via electrolysis further increase the capacity but the marginal electricity efficiency is reduced to 54-60% depending on the type of electrolysis used.

## 6.12 FLUIDIZED BED (FB) GASIFICATION

This sub-chapter describes the direct fluidized bed (FB) gasification process which is common to the two biofuel production pathways, producing methane and drop-in fuels, described in the following sub-chapters.

In a direct FB gasification system biomass is converted with steam and oxygen into a raw gas, Figure 36. The flow of oxygen is controlled to regulate the temperature of the process, since this controls the amount of oxidation. The heat needed for the gasification process is thus supplied by exothermic processes (oxidation by oxygen) in the bed, as opposed to DFB where heat is supplied indirectly through hot sand (bed material) with the heat coming from combustion in a separate reactor. Pure oxygen is required to avoid  $N_2$  in the produced gas as this would swell down-stream equipment and increase the heat demand. This gasification reactor type can be operated at elevated pressure, here assuming 25 bar, which makes for a significant reduction of the equipment size and gas compression energy. The biomass needs to be purged from air and pressurized using  $CO_2$  (from downstream AGR process), some of this  $CO_2$  will be lost to atmosphere and some will reenter the process. The raw gas needs to be cooled and cleaned from tar and other contaminants before it can be utilized as fresh gas for the synthesis.

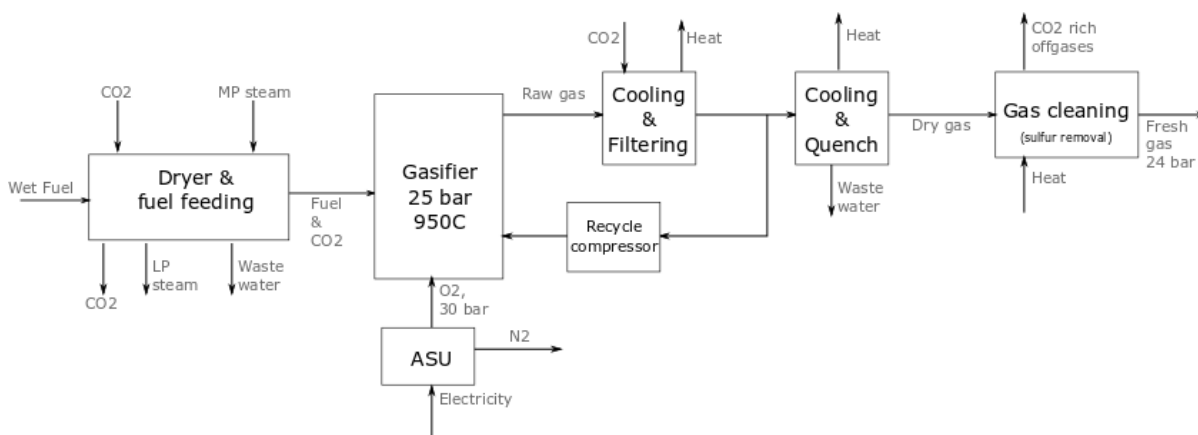


Figure 36: Direct  $O_2$ FB gasifier with primary gas cleaning.

Major contaminants such as particles, tar and steam are removed from the gas by cooling and water quenching. The bulk of H<sub>2</sub>S can be removed together with some of the CO<sub>2</sub> through amine scrubbing before final polishing using guard beds to produce a sulfur free fresh gas for the synthesis process.

### 6.13 FB GASIFICATION FOR SNG PRODUCTION

The SNG process was previously described in Section 6.10. Electricity can be introduced to the O<sub>2</sub>FB-SNG process to improve the carbon utilization and increased the marginal efficiency of biomass to SNG. The electricity can be introduced as H<sub>2</sub> produced through electrolysis. No scenario has been identified where using electricity to heat a process or process stream would have a significant impact on the process performance. Adding H<sub>2</sub> to the process will decrease the amount of CO<sub>2</sub> from the process which instead can be utilized in the process to produce additional SNG. Hydrogen can be added to replace the need for the WGS reactor where hydrogen would be produced by converting CO and H<sub>2</sub>O to CO<sub>2</sub> and H<sub>2</sub>. The water gas shift reaction will also occur in the pre-methanation reactor and therefore, adding the hydrogen up-stream of the pre-methanation will have a different impact than adding down-stream, therefore two alternatives for the addition of H<sub>2</sub> was considered here and are indicated as H<sub>2</sub> alt. 1 and H<sub>2</sub> alt. 2 in Figure 32 (As for the DFB SNG case). Three main scenarios have been simulated and are listed in Table 20. Scenarios involving electrolysis has been divided into sub scenarios based on different technologies used for the electrolysis a) PEM, and b) SOEC.

The performance and scale of the O<sub>2</sub>FB gasifier is based on the process design laid out in the BioMeet project by EcoTraffic R&D AB and Nykomb Synergistics AB (Brandberg et al. 2000). The unit operations used starting at the wet fuel feed all the way up to “Dry Gas” in Figure 6 mirror those of the BioMeet project. However, one deviation is using CO<sub>2</sub> for purging instead of N<sub>2</sub> due to a desire to limit the amount of N<sub>2</sub> going to the downstream process. Furthermore, in the cases where electrolysis is used, the oxygen demand of the gasifier is partially or fully covered by that produced in the electrolyzer thus reducing the load or eliminating the ASU. Apart from the above, the methodology for gas conditioning and synthesis is the same as described in the DFB SNG case, with the restriction of having to secure enough CO<sub>2</sub> to pressurize the fuel feeding.

**Table 20: Summary of simulation cases for the O<sub>2</sub>FB-SNG process.**

Notation	Case description
O <sub>2</sub> FB-SNG Base	Base case
O <sub>2</sub> FB -SNG 1a	Addition of H <sub>2</sub> produced with PEM to remove the need of the WGS reactor. Added down-stream of the pre-methanation (H <sub>2</sub> alt. 2 in Figure 31).
O <sub>2</sub> FB -SNG 1b	Addition of H <sub>2</sub> produced with SOEC to remove the need of the WGS reactor. Added down-stream of the pre-methanation (H <sub>2</sub> alt. 2 in Figure 31)
O <sub>2</sub> FB -SNG 2a	Addition of H <sub>2</sub> produced with PEM to remove the need of the WGS reactor. Added up-stream of the pre-methanation (H <sub>2</sub> alt. 1 in Figure 31). Recirculation of syngas is required to limit the temperature in the pre-methanation reactor.
O <sub>2</sub> FB -SNG 2b	Addition of H <sub>2</sub> produced with SOEC to remove the need of the WGS reactor. Added up-stream of the pre-methanation (H <sub>2</sub> alt. 1 in Figure 31). Recirculation of syngas is required to limit the temperature in the pre-methanation reactor.
O <sub>2</sub> FB -SNG 3a	Addition of H <sub>2</sub> produced with PEM to maximize the carbon utilization. Added up-stream of the pre-methanation (H <sub>2</sub> alt. 1 in Figure 31). Recirculation of syngas is required to limit the temperature in the pre-methanation reactor.
O <sub>2</sub> FB -SNG 3b	Addition of H <sub>2</sub> produced with SOEC to maximize the carbon utilization. Added up-stream of the pre-methanation (H <sub>2</sub> alt. 1 in Figure 31). Recirculation of syngas is required to limit the temperature in the pre-methanation reactor.

### 6.13.1 Mass and energy balances

Mass- and energy flows for the simulated cases are summarized in Figure 37 and Appendix 4 Table 16. Results shows that introducing electricity to the process has very little effect on the energy efficiency, but it increases the carbon efficiency from 0.33 in the base case to up to 0.75 in an optimized case,. The marginal efficiency for the electricity introduced is about 55% while using a PEM and about 65% when using a SOEC for the H<sub>2</sub> production. As this efficiency is constant for all the cases it stipulates that the production capacity of the plant will increase linearly with the amount of electricity added to the process via electrolysis. Using PEM requires more electricity but also increase the production of district heating.

Adding hydrogen from electrolysis to this type of SNG production plant will decrease the amount of CO<sub>2</sub> produced and instead increase the production of SNG as illustrated by the Sankey diagram in Figure 37. Part of the carbon in the fuel will end-up as almost pure CO<sub>2</sub> stream. Some of the CO<sub>2</sub> is recirculated to the fuel feeding where some will reenter the process, and some will be vented.

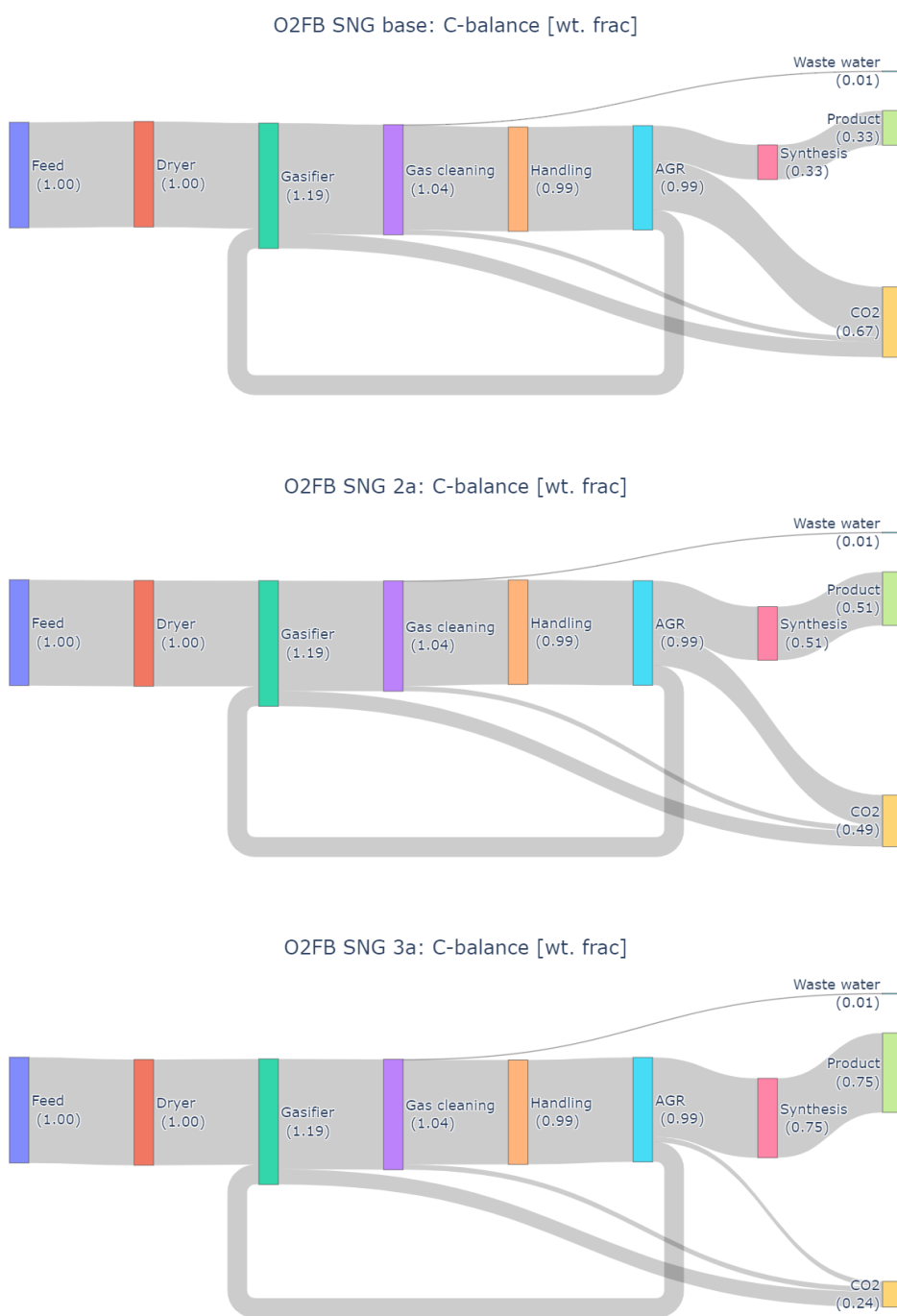


**Figure 37: Carbon Sankey diagrams – O<sub>2</sub>FB-SNG Base (no electrification), O<sub>2</sub>FB-SNG 2a, and O<sub>2</sub>FB-SNG 3a.**

### 6.13.2 Summary of electrification potential

SNG can be produced via an oxygen blown fluidized bed gasifier (O<sub>2</sub>FB-gasifier) with an energy efficiency of 56-62%. Electrification of the process has little impact on the energy efficiency, but it

can increase the carbon utilization from about 33% to up to 80%. The production capacity can be more than doubled through the electrification.

## 6.14 FB GASIFICATION FOR FISCHER TROPSCH (FT) PRODUCTION

The O<sub>2</sub>FB gasification process is described in section 6.13 and the FT-synthesis is described in section 6.11.

Electricity can be introduced to the O<sub>2</sub>FB-FT process to improve the carbon utilization and increased the marginal efficiency of biomass to FT-crude. The electricity can be added as heat or as H<sub>2</sub> produced through electrolysis. Adding electricity for heating is only considered for applications where it is not possible or impractical to cover the heat demand through process integration and heat recovery. One such scenario was identified using an electrically heated SMR process (eSMR) instead of burning part of the fresh gas.

Adding H<sub>2</sub> to the process will decrease the amount of CO<sub>2</sub> from the process which instead can be utilized in the process to produce additional SNG. Hydrogen can be added to replace the need for the WGS reactor where hydrogen would be produced by converting CO and H<sub>2</sub>O to CO<sub>2</sub> and H<sub>2</sub>. The water gas shift reaction will also occur in the SMR and therefore the hydrogen should be added up-stream of the SMR. When adding hydrogen to remove the need for a WGS-reactor, results were very similar to results where the carbon utilization was maximized. Therefore, only the scenario with a maximum carbon utilization is investigated for this technology.

### 6.14.1 Modelling methodology

Two main scenarios have been simulated and are listed in Table 21. The Scenario involving electrolysis has been divided into sub scenarios based on different technologies used for the electrolysis a) PEM, and b) SOEC.

**Table 21: Summary of simulation cases for the O<sub>2</sub>FB-FT-crude process.**

Notation	Case description
O <sub>2</sub> FB-FT Base	Base case.
O <sub>2</sub> FB -FT 1	Using eSMR for reforming of light hydrocarbons.
O <sub>2</sub> FB -FT 2a	eSMR and addition of H <sub>2</sub> produced with PEM to maximize the carbon utilization.
O <sub>2</sub> FB -FT 2b	eSMR and addition of H <sub>2</sub> produced with SOEC to maximize the carbon utilization.

The methodology for modelling the O<sub>2</sub>FB part of the process is described in section 6.12. For the gas handling and FT synthesis parts of the process the methodology is the same as described in section 6.11 for DFB-FT with the added requirement to recover enough CO<sub>2</sub> to satisfy the needs of the O<sub>2</sub>FB fuel feeding. The latter requirement is the reason why there is only 1 level of hydrogen addition.

### 6.14.2 Mass and energy balances

Results shows that introducing electricity to the process has very little effect on the energy efficiency, but it increases the carbon efficiency from 0.28 in the base case to up to 0.8 in an optimized

case, Figure 38. The marginal efficiency for the electricity introduced is about 55% while using a PEM and about 65% when using a SOEC for the H<sub>2</sub> production. As this efficiency is constant for all the cases it stipulates that the production capacity of the plant will increase linearly with the amount of electricity added to the process via electrolysis. Using PEM requires more electricity but also increase the production of district heating.

The carbon flows are illustrated in Sankey diagrams in Figure 38. This illustrates the recirculation flows of both CO<sub>2</sub> and tail gas. In the base case some of the carbon is lost as flue gas while this stream is removed by introducing the eSMR. Some of the carbon will also be lost with the wastewater in the form of tar and BTX and will require wastewater treatment.

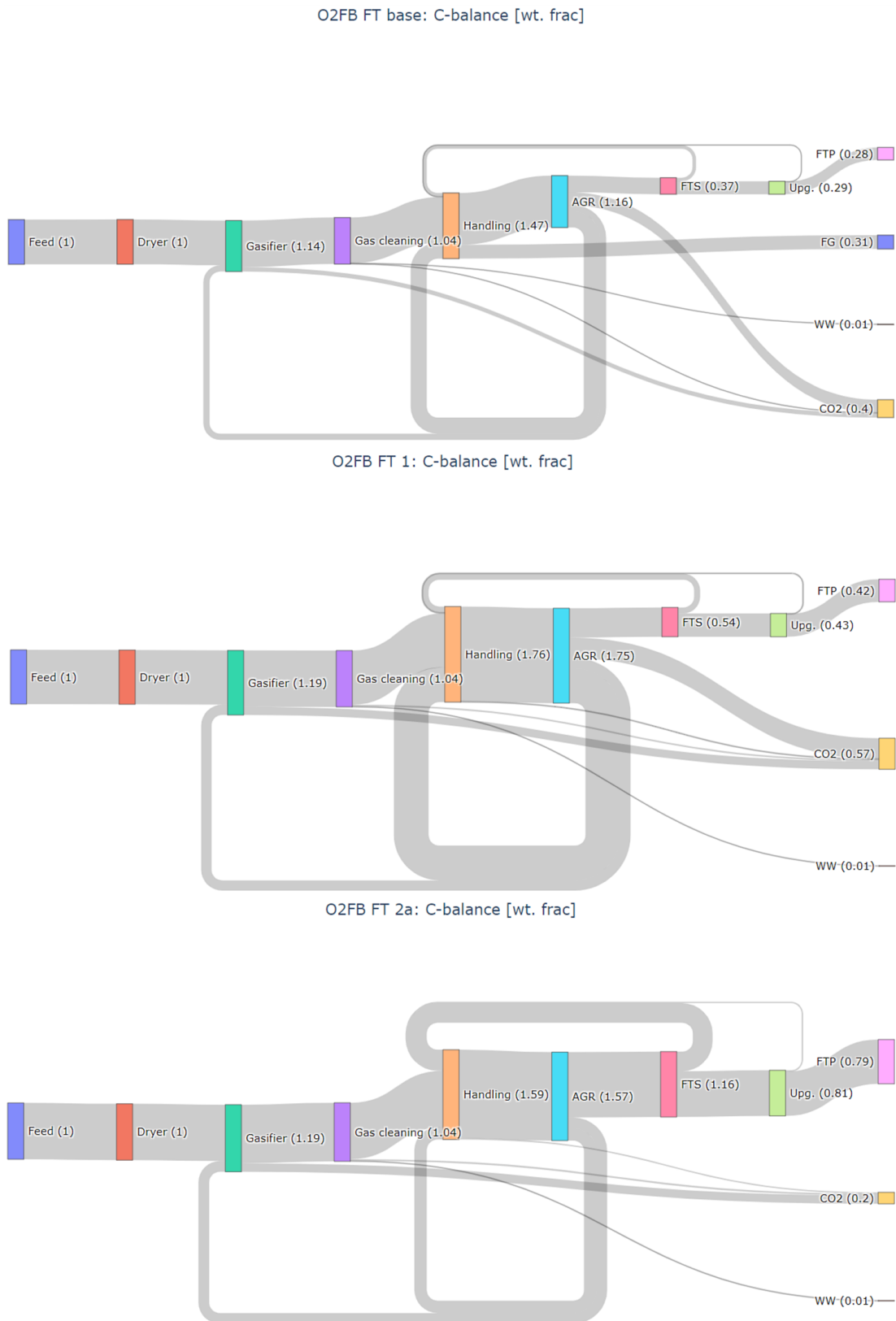


**Figure 38: Carbon Sankey diagrams – O2FB-FT Base (no electrification), O2FB -FT 1 (eSMR), and O2FB -FT 2a (max CO2 utilization).**

### 6.14.3 Summary of electrification potential

FT fuels can be produced via an oxygen blown fluidized bed gasifier (O<sub>2</sub>FB-gasifier) with an energy efficiency of 35-47%. Electrification of the process can increase the energy efficiency, as well as the carbon utilization from about 28% to up to 80%. Introducing electricity can most efficiently be done through an eSMR with a marginal electrical efficiency of 0.71. This also increase the production capacity with about 50%. The capacity can be further increased by introducing hydrogen through electrolysis to almost 3 times the base production.

## 6.15 REFERENCE ELECTROFUEL TRACKS

Electrofuel tracks, pathways that convert electricity and CO<sub>2</sub> into fuels, are evaluated for comparison to the bio-electrofuel concepts. A total of 3 electrofuel tracks aiming at production of FT fuels, methanol, and synthetic natural gas (SNG) are considered. In the first step, syngas suitable for the synthesis of advanced biofuel is produced from electrolysis-based hydrogen (PEM) and biogenic CO<sub>2</sub> in a reverse water-gas-shift (rWGS) process operated at 750°C and 30 bar. The equilibrium of the rWGS is controlled to favour syngas composition that satisfy conditions for optimal synthesis of desired biofuel downstream.

The CO<sub>2</sub> feed is assumed to be captured from biogenic sources such as biomass-based CHP plants, pulp and paper mill, biogas, bioethanol plants. Amine process, as one of the most mature techniques for carbon capture from flue gas or other CO<sub>2</sub> containing streams, is considered for CO<sub>2</sub> capture<sup>5</sup>. The amine scrubbing technique involves a stripping column to regenerate solvent in which the CO<sub>2</sub>-rich solution flows downwards against a counter-current flow of vapor generated in the reboiler (Liang et al. 2015). The energy demand of the reboiler makes amine scrubbing technique energy intensive. A typical MEA-based system in industrial configuration is expected to have energy consumption 3.2–4.2 MJ per kg-CO<sub>2</sub> separated, depending on the CO<sub>2</sub> concentration in feed, CO<sub>2</sub> removal rate (85%–90%), and system operating conditions (Xie et al. 2017). Energy consumption 1MWh/tCO<sub>2</sub> (90% in form of heat and 10% in form of electricity to drive the system, excluding compression electricity) is used for the cases evaluated in this work. The heat demand of the reboiler can be satisfied by LPS (3-5 bar or 133°C -150°C) with a return temperature well above 100°C (Xie et al. 2017).

The production capacities of the electrofuel cases are selected to match available biogenic CO<sub>2</sub> sources in Sweden at scales 300 kt/y or higher (“Stora Källor För Biogen CO<sub>2</sub> Lista” 2019). 300 kt/y CO<sub>2</sub> correspond to biofuel production capacities for FT fuels (144 MW HHV), methanol (144 MW HHV) and SNG (201 MW HHV) assuming 90% annual plant availability. The mass and energy balances of the electrofuel tracks are taken from Brynolf et al. (Brynolf et al. 2018) for 2030 base case scenario, see Table 22.

<sup>5</sup> The hot potassium carbonate (HPC) technology, which is for example considered by Stockholm Exergi for a commercial bio-CCS installation, is also a mature technology, which uses more electricity and less heat. When combined with electrofuel production that gives excess heat, the amine process is judged more efficient.

Useful excess heat generated during synthesis is utilized to supply part of the energy demand of the amine process. Any heat deficit for the CO<sub>2</sub> removal process is assumed to be supplied from an integrated MVR heat pump that run with a COP 3. The MVR lifts temperature of water vapor generated by flashing reboiler condensate and by utilizing heat recovered from low-temperature streams available onsite, 85°C -100°C.

**Table 22 Electrofuel tracks – inputs and outputs.**

Electrofuel track		e-FT liquids	e-methanol	e-SNG
Input	Unit			
H <sub>2</sub>	MWh <sub>LHV</sub>	1.37	1.25	1.30
CO <sub>2</sub>	ton	0.28	0.32	0.21
Output				
Fuel	MWh <sub>LHV</sub>	1.00	1.00	1.00
Heat (useful)	MWh <sub>th</sub>	0.20	0.10	0.20

## 6.16 SUMMARY AND CONCLUSIONS

This sub-chapter aggregates and summarizes the results from all individual biofuel production tracks presented above in this chapter. The efficiency metrics, which are uses as KPIs for process performance are defined in 2.3.

Figure 39 (left) shows the fuel carbon efficiency, i.e. the fraction of biogenic feedstock carbon atoms that end up in the main biofuel product, for all studied tracks and electrification options. The carbon efficiency is shown as a function of the fraction of electric energy input to the process, which can be seen as a measure of the degree of integrated electrification. The base case process options have electricity inputs between -10% and 10% (negative numbers means electricity production) and carbon efficiencies between 20% and 50%.

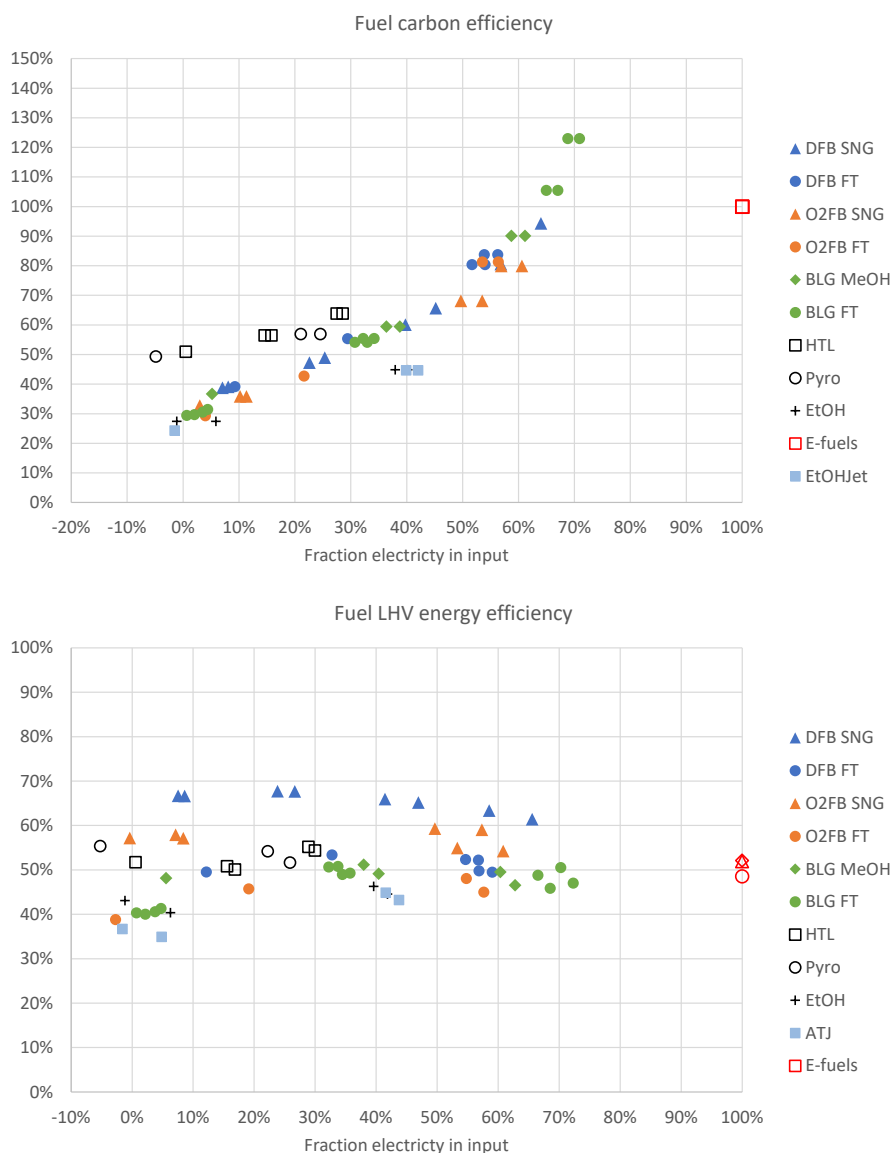


**Figure 39. Fuel carbon efficiency (top) and fuel energy efficiency (bottom) for all studied tracks and electrification options. The different e-fuel products differentiated by symbols in the right plot.**

It is evident that indirect electrification can be used to increase the biomass resource efficiency dramatically compared to the biofuel production pathways in their base configuration. There is a clear increase in fuel carbon efficiency with electrification for all production pathways. It is also striking how well all tracks of the same technology category (gasification or liquefaction or ethanol) align although these have been modelled independently with varying degrees of integration to other processes.

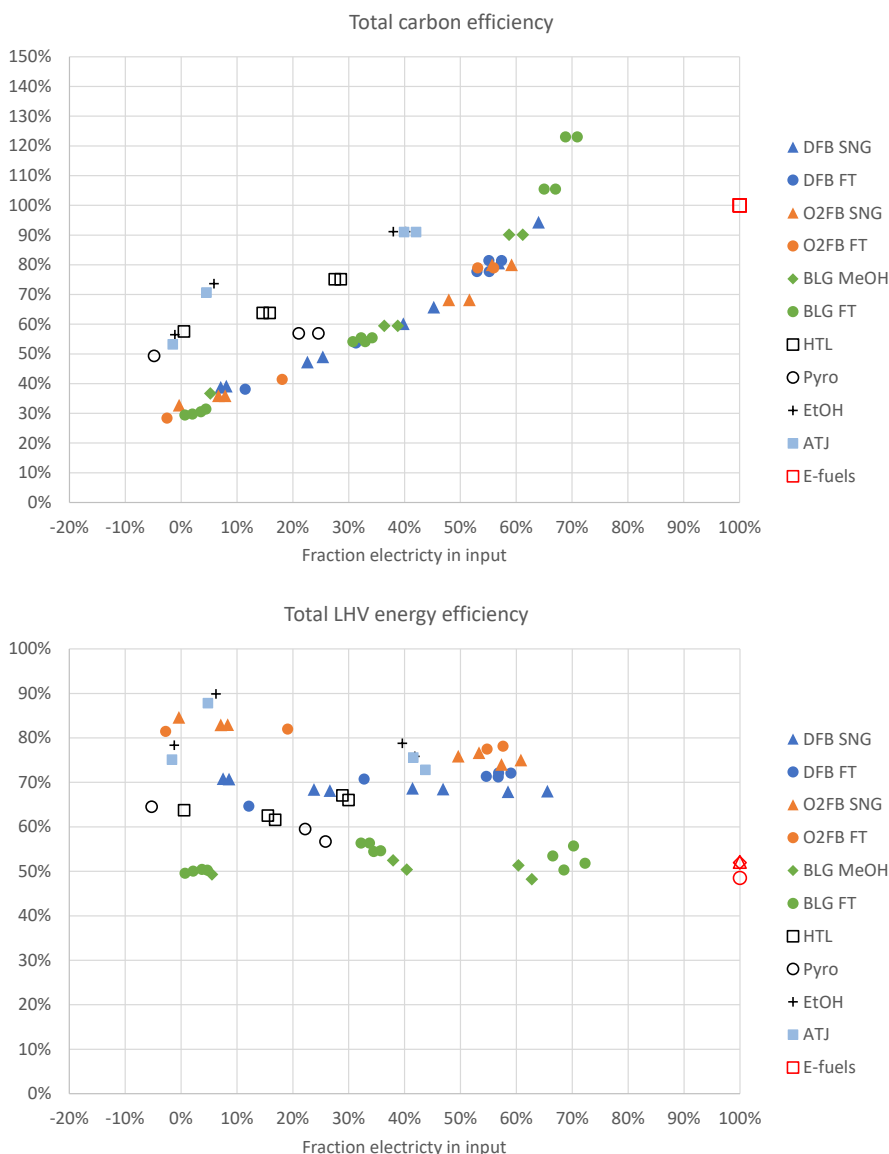
The most electrified cases with the highest potential carbon efficiencies are based on gasification. These have electricity inputs that are around 2/3 of total input, which means that there is around twice as much electric energy used as biomass energy, truly motivating the nomenclature “bio-electrofuels”. The main electrification technology used in these cases is addition of electrolysis-based

hydrogen to the syngas but also electric heating can contribute. Production based on other technologies than gasification can be electrified to a lower extent and show a little bit lower increase in efficiency.

It can be noted that carbon efficiency exceeds 100% for the BLG FT track with extensive electrification. The reason, discussed more in detail in 6.6-6.8 above, is the heat integration with the pulp mill. The large amount of excess heat exported to the pulp mill from the biofuels plant decreases mill fuel demand, which is accounted for.

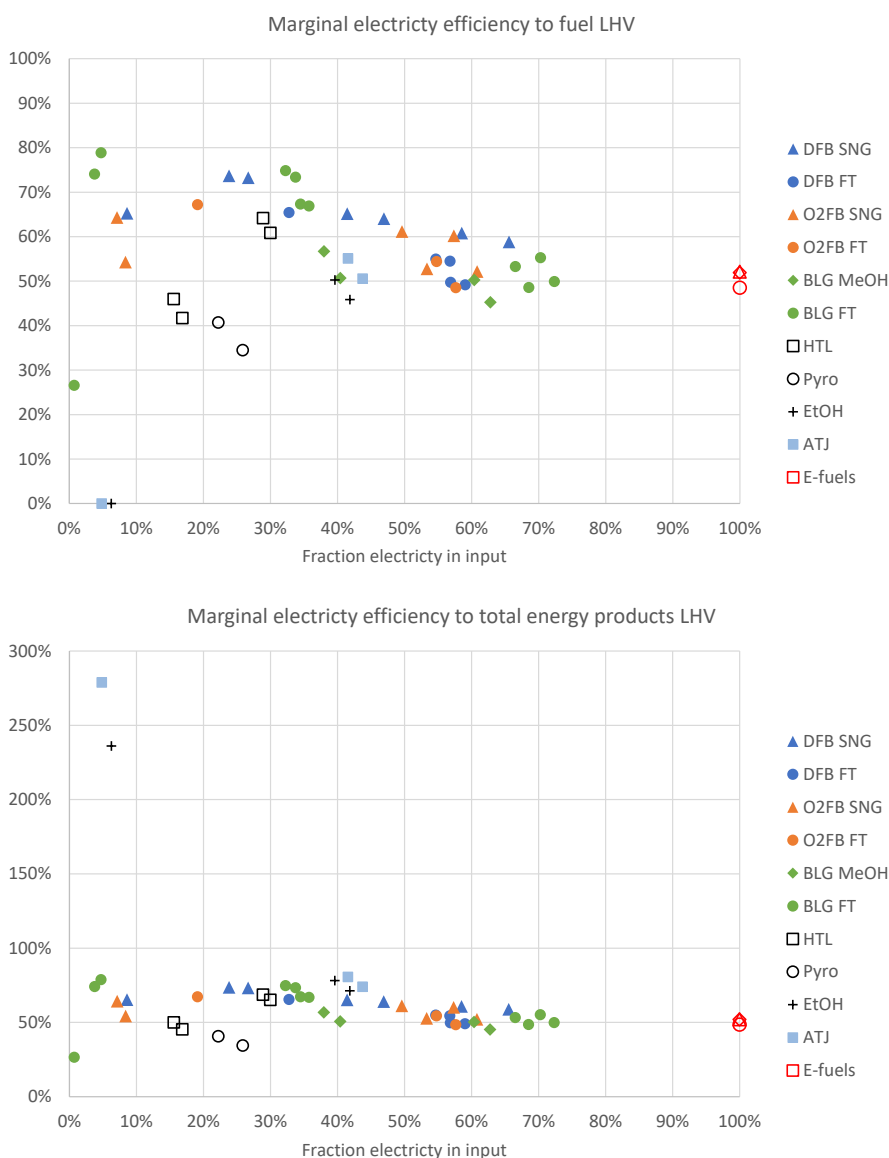
The electrification does not have a major generic systematic impact on the fuel production energy efficiency as is shown in Figure 39 (right). This means that the conversion of added electricity to biofuel product is not less efficient (on energy terms) than the original process from biomass to biofuel. There are certain processes that even show an increased energy efficiency, for example ethanol production and black liquor gasification. The efficiency from electricity to e-fuels is also similar.

Figure 40 show *total* carbon and energy efficiencies, i.e. also including *energy by-products* (such as lignin pellets from ethanol production) and heat. The trends are similar to the fuel-based efficiencies in Figure 39 but the improvement in efficiency with electrification for most non-gasification-based tracks is now larger, since by-products are more important for these. Concerning total energy efficiency, the differences between the production pathways are larger than for fuel energy efficiency but the effect of electrification is even smaller on the individual tracks.



**Figure 40. Total carbon efficiency (top) and total energy efficiency (bottom) for all studied tracks and electrification options. E-fuel products indicated by symbol for right plot.**

The discussion above, including Figure 39 and Figure 40, show clearly how carbon efficiency increases with indirect electrification and that overall energy efficiency was, on a general level, similar for varying degrees of electrification. But it can still be of interest to investigate the marginal efficiency for electricity addition for each of the electrified cases. Figure 41 shows the results from such a calculation, which provides more detail than the general energy efficiencies since each electrification option is in this case compared to the base case of the same technology track.



**Figure 41. Marginal electricity efficiency to fuel product(s) (top) and total energy products (bottom). Both base cases (non-electrified options) are not shown since these constitute the baseline to which the marginal efficiency of added electricity is measured.**

For the gasification-based tracks, Figure 41 (left) shows a relatively consistent trend of decreasing marginal electricity efficiencies with increasing electricity addition. For high degrees of electrification, >50% electricity input, the marginal efficiency approaches the 50% efficiency for the e-fuel tracks. For lower degrees of electrification (5-35% electric energy input), the marginal efficiency can be >70%. Specifically, for the gasification-based tracks it is most energy-efficient to use electric energy in an electrolyzer to eliminate the WGS process rather than implementing an rWGS (see for example 6.7 and 6.10 for details). However, the latter option (rWGS) offers much higher carbon-efficiency, which can motivate this option anyhow. It is also clear that using an electric heated SMR is very energy-efficient, as indicated by 75-80% marginal efficiency for BLG-FT.

For the non-gasification tracks, adding electrolysis hydrogen to the HTL process stands out as the most energy-efficient option, while marginal efficiencies are in general somewhat lower for pyrolysis and ethanol-based tracks.

When the marginal efficiency from electricity to total energy outputs is reviewed (Figure 41, right), it is striking that two cases related to ethanol production have marginal efficiencies >200%. The explanation is that these cases use a high-efficiency heat pump to make lignin pellets (an energy by-product) available instead of being used internally for heat production. Also, the more electrified options for ethanol production have higher marginal electric efficiency to total energy products than to fuel products, due to lignin pellet export.

Exergy efficiency to fuel and total products is shown in Figure 42. As expected, the exergy efficiency decreases with increased electrification, but the relevance of this performance parameter can be questioned in the emerging paradigm with increased low-cost renewable electricity production.

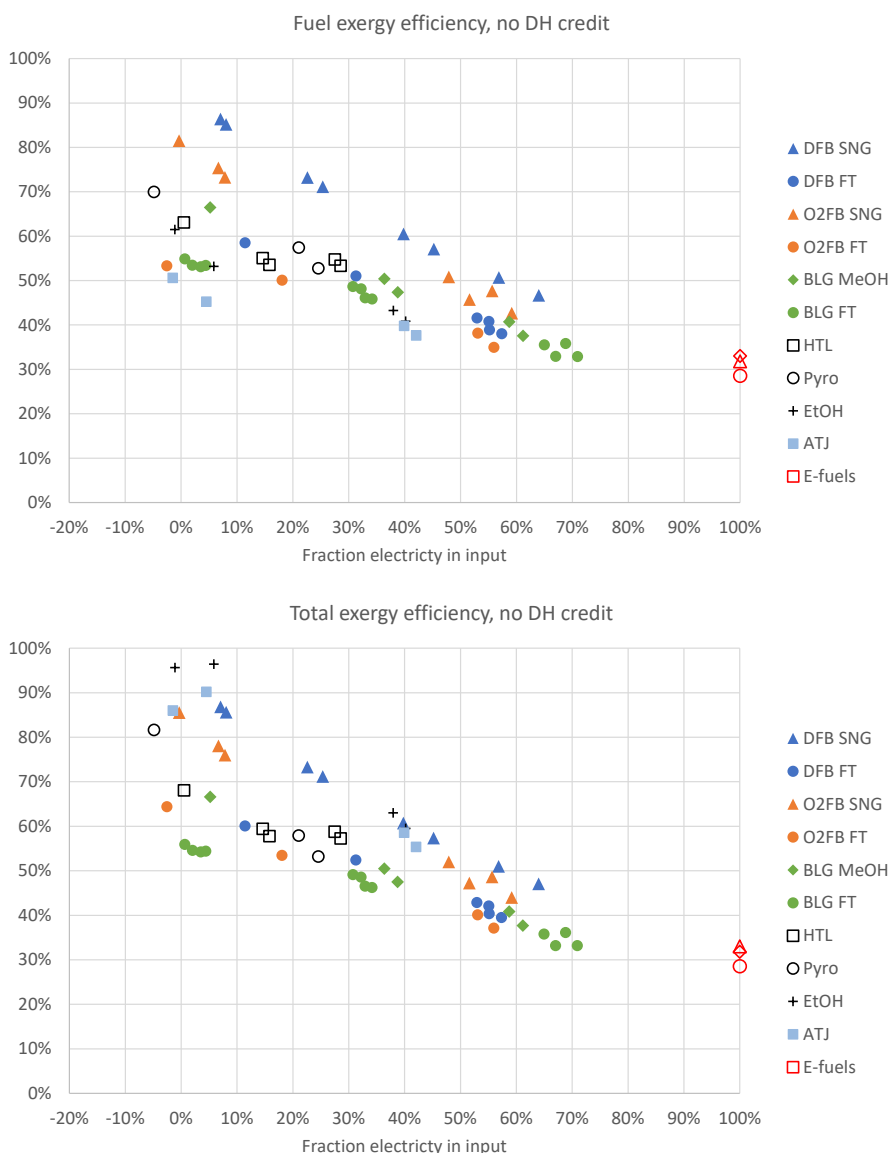


**Figure 42 Fuel (left) and total exergy efficiency (right) for all studied tracks and electrification options.**

### 6.17 EXCESS HEAT IN DITRICT HEATING NETWORKS

In order to illustrate the importance that low grade excess heat from biofuel production can have in a future bioeconomy, a separate analysis was carried out in which it was assumed that excess heat on district heating temperature level could replace district heat produced in today’s bio-based heat and/or CHP plants. In this analysis, the biomass used to produce the original district heat, which is no longer produced by combustion, is credited as a decreased feedstock demand.

The result is shown in Figure 43, left part. The right part of Figure 43 shows carbon efficiency without consideration of district heating (same as Figure 40 but re-scaled to facilitate comparison). The gasification-based drop in biofuel production tracks DFB FT (see 6.11) and O2FB FT (see 6.14) with the greatest electrification show a remarkable 120%-300% carbon efficiency using this

methodology. The BL gasification-based FT pathway shows >120% carbon efficiency when accounting for reduced district heat fuel demand.

The most important reasons that the gasification-based drop in (Fischer Tropsch) fuel tracks stand out in this analysis are: 1) the highly increased carbon efficiency obtained by hydrogen addition, since the carbon losses become very small with hydrogen addition for these tracks, and 2) the relatively large amount of heat released by these processes, caused both by the high-temperature gasification and the FT process. The results shown in Figure 46 (left) can be viewed as a “limiting case”, since it is not realistic that it would be feasible to use all excess heat to replace biomass combustion-based heating. It can, however, be seen as a strong argument to design and locate biofuel production plants to facilitate waste heat recovery and use in a biomass resource-constrained future society.

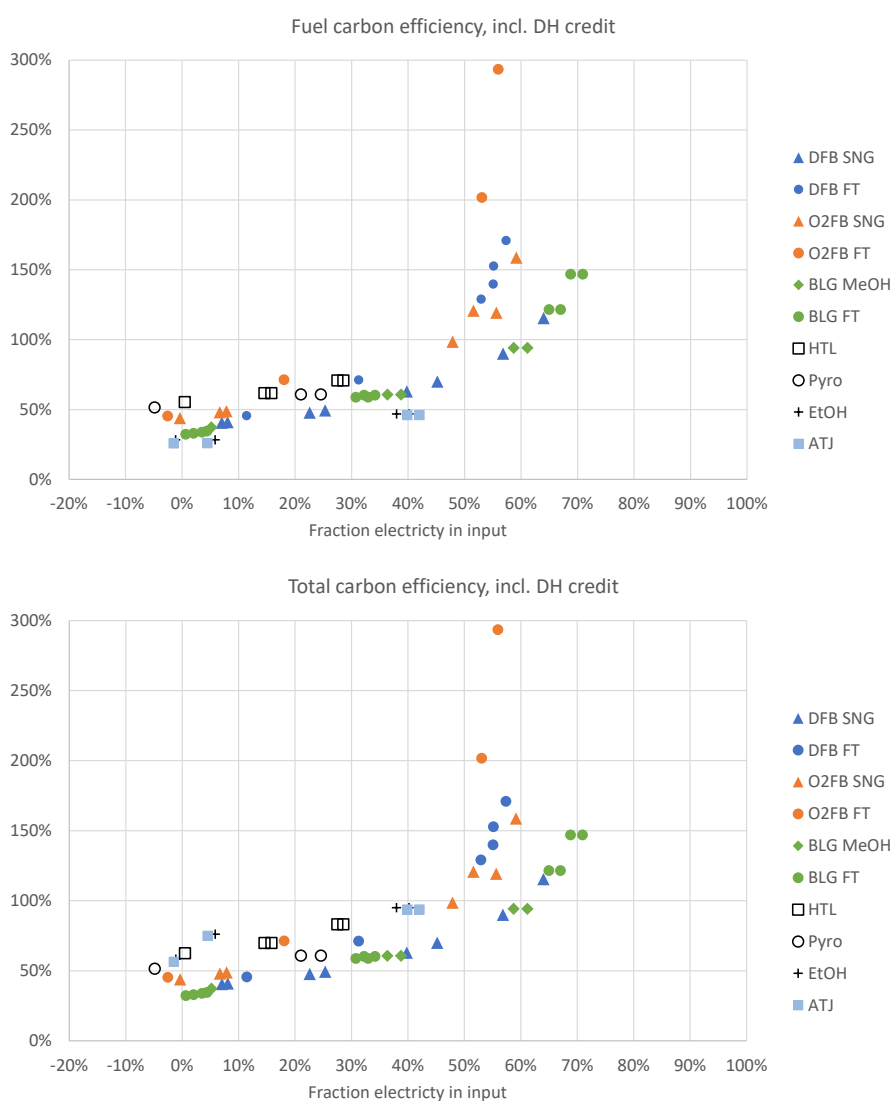


**Figure 43. Total carbon efficiency, i.e. including energy by-products, with (top) and without (bottom) system expansion to account for potential reduced bio-based combustion district heat production.**

## 7 ECONOMIC PERFORMANCE

This chapter contains the results of the techno-economic analysis applied to estimate production costs for biofuels and bio-electro fuels according to the methodology described in 2.4.

### 7.1 INVESTMENT COST ESTIMATES

Figure 44 and Figure 45 show the total capital expenditure (CAPEX) and specific investment of the technology tracks studied, respectively. In Figure 44, every box and whiskers plot correspond to CAPEX data set of the different configurations for a given technology track. Figure 45 shows the corresponding specific investment data set, in €/kW-biofuel product. The numbers behind these figures are documented in Appendix 3. CAPEX and Specific Investment.

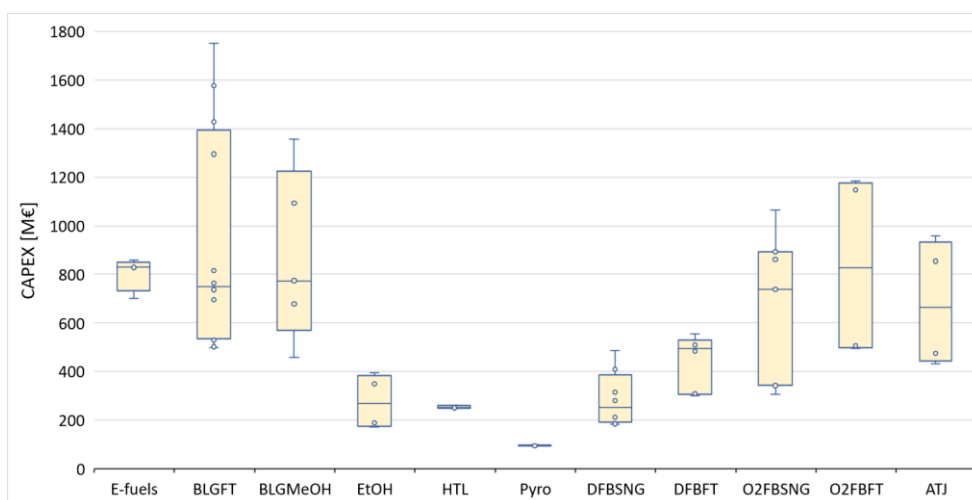


**Figure 44** Total CAPEX for all biofuel production tracks, including all configurations (base and electrified to varying extents).

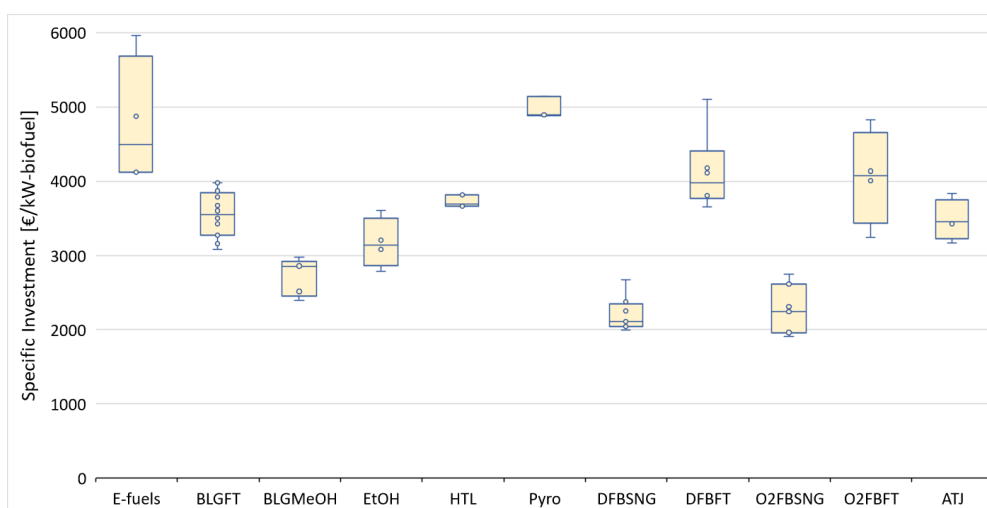


**Figure 45** Specific investment for all biofuel production tracks, including all configurations (base and electrified to varying extents).

The total CAPEX for each technology, ranging from 95 M€ for fast pyrolysis to as high as 1750 M€ for the BLGFT rWGS SOEC configuration, is influenced by the capital intensity of the technology and the assumed scale, see Figure 44. Generally, for bio-electrofuel tracks the CAPEX increases with increasing electrification, i.e., the lowest-ends of the whiskers correspond to basecase and the highest-ends to the most electrified configurations involving SOEC electrolyser. This is caused by the increasing production capacity with increasing electrification, since all configurations for each track use the same amount of biomass feedstock. The CAPEX span is in general a good indicator for electrification potential of the tracks, i.e., the wider the CAPEX span the higher the electrification potential thus the wider the room for improving carbon conversion efficiency to biofuel products. The basecase CAPEX of the BLGFT configuration is about 500 M€, which progressively increased to a maximum of about 1750 M€ with electrification.

A more relevant indicator of capital intensity is perhaps specific investment, which considers both the CAPEX and production capacity of the plant. The ranking of the configurations within a technology track do not necessarily follow the same order as that of the CAPEX. For example, the basecase configuration of the BLGFT track has the highest specific investment, about 4000 €/kW-biofuel, whereas the most electrified case BLGFT rWGS PEM configuration resulted in the lowest, 3100 €/kW-biofuel, see Figure 45. For some technology tracks, the situation is the opposite with increasing specific investment with increasing electrification.

Most of the bio-electrofuel tracks have narrower margins for specific investment than for CAPEX, exceptions are the direct liquefaction cases which had a limited electrification potential to begin with. The trend indicates that the CAPEX added due to electrification is compensated by increased productivity, i.e., better carbon conversion to biofuel products.

Specific investment covers only capital intensity aspect of economic performance of the technology tracks, hence additional indicator that brings in operating costs into the equation is necessary. In the next section, production cost of biofuels is estimated, compared, and discussed.

## 7.2 PRODUCTION COST ESTIMATES

Figure 46 shows the production cost (PC) of biofuels for all technology tracks evaluated under electricity market prices of 30 €/MWh (left) and 40 €/MWh (right), as discussed in chapter 5, plotted against electricity input fraction (top), carbon conversion to biofuels (middle) and carbon conversion to total products (bottom). The PC for all bio-electrofuel tracks evaluated fall between 60 and 140 €/MWh under both electricity prices. This is because the lower and upper PC values derive from basecase configurations and are insensitive to changes in electricity price. The higher-end of the range, 100–140 €/MWh, correspond to direct liquefaction (HTL and fast pyrolysis) and FT technologies. It should be noted that the assumed biogas-based hydrogen contributes to high costs for the liquefaction-based tracks in their base configuration.

The lower end of the PC range, 60–100 €/MWh, correspond to methanol, SNG, bioethanol and ATJ technologies. The PC of the reference electrofuel tracks eMeOH and eSNG also fall within these limits under both electricity prices, whereas eFT ends up between 140 and 165 €/MWh. Stacked plots showing PC build-up of all tracks are presented in Appendix 6. production cost build-up. Figure 47 shows PC build-up for BLGFT tracks as an example.

The change in PC with increasing electrification and carbon efficiency is different for different tracks. Typically, the specific PC increases with increasing electrification for the low cost tracks (SNG, methanol, ethanol) but still in all cases staying below the eSNG and eMeOH production costs.

For gasification-based drop-in fuels (FT), the change in PC with increasing electrification is much smaller and can go either up or down, depending on the gasification technology and configuration. In general, there is no or very small cost for increasing the biomass resource efficiency for these tracks.

For the liquefaction-based tracks, the PC decreases with increasing electrification. As described above this is due to the assumption of using biogas-based hydrogen in the base cases, which was done in order to have comparable climate performance between configurations.

In general, the gain in carbon conversion efficiencies to biofuels is high relative to the corresponding marginal change in PC, which for some tracks could even be lower than the basecase PC under the 30 €/MWh electricity price scenario (Figure 46 middle and bottom). Carbon conversion efficiencies to biofuels and to total products are the same for tracks that do not have carbon containing non-biofuel co-products, such as lignin and char. EtOH, ATJ and HTL tracks have different carbon conversion efficiency to biofuels and to total products. Thus, except for these 3 tracks, Figure 46 (middle and bottom plots) are essentially the same.

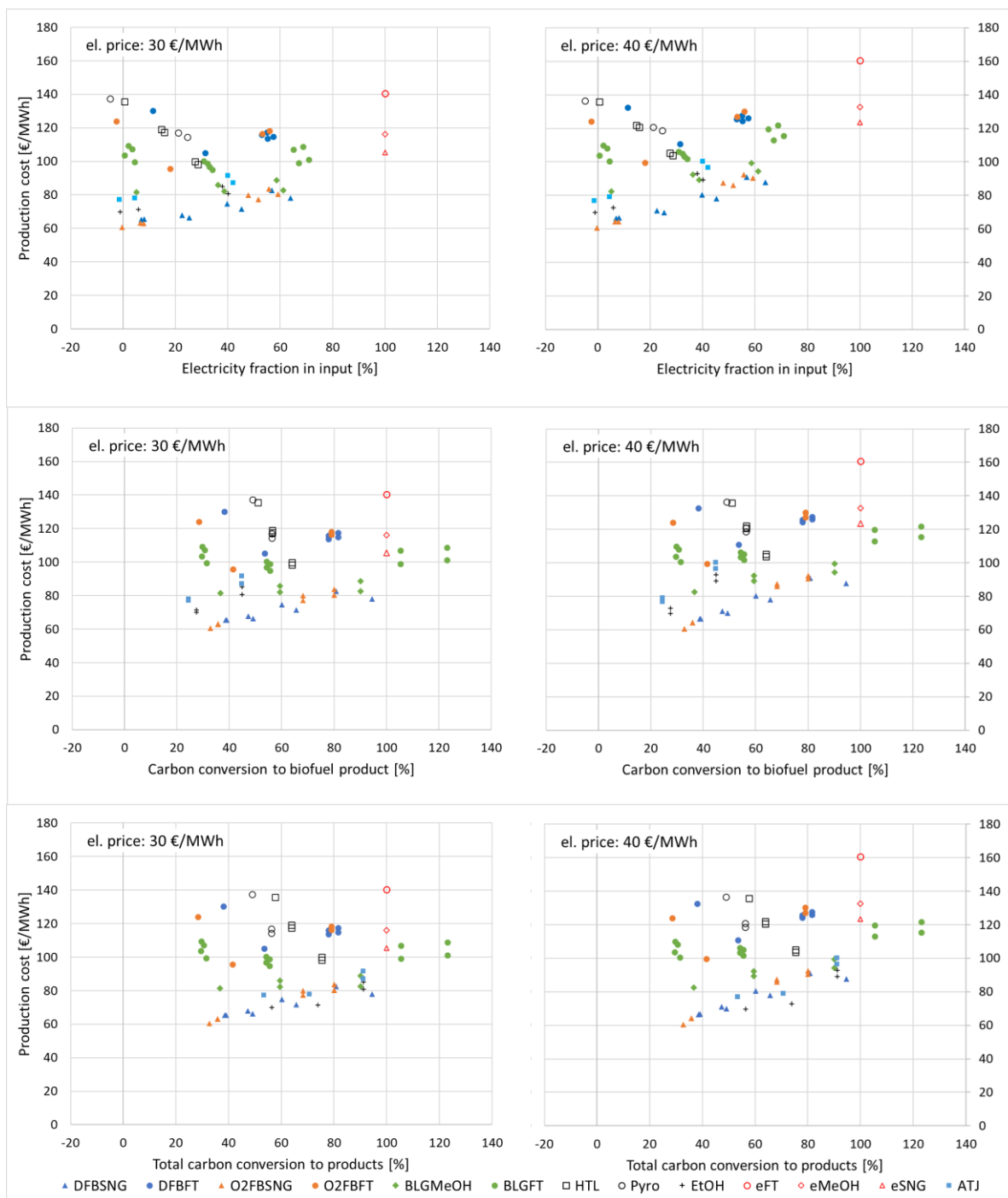


**Figure 46.** PC of bio-electrofuel tracks under electricity prices (€/MWh) 30 (left) and 40 (right) plotted against electricity input fraction (top), carbon conversion to biofuels (middle) and total carbon conversion to products (bottom).

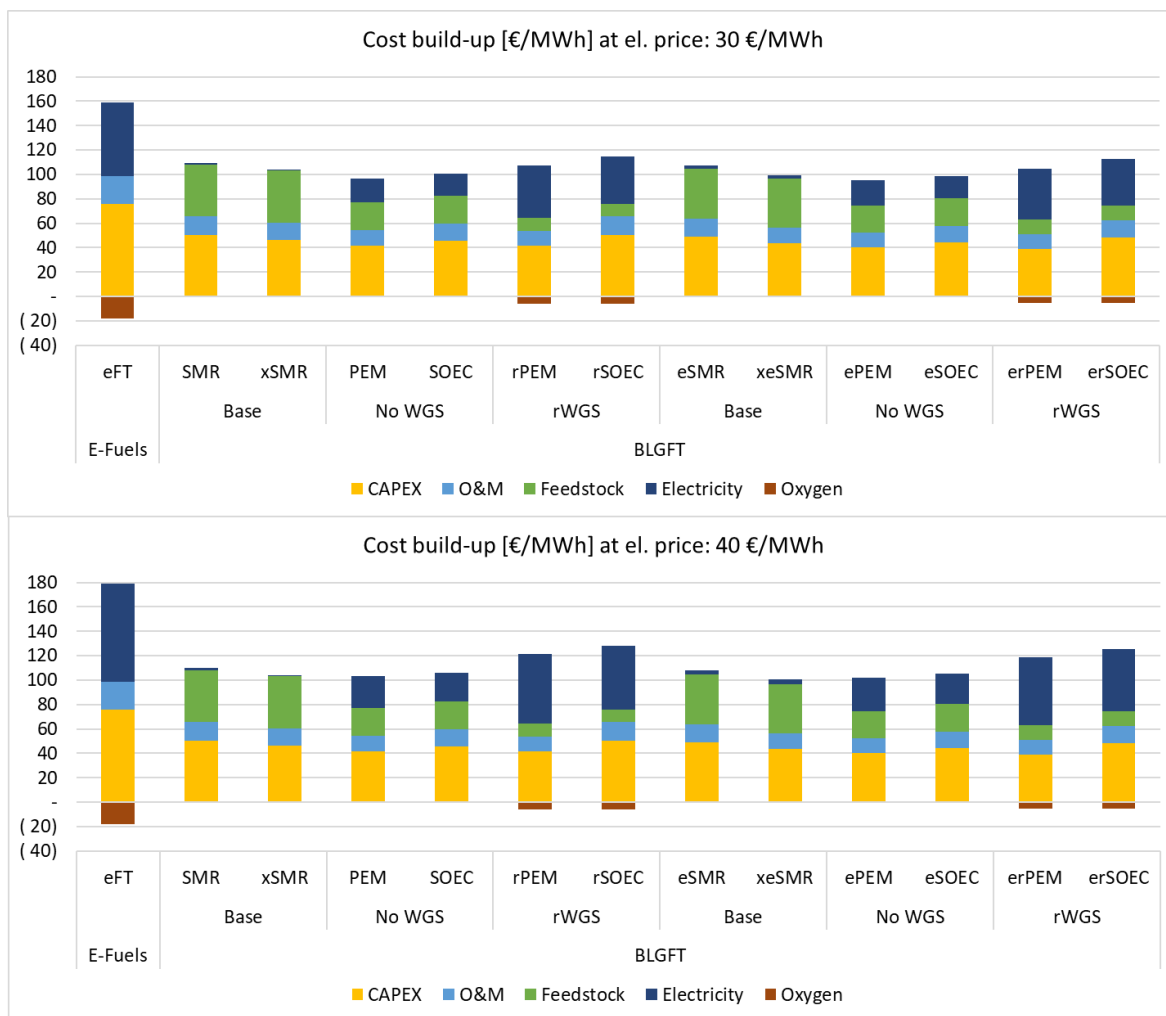


**Figure 47 PC build-up for BLGFT tracks under electricity prices (€/MWh), 30 (top) and 40 (bottom).**

The PC of FT fuels via fluidized bed gasification DFB-FT and O<sub>2</sub>FB-FT are estimated to be in the ranges 105 (111)–130 (133) and 96 (100)–124 (130), respectively (numbers before brackets for 30 €/MWh, within brackets 40 €/MWh). The use of an electrified SMR lead to decreased costs and eSMR configurations correspond to the lower end of the PC ranges. Further electrification to avoid WGS resulted in increased PC by 22-30% for O<sub>2</sub>FB-FT and 8-13% for DFB-FT. The high electricity consumption of PEM (compared to SOEC) technology resulted in higher PC for the configurations involving PEM option. Figure 46 (middle) illustrates the corresponding carbon conversion efficiency from feedstock to final biofuel which for DFB-FT track increased from 38% in the base case to 78% for no WGS configuration to a maximum of 81% for rWGS configuration. For O<sub>2</sub>DFBFT track the carbon conversion efficiency to biofuel increased from 28% to 41% to 79% for base case, eSMR and eSMR no WGS configurations, respectively.

The PC of the BLG-FT track resulted in a range, 97 (101) – 109 (122) €/MWh. The variation of PC for BLG-FT track between SMR and eSMR configurations is not as significant as for fluidized bed configurations since these units are primarily used to reform FT tail gas in this case, due to the low methane content of the syngas from the gasifier.

Further electrification of the BLG-FT with PEM or SOEC technology to avoid WGS and to integrate rWGS resulted in somewhat lower PC for the 30 €/MWh electricity scenario but not for the 40 €/MWh scenario. The corresponding carbon conversion efficiencies for BLG-FT tracks with SMR are 30% (base), 54% (no WGS) and 123% (rWGS) and for eSMR 31% (base), 56% (no WGS) and 105% (rWGS). More than 100% carbon efficiencies derive from integration benefits, i.e., carbon in additional biomass supplied to cover energy deficit in the pulp mill due to BL gasification is less than the carbon in the gasified BL itself.

The PC of BLG-MeOH tracks increased with electrification from 81 (82) €/MWh in the base case to 89 (99) for the rWGS track involving SOEC technology. Compared to the base case, the PC of the BLG-MeOH tracks with no WGS and rWGS involving PEM technology increases by 1-9% for 30 €/MWh electricity and 5-20% for 40 €/MWh electricity. The carbon conversion efficiency of BLG-MeOH track progressively increased from 37% (base) to 59% (no WGS) to 90% (rWGS).

SNG can be produced to a cost range 65 (66) – 83 (91) €/MWh and 61 (61) – 84 (92) €/MWh via DFB and O2FB configurations, respectively. For both technologies, DFB and O2FB, the PC of SNG increases with increasing share of electricity input to the systems. The PC cost increase for the most electrified cases is 30-50% depending on technology and electricity price scenario. But the production cost is still lower than the corresponding electro-SNG production cost. The carbon conversion efficiency for DFB increased from 39% to 66/60% (no WGS) to 95/81% (full CO<sub>2</sub> utilization). The O2FB track carbon efficiency increased from 33% (base) to 68% (no WGS) to 80% (full CO<sub>2</sub> utilization).

The PC of lignocellulosic EtOH tracks increase with increasing electrification from about 70 (70) €/MWh in the base case to 71 (73) €/MWh for the heat pump (MVR) option to 81 (89) €/MWh for the MVR plus PEM-based rWGS. The EtOH track implementing MVR plus SOEC-based rWGS resulted in the highest PC 85 (93) €/MWh. The carbon conversion efficiency to bio-fuels for EtOH increased from 28% (base and MVR tracks) to 45% (MVR plus rWGS track), whereas carbon conversion to total products (i.e., including lignin pellets) increased from 56% (base) to 74% (MVR) to 91% (MVR plus rWGS).

The PC for ethanol-to-jet track in the so-called ATJ pathway increases from 77 (77) €/MWh to 78 (79) €/MWh to 87 (97) €/MWh for the base case, MVR and MVR plus PEM-based rWGS configurations, respectively. The MVR plus SOEC-based rWGS configuration resulted in the highest PC 92 (100) €/MWh. It should be noted that the ATJ track benefits from economy-of-scale effect as the capacity was magnified to about 2.5 times, compared to the capacity of the lignocellulosic EtOH track, to show the impact of large ATJ plant that convert ethanol produced in multiple facilities. The carbon conversion efficiency to biofuels increased from 24% (base and MVR) to 45% (MVR plus rWGS) and to total products (i.e., including lignin pellets) from 53% (base) to 71% (MVR) to 91% (MVR plus rWGS).

Direct liquefaction tracks resulted in PC ranges 114 (119) – 137 (136) €/MWh and 98 (104) – 136 (136) €/MWh for fast pyrolysis and HTL, respectively. The PC of liquefaction cases reduced by 17% (13%) and 11% (9%) from base cases to electrified configurations implementing PEM for fast pyrolysis and HTL, respectively. The corresponding SOEC configurations has slightly higher PC, which compared to the base cases reduced by 15% (12%) for pyrolysis and 10% (8%) for HTL. The economic performance of base case configurations for fast pyrolysis and HTL suffer from high

cost of biogas (90 €/MWh). Carbon conversion improvement margins for pyrolysis and HTL are limited to replacement of biogas with electricity. Thus, carbon conversion to biofuels for fast pyrolysis increased from 49% (base) to 56% (no biogas) and for HTL from 51% (base) to 64% (no biogas).

Figure 48 shows the impact of changing electricity price from 30 to 40 €/MWh on the PC of the bio-electrofuel and electrofuel tracks plotted against electricity input fraction (top), carbon conversion efficiency to biofuels (middle) and total carbon conversion efficiency (bottom). In general, the cost increase is (of course) higher for more electrified options (to the right in Figure 48) and reaches maximum 18%, which is around half of the electricity price increase of 33%. The relation of the PC increase to the fraction electricity input is almost linear (Figure 48 top). The highest is found for eSNG track (17%), followed by rWGS tracks (10%–15%), no WGS tracks (4%–10%), eSMR and liquefaction tracks (<4%).

### 7.2.1 Sensitivity analysis on production cost

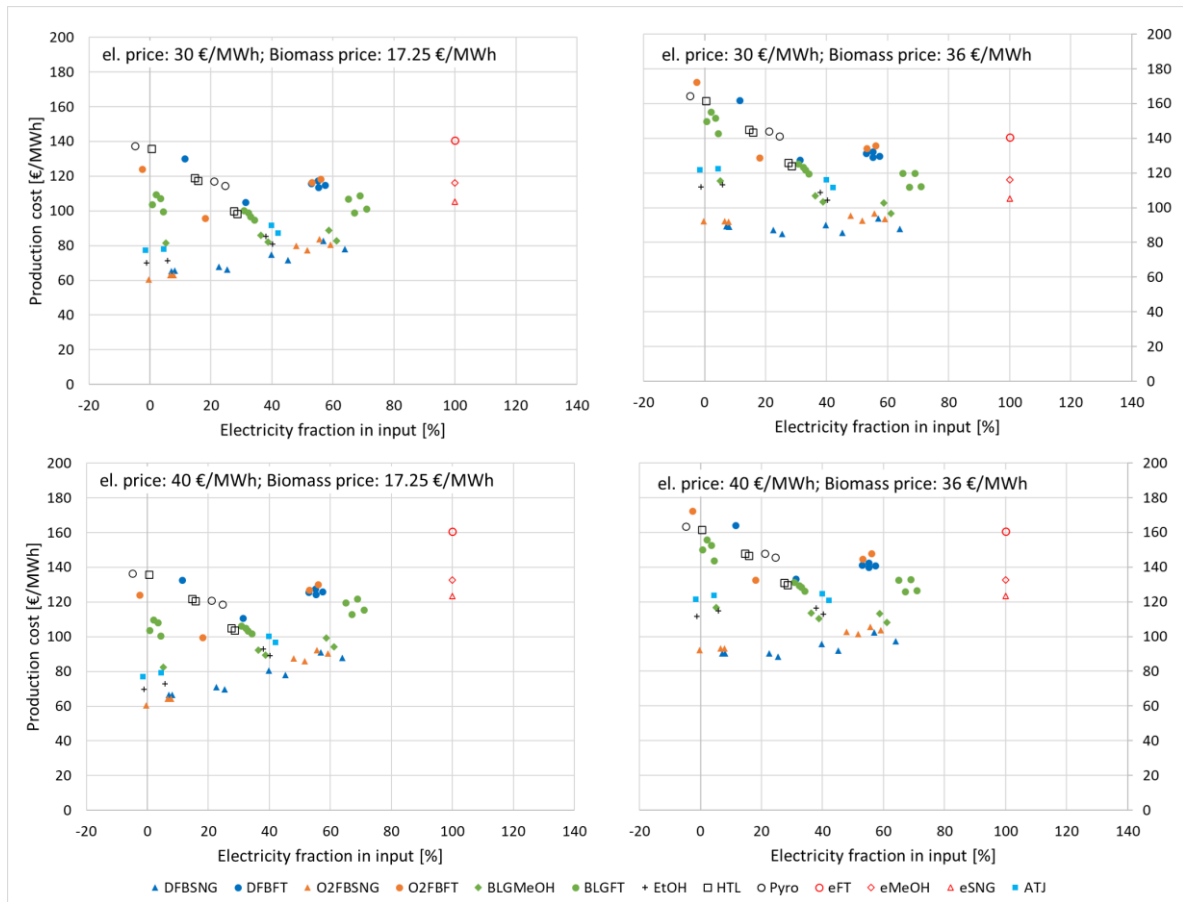
A sensitivity analysis was performed for the biomass price (17.25 €/MWh as reported by the Swedish statistics office (“Wood Fuel and Peat Prices” 2018) used in the base case) and a tentative value of district heating export (no value assumed in the PC above). The sensitivity analysis is performed for both electricity price scenario, i.e., 30 & 40 €/MWh, and only one parameter is varied at a time while others are held at their base values. Excess heat utilization for district heating (DH) is assumed for only half of the annual operation hours, about 4000 hours.

Figure 49 shows PC sensitivity to biomass price which was increased from 17 €/MWh to 36 €/MWh (based on an assumed increase as the energy mix transforms from fossil to renewable sources (Energiforsk 2021)). Doubling the biomass price increased the PC of all bio-electrofuel tracks but with a varying degree, from 10% to as much as 60% under both electricity price scenarios. The lower end of the range corresponds to highly electrified configurations whereas the high-end correspond to the base cases.

Figure 50 shows the impact of utilizing excess heat for DH assuming 35 €/MWh, attempting to reflect a representative production cost for DH. In general, this does not change the overall picture of PC levels or trends. The PC of the tracks with high excess heat reduces most, such as O2FB tracks reduces by about 14%.



**Figure 48** Impact of electricity price change on PC plotted against electricity input fraction (top, negative values mean electricity production), carbon conversion to biofuels (middle) and total carbon conversion to products (bottom).



**Figure 49 Sensitivity of PC to changes in biomass price in €/MWh, 17 (left) and 36 (right) plotted against electricity input fraction.**

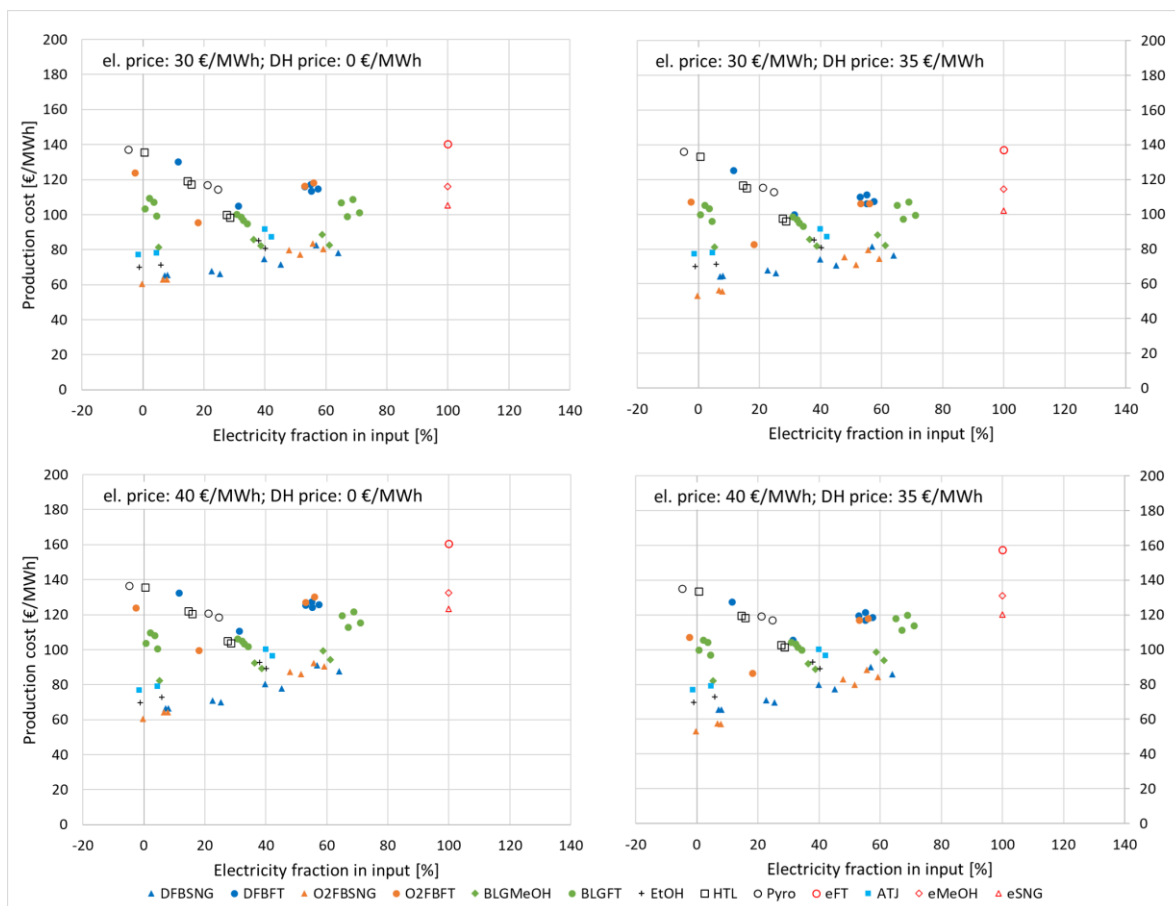


**Figure 50** Sensitivity of PC to excess heat sales in €/MWh, 0 (left) and 35 (right) plotted against electricity input fraction.

### 7.3 CONCLUSIONS

In summary, the techno-economic analysis of this chapter shows that the production cost for all bio-electrofuel tracks evaluated fall between 60 and 140 €/MWh assuming 30-40 €/MWh electricity costs. The higher-end of the range, 100–140 €/MWh, correspond to direct liquefaction (HTL and fast pyrolysis) and gasification-FT technologies, which are all tracks for drop in fuels. The lower end of the production cost range, 60–100 €/MWh, correspond to methanol, SNG, bioethanol and ATJ technologies. This shows that the extensive chemical transformation from biomass to pure hydrocarbons (very different elemental composition as discussed in chapter 3) has a high cost. The production cost of the reference electrofuel tracks eFT, eMeOH and eSNG are in each case higher than the corresponding bio- and bio-electrofuel tracks.

The production cost changes with increasing electrification and carbon efficiency.

- For the non-drop in fuels (SNG, methanol, ethanol), with lower base case production cost, the specific cost increases with increasing electrification but still in all cases staying below the corresponding electrofuel (eSNG and eMeOH) production costs.

- For gasification-based drop-in fuels (FT), the change in production cost with increasing electrification is much smaller and can go either up or down, depending on the gasification technology and configuration.
- For the liquefaction-based tracks, the production cost decreases with increasing electrification. This is due to the assumption of using biogas-based hydrogen in the base cases, which was done in order to have comparable climate performance between configurations.

The sensitivity analysis with respect to biomass and electricity cost shows, not surprising, that bio-fuels tracks are sensitive to biomass price, electrofuel track are sensitive to electricity price and bio-electrofuels tracks fall in between.

For the high biomass price scenario, bio- and bio-electro-SNG, methanol and ethanol still have lower production cost than the corresponding e-tracks but for drop-in fuels, the base case biofuel production cost is now higher than e-FT. It decreases clearly with increasing electrification and the bio-electrofuel options have lower production costs than e-FT.

## 8 GREENHOUSE GAS FOOTPRINTS

This chapter contains the results of the greenhouse gas footprint estimation for biofuels and bio-electro fuels according to the methodology described in Section 2.5.

Figure 51 shows GHG emissions reduction potential of the bio-electrofuel and electrofuel tracks compared to respective fossil counterparts indicated in Table 2. The GHG performance of all base case configurations was high, as all fossil inputs were avoided by the choice of design, and the emissions were primarily driven by the biomass supply chain.

As the share of electricity in the input increases, the GHG performance becomes more sensitive to electricity emission factors, Figure 51. For the 13.1 kgCO<sub>2</sub>eq/GJ electricity emission factor scenario, the bio-electrofuel tracks can achieve as much as 76%–98% GHG emission reduction potential while the electrofuel tracks achieved 61%–75%, Figure 51 (left). Lower-end of the ranges correspond to SNG tracks since SNG requires more hydrogen for a given amount of carbon atoms, which in turn requires more electricity. Reducing the electricity emission factor to 7 kgCO<sub>2</sub>eq/GJ has significant impact on the GHG emissions reduction potential of the electrified cases which increased to 86% – 99% for bio-electrofuel tracks and 79%–87% for electrofuel tracks, Figure 51 (right).

Ideally, a zero-emission electricity source would enable the heavily electrified bio-electrofuel tracks achieve over 97% GHG emissions reduction, while all electrofuel tracks converge at 100%, Figure 52. The remaining GHG emissions for the bio-electrofuel tracks come from collection and transport of the biomass feedstock.

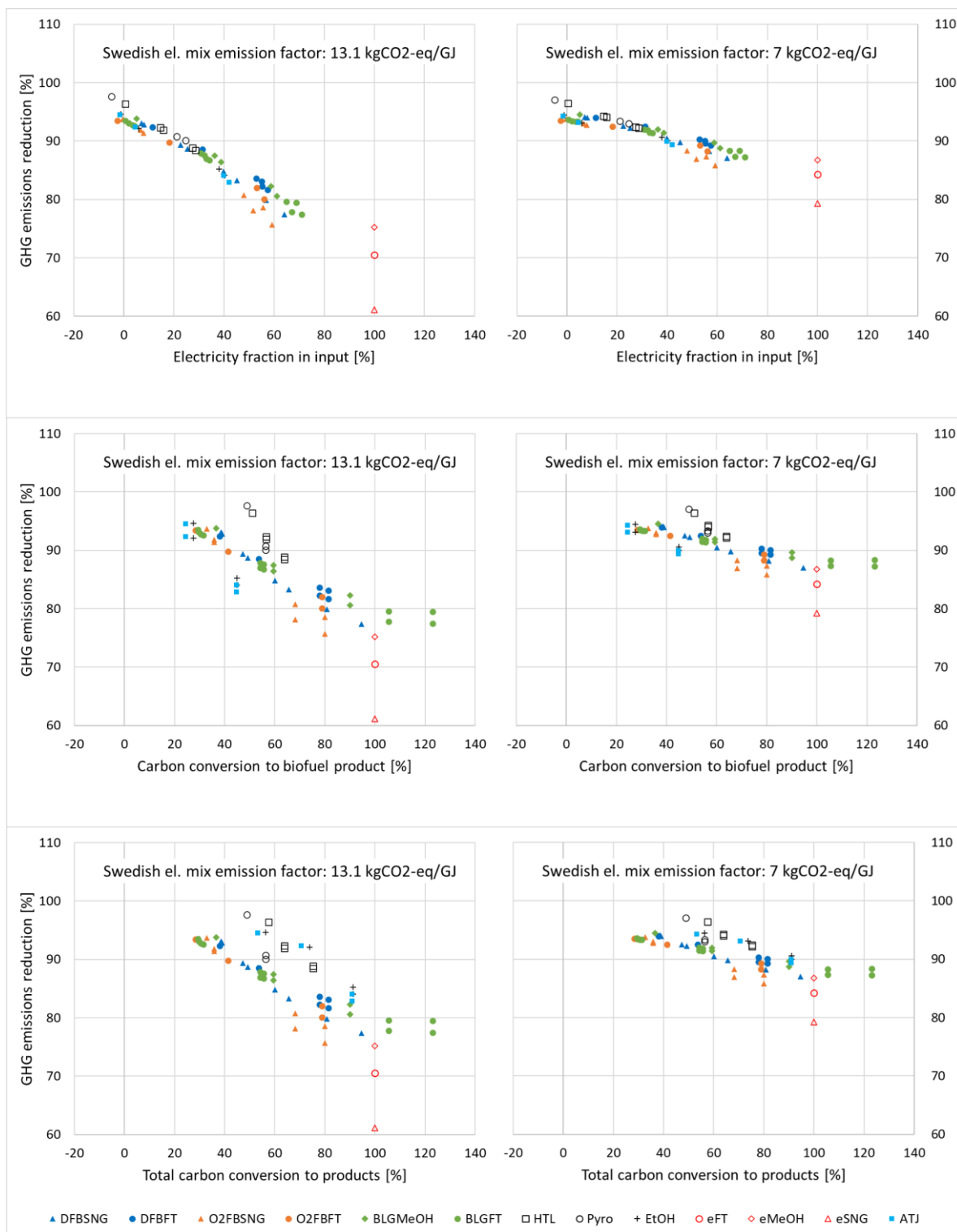


**Figure 51** GHG emissions reduction potential of all the biofuel tracks under electricity emission factors (kgCO<sub>2</sub>eq/GJ) 13.1 (left) and 7 (right) plotted against electricity input fraction (top), carbon conversion to biofuels (middle) and total carbon conversion to products (bottom).

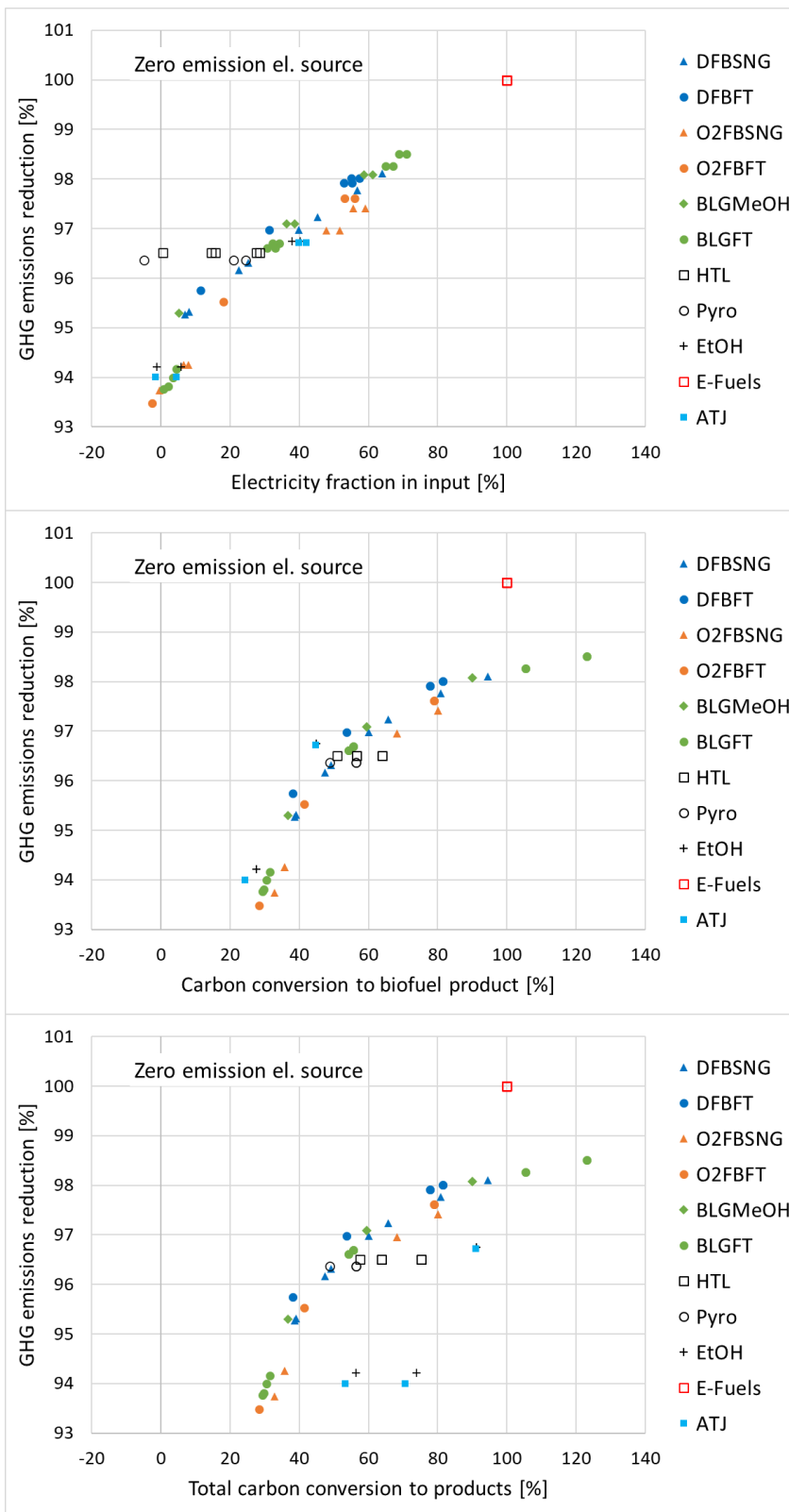


**Figure 52** GHG emissions reduction potential under zero emission electricity source plotted against electricity input fraction (top), carbon conversion to biofuels (middle) and total carbon conversion to products (bottom).

## 9 SCENARIOS FOR LARGE SCALE IMPLEMENTATION

This chapter attempts to describe some aspects of large-scale commercial implementation of the bio-electrofuels technology. In order to illustrate the impact, scenarios are developed that describe how the Swedish biofuel demand 2030 and 2045 could be met from domestic feedstocks using combinations of (“traditional”) biofuels, bio-electrofuels and electrofuels. We illustrate the impact on biomass demand, electricity demand, total cost and total greenhouse gas emissions in order to assess the societal benefit of the respective solution.

It is important to point out that the scenarios developed are to be seen as illustrative examples to visualize the effects more clearly. It is not likely that scenarios would occur that uses 100% e-fuels or 100% gasification-based bio-electrofuels to meet the demand for liquid and gaseous transportation fuels, for example.

### 9.1 BIOFUEL DEMAND SCENARIOS

The present Swedish use of biofuels for transport is 20 TWh/y but this is mostly imported. The use is mainly driven by the reduction obligation system, obliging fuel distributors to reduce the greenhouse gas emissions of their products by blending of sustainable fuels. There have, however, not been corresponding incentives on the biofuel production side. Only 3.5 TWh/y of biofuel is presently produced from domestic feedstocks: ethanol from wheat (1.5 TWh/y), HVO from tall oil (0.6 TWh/y) and biogas from various substrates (1.5 TWh/y).

There are many different scenarios for the future volumes of sustainable liquid and gaseous fuels required for the transformation of the Swedish transport system, for example by the government initiative Fossil Free Sweden (FossilfrittSverige 2021), Swedish Energy Agency (Energimyndigheten 2019) and Swedish Transport Administration (Trafikverkets 2020). The differences among these are to a large extent depending on the assumptions regarding how fast the electrification of road transport will take place, but there is consensus that biofuel demand for domestic road transport will peak in the period 2030-2040. There are also differences with respect to if international transport fueled in Sweden is included or not.

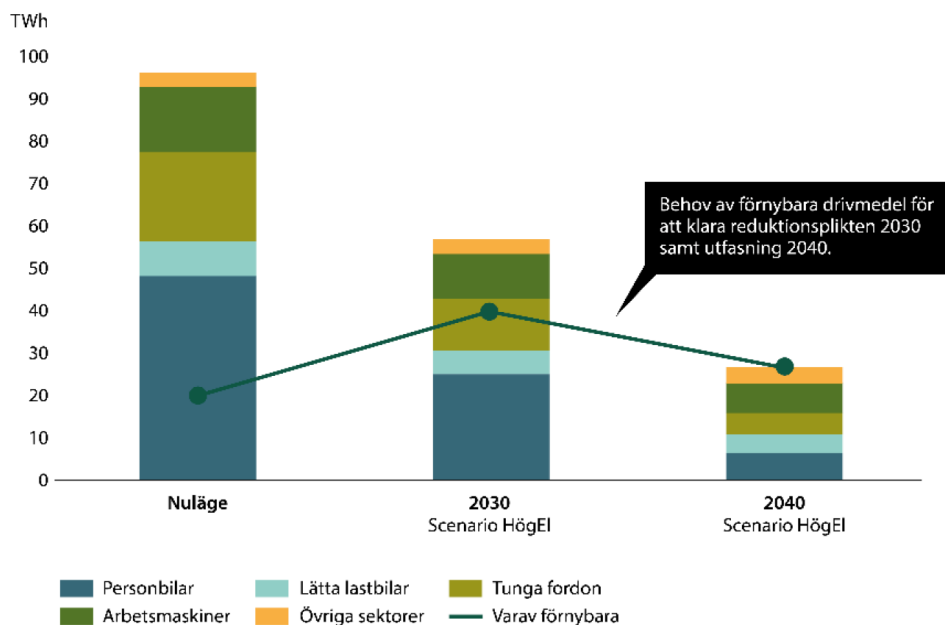
A recent and highly relevant source for domestic biofuel demand scenarios is the government-initiated Inquiry regarding phase out of fossil fuels in the transport sector<sup>6</sup> (Miljödepartementet 2021). The inquiry proposes that fossil fuels are completely phased out 2040. An important factor is that all new passenger cars are electric from 2030 and onwards. The Inquiry also proposes changes to the current system mandating biofuel blending, the reduction obligation system.

Figure 53 shows the estimated demand of liquid and gaseous fuels for domestic transportation in a high electrification scenario. The demand for renewable fuels is 41 TWh/y 2030 and 20 TWh/y 2045. We have selected this as our low demand liquid fuel demand scenario in the analysis carried out in this project, but from Figure 54, it is very clear that less optimistic scenarios for electrifica-

---

<sup>6</sup> Utfasningsutredningen (M 2019:04).

tion would create a substantially higher demand. The high demand scenario used in this study, corresponding to “average electrification rate” (“MellanEI” in Figure 54) is 48 TWh/y 2030 and 34 TWh/y 2045 for domestic transport.



**Figure 53. Domestic demand of liquid and gaseous fuels in a high electrification scenario, from (Miljödepartementet 2021).**

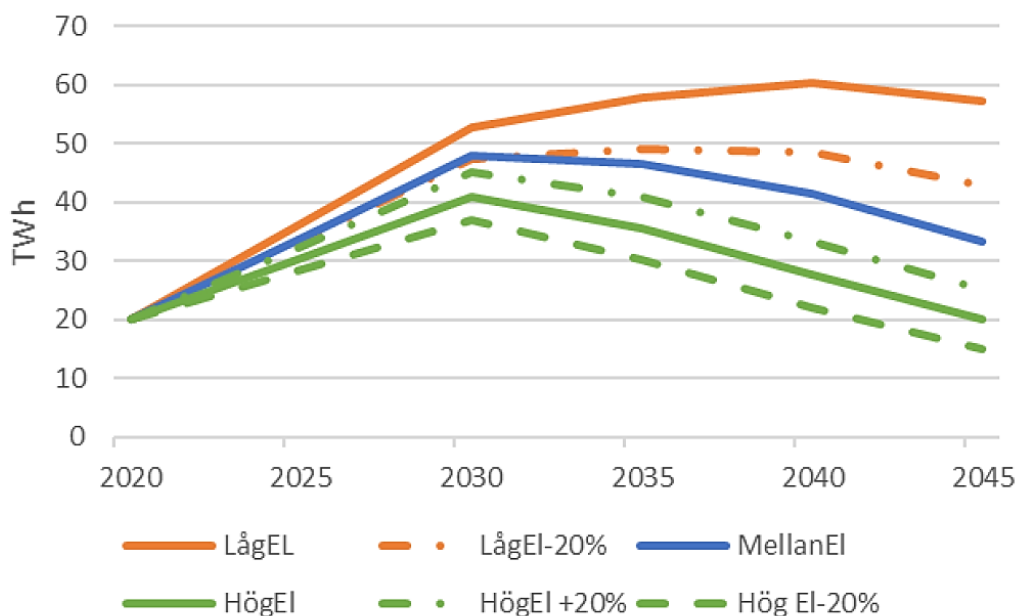


**Figure 54. Domestic demand of renewable liquid and gaseous fuels for different electrification and transport demand scenarios, from (Miljödepartementet 2021).**

The demand scenarios discussed above do not include international transport originating (and fueling) in Sweden. The pre-pandemic energy consumption for international aviation was 10 TWh/y and for international maritime transport 24 TWh/y. We have selected to include international transportation only in the 2045 demand scenarios, either 50% of energy demand (low demand scenario) or 100% (high demand scenario).

Based on this, the demand scenarios shown in Table 23 were used.

**Table 23. Biofuel demand scenarios.**

	2030 only domestic	2045 incl. international
High fuel demand scenario	48 TWh/y	68 TWh/y (34+34)
Low fuel demand scenario	41 TWh/y	37 TWh/y (20+17)

## 9.2 NATIONAL SUSTAINABLE BIOMASS SUPPLY SCENARIOS

A recent and widely used source for Swedish sustainable biomass supply potential is (Börjesson 2021) and this is also the basis of our sustainable biomass supply scenarios.

In 2030, it is estimated that 50 TWh/y more than today of sustainable biomass resources can be used. Forest-based biomass account for two thirds of the total biomass potential whereas agriculture-based account for one third. In 2040, the estimated increase in sustainable biomass supply potential compared to today is 67 TWh/y. In this case, forest-based biomass account for 60% of the total biomass potential and agriculture for 40%.

There will be demand for the sustainable biomass supply from several sectors. According to Fossil Free Sweden, we can expect approximately equal shares of biomass energy use for transport, industry and heat/power in 2045 (FossilfrittSverige 2021). But use of biomass for industry and heat/power is substantial already today so it is reasonable to expect that production of transport fuel will take a much larger share of the increased biomass supply potential. As an example, we have, somewhat arbitrarily, used a scenario in which 75% of the increased biomass supply potentials 2030 and 2045 can be used for production of fuels for the transport sector, as shown in Table 24.

**Table 24. Biomass supply scenarios.**

	2030	2045
Total increased biomass potential, (Börjesson 2021)	50 TWh/y	67 TWh/y
75% of potential, assumed available for transport sector	37.5 TWh/y	50 TWh/y

## 9.3 BIOFUEL PRODUCTION SCENARIOS

Based on the fuel demand scenarios (low and high, 2030 and 2045) in Table 23 and the biomass supply scenarios (2030 and 2045) in Table 24, we have modelled a number of theoretical scenarios to meet the transport fuel demand using the domestic biomass supply.

The scenarios include different technologies for fuel production according to Table 25. In this scenario work we selected to include only drop-in hydrocarbon fuels, which means that we have included gasification with Fischer Tropsch, liquefaction with hydrotreatment (refinery-based) and Fischer Tropsch-based electrofuels, the latter using flue gas as biogenic CO<sub>2</sub> source.

The data in Table 25 is formed by interpolation and local averaging from the data in chapter 6 (Figure 39 and Figure 40) and chapter 7 (Figure 46, 40 €/MWh electricity cost). Gasification track data are based on all three gasification technologies in combination with FT, since it is assumed that a mixture of these would be more realistic to meet demand than a single technology (and similarly for liquefaction with hydrotreatment). Data from chapter 8 has also been used for GHG footprint but is not shown in the table above, since there are several cases depending on electricity mix assumptions.

**Table 25. Technologies for drop-in biofuel supply scenarios.**

Biofuel production technology	Fraction el input	C eff.	LHV eff.	Prod. Cost (€/MWh)
Gasification FT base (biofuel)	5%	30%	45%	110
Gasification FT 50% (bio-electro)	30%	55%	52%	105
Gasification FT 90% (bio-electro)	60%	90%	52%	120
Refinery base (biofuel)	0%	50%	55%	135
Refinery electrified (bio-electro)	28%	65%	55%	105
Electrofuels	100%	100%	50%	160

The resulting sustainable fuel production scenarios are shown in Figure 55. A general principle that has been used is that if the biomass supply is not enough to meet transport fuel demand in the scenario, electrofuel production is used to meet the remaining demand, which can be seen by the green bars that constitute the upper part of the bars for almost all technology options.

It is only the most carbon efficient option (Gasification FT 90%, grey bars) that manages to meet fuel demand for all cases using biomass supply (almost, small deviation for 2045H). For remaining technology options, a substantial amount of electrofuel production is required to meet fuel demand, due to shortage of biomass supply. The largest volumes of electrofuels are for the least efficient track (Gasification FT base). The case with only green bars in Figure 55 (rightmost in each group) is the electrofuels only case, with no biomass demand at all. For the 2045L scenario, with lowest fuel demand and highest biomass potential, all three bio-electrofuel options can meet the demand.

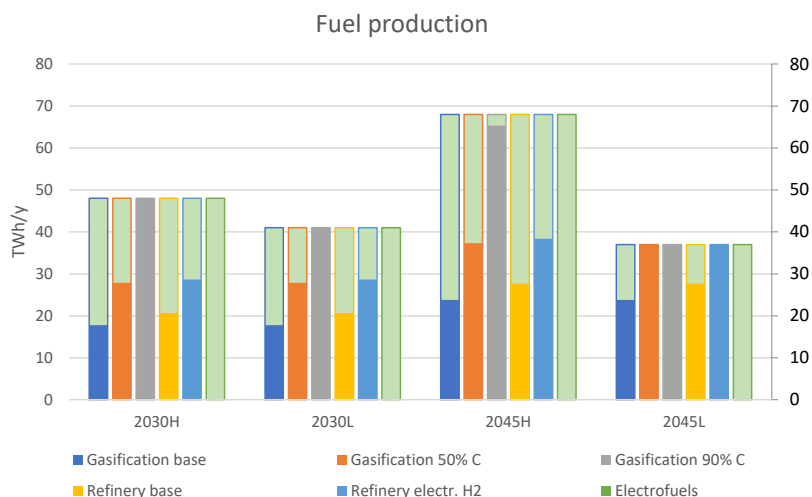


**Figure 55. Sustainable transport fuel production for the four scenarios (Table 23) and the six technology options (Table 25).**

Figure 56 shows the biomass (top) and electricity (bottom) demand for each sustainable fuel production scenario. The biomass use is for the biofuel or bio-electrofuel production in the scenarios, which is zero in the electrofuels only case. In most cases, the biomass use is equal to the maximum, i.e. 75% of the additional sustainable supply potential, as indicated Table 24. The only production technology that does not use the full available biomass supply is the high carbon efficiency gasification case (grey in Figure 56).

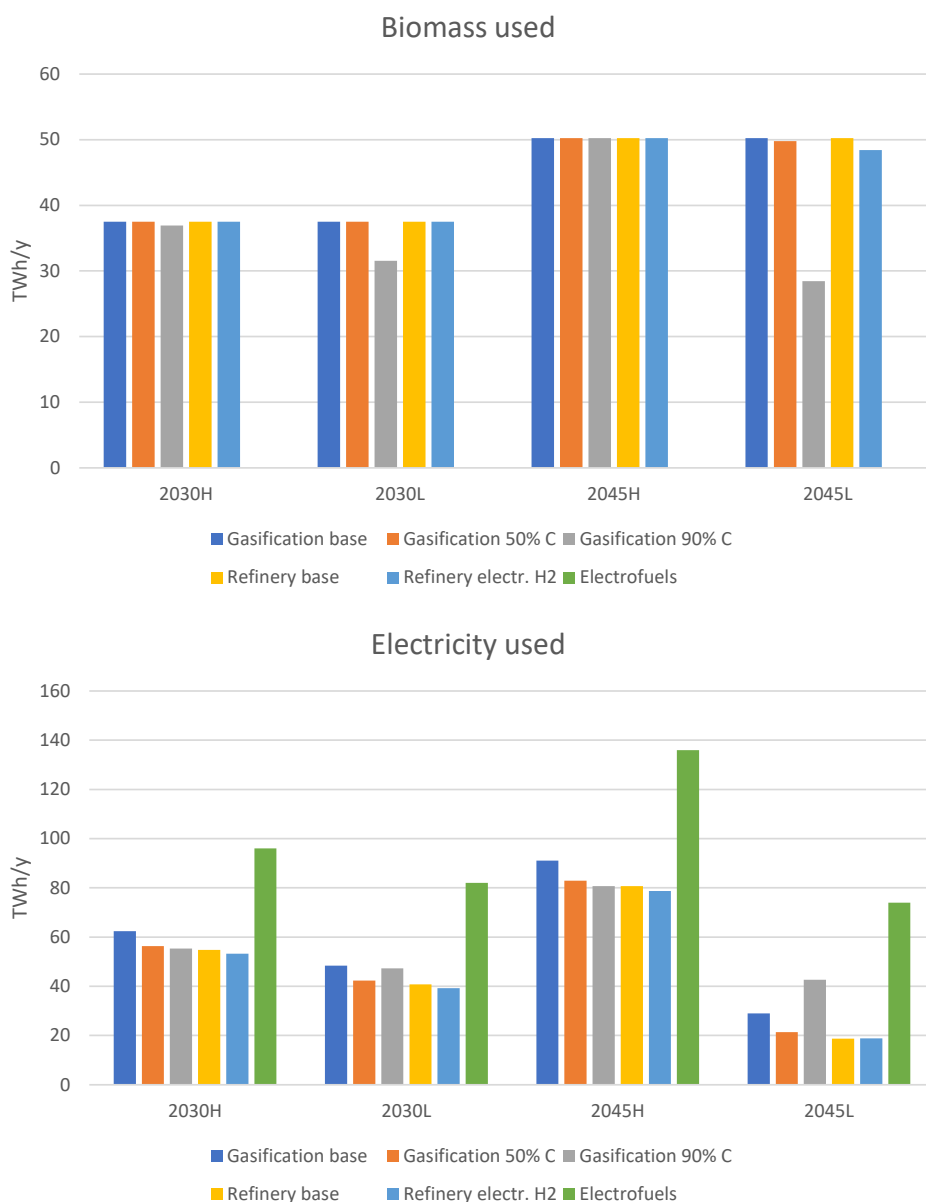


**Figure 56. Biomass (top) and electricity (bottom) use to meet the biofuel production scenarios in Figure 55. Electricity use is for the bio-electrofuel production and any electrofuel production combined.**

The electricity demand is substantial for all cases and scenarios. The electrofuels only cases (green bars in Figure 56, lower part) have electricity demands of 75-140 TWh/y, which is 50%-100% of current total Swedish electricity consumption. This is most likely not a feasible scenario.

The scenarios using biomass feedstocks, either as biofuels + electrofuels, or bio-electrofuels, require much less electricity but still very large amounts. For 2030, 40-60 TWh/y (around half compared to 80-100 TWh/y for electrofuels only) is still too much to be realistic, which indicates that at this time, Sweden will still be dependent on biofuels (or biomass feedstock) import to supply our transport system.

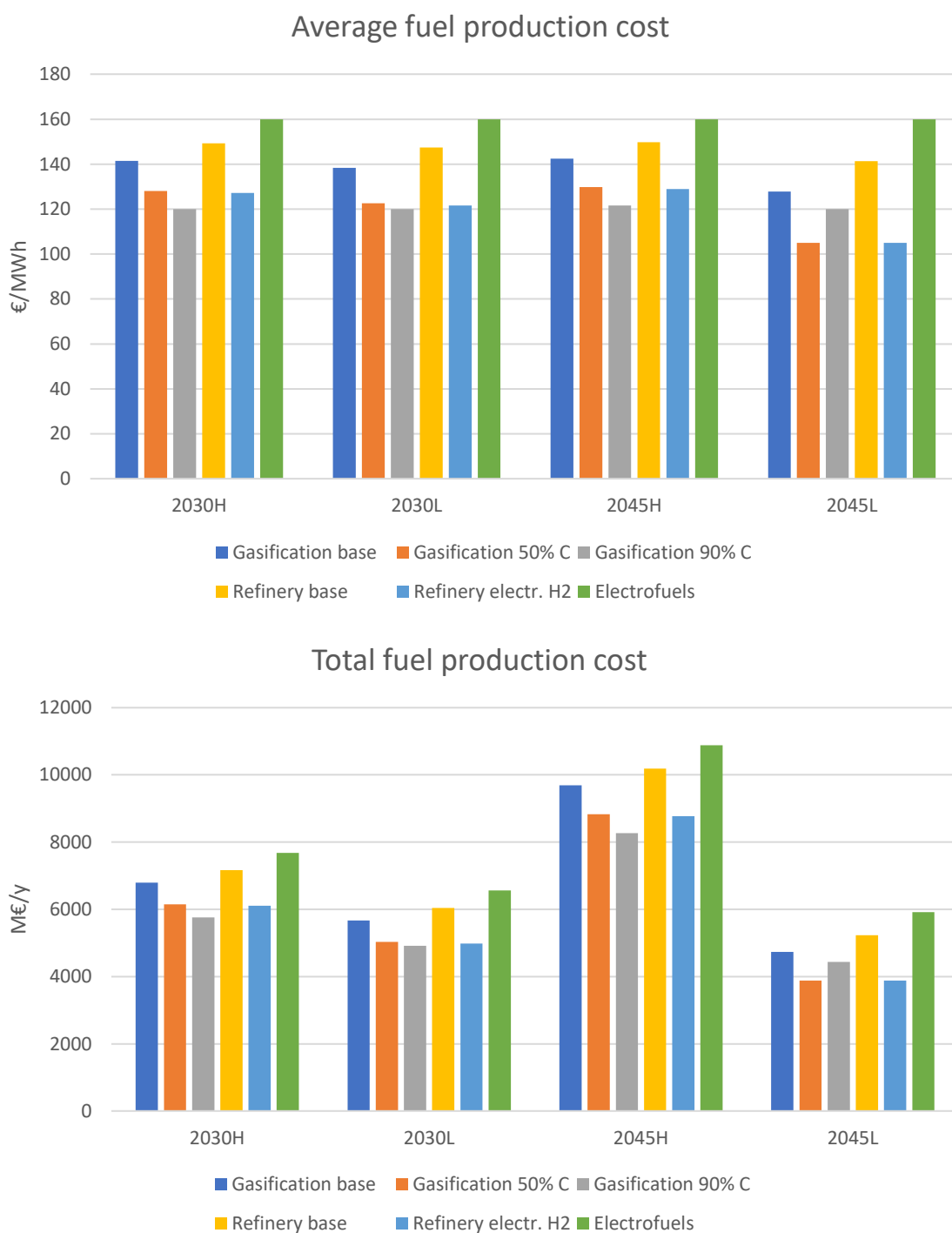
In 2045, the two biofuel demand scenarios are very different, with only 20-40 TWh/y of electricity demand for the low scenario 2045L, compared to 75 TWh/y for electrofuels only. For the 2045H, electricity demand is 80 TWh/y using biofuels or bio-electrofuels as the main option, which is much less than the electrofuels only at 140 TWh/y but still most probably too much to be realistic, indicating that the biofuel demand should be pushed towards the low scenario through extensive battery-based electrification.

Figure 57 shows production costs for the biofuel demand scenarios. The average biofuel production costs are not dramatically different between the different options, ranging from 120 to 160 €/MWh. The values shown in Figure 57 (upper part) are average for the fuel production scenarios, meeting the fuel demand, i.e. including the whole production mix. As noted in chapter 7 (Figure 46) above the electrofuel production fraction of the mix is more expensive than the biofuel or bio-electrofuels, which is consistent with the fact that the electrofuels only cases in Figure 57 always show the highest cost.

It can also be noted that the case with the lowest cost for each year and demand scenario is, for all demand scenarios and years, a bio-electrofuels case. In three out of the four cases, it is the highly electrified gasification case (“Gasification 90% C”). In the 2045L demand scenario, the other two bio-electrofuel cases, with lower carbon efficiency has higher costs. It can be noted that this coincides with that that these two cases can meet demand without electrofuels supplement (compare Figure 55), indicating that it is cost efficient to electrify biofuels (into bio-electrofuels) to the extent enough to avoid pure electrofuel production, but not necessarily more. Or in other terms, it is efficient to use the biomass resource available first and then to turn to electricity as a second option.

As noted above, it has been assumed that drop-in hydrocarbon fuels are used to meet the full demand. It can be noted from chapter 6 (Figure 39 and Figure 40) and chapter 7 (Figure 46) that costs would be lower and efficiencies higher if methanol and/or methane were produced by gasification and electrofuel technology. Since much of the demand in 2045 is for international maritime transport, it is not unlikely that methanol or methane could be an important part of a fuel mix. Such an assumption would decrease the overall costs, but it would not dramatically change the comparison between biofuels, bio-electrofuels and electrofuels, which is the main purpose of these scenarios.

Figure 58 shows average and total GHG emissions for the biofuel production scenarios for 7 g CO<sub>2</sub>/MJ and zero CO<sub>2</sub> electricity. The electrofuels case has the highest (for 7 g CO<sub>2</sub>/MJ electricity) and lowest (for zero CO<sub>2</sub> electricity) GHG footprint, with biofuels and electrofuels cases lying in between. All of the cases shown in Figure 58 have good GHG performance with >80% savings compared to fossil fuels. As noted in chapter 8, this was not the case for electrofuels with 13 g CO<sub>2</sub>/MJ electricity.



**Figure 57. Average (top) and total (bottom) fuel production cost for the biofuel production scenarios in Figure 55. Note that this is the total production cost for sustainable fuels, not an increase compared to fossil fuel.**

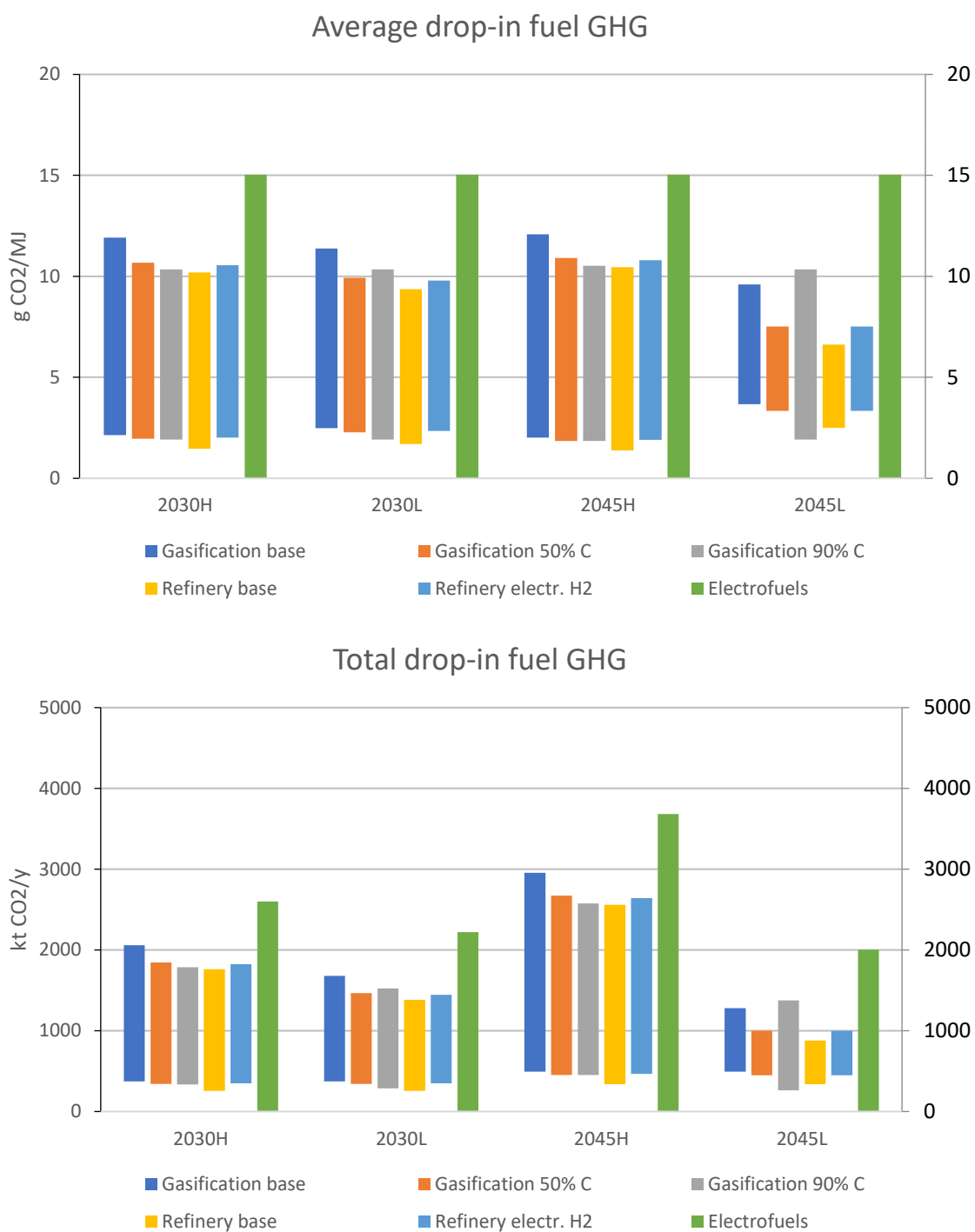


**Figure 58. Average (top) and total (bottom) GHG emissions for the biofuel production scenarios in Figure 55. Top of bars indicate 7 g Co2/MJ electricity and bottom of bars zero CO2 electricity. Note that this is the total GHG emissions for sustainable fuels, not an increase compared to fossil fuel.**

## 10 SUMMARY AND CONCLUSIONS

Sustainable biofuels will be an important part of the transition of the transport sector towards sustainability. Despite extensive electrification, primarily in road transport, the demand for gaseous and liquid fuels is expected to be significant in both 2030 and 2045.

Sustainable biomass is a limited resource. In this respect, the relatively low carbon efficiency in the transformation of lignocellulosic biomass to transportation fuels and chemicals using emerging biorefinery technologies, such as gasification, pyrolysis and fermentation, could become a challenge. It leads to lower climate benefit and lower amount of displaced fossil products from a certain amount of biomass.

This research project investigates how integrated electrification of biorefinery processes can be used to improve the carbon efficiency. Process modelling of different process configurations, based on openly available data for process units' performance, was used as the main tool. The results of the modelling were used to estimate performance indicators for the configurations, such as efficiency, production cost and greenhouse gas emissions.

A major factor limiting the carbon efficiency in biorefineries is the elemental composition of the feedstock and the product. The initial analysis of theoretical efficiencies of biofuel production, not requiring energy self-sufficiency, indicates that a theoretical carbon efficiency for biomass conversion to fuel products is 50-80% for lignocellulosic feedstock. The exact number is highly dependent on the desired product molecule, especially its elemental composition. Carbon efficiency is in general lower for products that have high H/C ratio, for example methane. Hydrogen addition can dramatically change the picture and always gives 100% theoretical carbon efficiency. Theoretical energy yields with hydrogen addition (on biomass feedstock basis) is >100% and as high as 180% for methane from lignocellulose. This means that a large amount of hydrogen needs to be added to reach this efficiency and that this energy can be stored in the methane product.

An initial screening of emerging biofuel production technologies for lignocellulosic feedstock shows that the carbon efficiencies that can be obtained practically, using current “state-of-the-art” process configurations, are 25-50%, i.e. significantly lower than the theoretical efficiencies. There are several reasons for this

- 1) the limitation posed by the different element composition of feedstock and product, studied in the theoretical analysis
- 2) biomass feedstock is used both as carbon source and as energy source, which usually means that some of the feedstock is combusted in the process
- 3) by-product formation and side reactions, which lead to the formation of carbon-containing streams other than the main desired product

Integrated electrification can provide means to improve the carbon efficiency. Previous research studies have investigated the effects for specific combinations of biofuel production technologies and electrification options. The broader analysis and synthesis done in this project for a large number of combinations show that the two most important technology categories for electrification were

- 1) Electrolysis of water for hydrogen addition to the biomass conversion process, which can address the limitations posed by the different element composition of feedstock and product.
- 2) Electric heating, which can address the use of part of the biomass feedstock as energy source, by replacing this with electric energy. The technology used differs depending on the specific process, and ranges from high temperature direct heating of chemical reactors to (relatively) low temperature heat pumps that can supply low pressure process steam demands.

Ten different specific lignocellulosic-based biofuel production pathways were selected to study in more detail the effect of integrated electrification on carbon efficiency, energy efficiency, production costs and GHG performance. The selection was done based on relevance in a future Nordic context and electrification potential. The tracks are

- Gasification-based drop-in fuels through Fischer-Tropsch synthesis combined with entrained flow BL gasification, oxygen-blown FB gasification, and indirect dual-FB gasification
- Gasification-based methane/synthetic natural gas through catalytic methanation combined with oxygen-blown FB gasification and indirect dual-FB gasification
- Gasification-based methanol through catalytic synthesis combined with entrained flow BL gasification
- Pyrolysis-based drop-in fuels through fast pyrolysis and catalytic hydrotreatment
- HTL-based drop-in fuels through hydrothermal liquefaction and catalytic hydrotreatment
- Ethanol through lignocellulosic sugar-based fermentation
- Jet fuel through ethanol production (see above) in combination with catalytic dehydration and oligomerization (so called alcohols to jet)

A fairly detailed process modelling-based analysis of these tracks shows clearly that integrated electrification has a great potential to improve carbon efficiency (as illustrated in Figure 39 above). The base case process options have electricity inputs between -10% and 10% (negative numbers means electricity production) and carbon efficiencies between 20% and 50%. There is a clear increase in fuel carbon efficiency with electrification for all production pathways.

The most electrified cases with the highest potential carbon efficiencies are based on gasification. These have electricity inputs that are around 2/3 of total input, which means that there is around twice as much electric energy used as biomass energy, truly motivating the nomenclature “bio-electrofuels”. The main electrification technology used in these cases is addition of electrolysis-based hydrogen to the syngas, but also electric heating can contribute. The increase in carbon efficiency, and thus production potential for a given amount of biomass, can be increased threefold for many gasification tracks. The resulting carbon efficiency can approach 100%, in agreement with previous studies of gasification (Hannula 2016), and even increase that, if integration effects are included.

Production based on other technologies than gasification can be electrified to a lower extent and show a little bit lower increase in efficiency. For biomass liquefaction-based tracks, around 60% carbon efficiency can be reached at around 25% electricity input.

The *total* carbon and energy efficiencies, i.e. also including *energy by-products* (such as lignin pellets from ethanol production) and heat, show similar trends as the fuel-based efficiencies but the improvement in efficiency with electrification for most non-gasification-based tracks is now larger, since by-products are more important for these, especially ethanol-based tracks.

The electrification does not have a major generic systematic impact on the fuel production energy efficiency, which means that the conversion of added electricity to biofuel product is not less efficient (on energy terms) than the original process from biomass to biofuel.

The marginal efficiency for electricity addition for each of the electrified cases provides more detail than the general energy efficiencies since each electrification option is in this case compared to the base case of the same technology track. The marginal electricity efficiency is varying between 30% and 80% depending on track and electrification technology. The pure electrofuel tracks show an electricity-to-fuel efficiency of approximately 50%, using the same assumptions and methodology.

For the gasification-based tracks, marginal electricity efficiencies can reach as high as 80% and in general shows a trend of decreasing marginal electricity efficiencies with increasing electricity addition. For high degrees of electrification, >50% electricity input, the marginal efficiency approaches the 50% efficiency for the e-fuel tracks. For lower degrees of electrification (5-35% electric energy input), the marginal efficiency is often >70%. It is clear that using an electric heated reformer, where relevant, is very energy-efficient with 75-80% marginal efficiency.

For the non-gasification tracks, adding electrolysis hydrogen to the HTL process stands out as the most energy-efficient option, while marginal efficiencies are in general somewhat lower for pyrolysis and ethanol-based tracks.

If it is assumed that the excess heat from biofuels production can replace bio-based CHP, very high overall carbon efficiencies are obtained due to the avoided incineration of biomass for CHP in combination with the high carbon efficiencies of the bio-electrofuel tracks that generate the excess heat. Several tracks obtain carbon efficiencies >150% with these system boundaries. The efficiencies calculated by this approach from can be viewed as a “limiting case”, since it is not realistic that it would be feasible for all excess heat to replace biomass combustion-based heating. It can, however, be seen as a very strong argument to design and locate biofuel production plants to facilitate waste heat recovery and use in a biomass resource-constrained future society.

Assessment of the potential for cost savings or additional revenues from intermittent operation and flexibility services, based on electrolyzer over-capacity and hydrogen storage, was carried out. The analysis was based on scenarios for future electricity price variability and historical values for flexibility services. The uncertainty in future electricity prices and the lack of scenarios for future values of flexibility services make the results are highly uncertain. A conclusion is that intermittent on/off operation and hydrogen storage to decrease average electricity purchase price does not seem to show a significant potential to decrease production costs for bio-electrofuels production. The potential to offer flexibility services to the grid operator can decrease the net electricity cost by

4-7 €/MWh, i.e. 10-20% of the average electricity price in the electricity system scenarios used. We have chosen not to explicitly include intermittent operation, hydrogen storage and flexibility services in the techno-economic calculations. Instead, they are implicitly included in the electricity price scenarios.

A techno-economic analysis conducted with assumptions relevant for Nordic conditions shows that the production cost for all bio-electrofuel tracks evaluated fall between 60 and 140 €/MWh assuming 30-40 €/MWh electricity costs. The higher-end of the range, 100–140 €/MWh, correspond to direct liquefaction (HTL and fast pyrolysis) and FT technologies. The lower end of the production cost range, 60–100 €/MWh, correspond to methanol, SNG, bioethanol and ATJ technologies. The production cost of the reference electrofuel tracks eFT, eMeOH and eSNG are in each case higher than the corresponding bio- and bio-electrofuel tracks.

The change in production cost with increasing electrification and carbon efficiency is different for different tracks. Typically, the specific cost increases with increasing electrification for the low cost tracks (SNG, methanol, ethanol) but still in all cases staying below the eSNG and eMeOH production costs. For gasification-based drop-in fuels (FT), the change in production cost with increasing electrification is much smaller and can go either up or down, depending on the gasification technology and configuration. In general, there is no or very small cost for increasing the biomass resource efficiency for these tracks. For the liquefaction-based tracks, the production cost decreases with increasing electrification. This is due to the assumption of using biogas-based hydrogen in the base cases, which was done in order to have comparable climate performance between configurations.

A sensitivity analysis with respect to biomass cost shows somewhat changing trends for a scenario of doubled biomass prices. For SNG, methanol and ethanol, bio-fuels and bio-electrofuels still have lower production cost than the corresponding e-tracks. But for drop-in fuels, the base case biofuel production cost is now higher than e-FT. It decreases clearly with increasing electrification and the bio-electrofuel options have lower production costs than e-FT.

The GHG performance of all base case biofuel production configurations were high, as all fossil inputs were avoided by the choice of design, and the emissions were primarily driven by the biomass supply chain. The use of biogenic residues, according to the renewable energy directive, only carries the GHG footprint of collection and transport. As the share of electricity in the input increases, the GHG performance becomes more sensitive to electricity emission factors. For a 13.1 kgCO<sub>2</sub>eq/GJ electricity emission factor scenario, the bio-electrofuel tracks can achieve 76%–98% GHG emission reduction potential while the pure electrofuel tracks achieved 61%–75%. A zero-emission electricity source would enable the heavily electrified bio-electrofuel tracks achieve over 97% GHG emissions reduction, while all electrofuel tracks converge at 100%.

A scenario analysis was made in order to assess the impact that large-scale implementation of bio-electrofuels technology could have on the possibility to supply transport fuel for Swedish demands. The analysis shows that using “base case” biofuels technology, with limited carbon efficiency, leads to very large biomass demand for meeting the transport fuel demand, which indicates that biofuels alone is not a realistic option. For the 2030 scenarios, only 30-50% of the demand can be supplied by the biofuel production technologies (“gasification base” and “refinery base”) from domestic sustainable biomass resources. On the other hand, the electricity demands for meeting the

liquid transport fuel demands by electrofuels only are huge, 80-140 TWh/y, despite assumed significant electrification of road transport.

Hence, it is clear that a combination of biofuels and electrofuels is required. From the electricity demand and production cost scenarios, it is clear that bio-electrofuels, i.e. combining the “bio” and the “electro” in a single production process is more efficient and has lower cost than building separate processes.

Another benefit of the bio-electrofuels processes, with high carbon efficiencies, is the avoided direct emissions of CO<sub>2</sub> from the biofuel production process. These emissions do not substitute any fossil emissions and are, hence, not creating any benefit. If the carbon is instead bound in fuel products, it is still released as CO<sub>2</sub> to the atmosphere when the fuels are used, but since the biofuel products substitute fossil fuel products, there is a climate benefit. Using dynamic LCA or other comparable methodologies that quantify this aspect of the bio-electrofuels technology is something that would be an interesting topic of further research (Cintas et al. 2017).

The production and electrification technologies included in this study are either commercial or currently being commercialized. Most of the technology options being looked at can be implemented already now, even if the cost and technology risk will decrease with time. All technologies are believed to be commercially available until 2030, allowing large scale implementation without an extensive technology risk. In the present situation, there are currently not always incentives for project developers and investors to choose novel carbon-efficient production technologies over technologies with lower resource efficiency. The demand for residue-based biogenic feedstocks, for example bark and saw dust, is today not large enough to lead to increased prices, which would make bio-electrofuels more cost-competitive. The plants being planned today will, however, operate for at least 15-20 years, which from a societal point-of-view makes it motivated to support resource efficient and future proof process configurations. Development of policy/incentives that promotes resource efficient use of limited biogenic resources in biorefineries is thus highly motivated.

Legislation is and will be an important factor in the commercialization of bio- and electrofuels and the construction of large-scale production plants. A major aspect is the sustainability criteria and the “fuel type classification” in the EU legislation, since these determine the conditions for a number of other aspects of great importance, such as the minimum tax rates, the possibility to fulfill specific quotas towards renewable energy, etc. In the current Renewable Energy Directive, two relevant definitions of fuel types are:

- advanced biofuels – “means biofuels that are produced from the feedstock listed in Part A of Annex IX”;
- renewable liquid and gaseous transport fuels of non-biological origin (RFNBO) – “means liquid or gaseous fuels which are used in the transport sector other than biofuels or biogas, the energy content of which is derived from renewable sources other than biomass”

From the results of this study, it is clear that the most carbon efficient bio-electrofuels (produced by extensive indirect electrification of biofuels production) are produced from feedstocks qualifying as “advanced biofuels”. At the same time, most of the energy “is derived from renewable sources other than biomass”, which is normally associated with RFNBO (or electrofuel). Classification of the fuel is of great importance, since sustainability criteria and the methodology for estimating

GHG performance may be different. The current view is that there may be significant restriction on what electricity can be used for RFNBO production<sup>7</sup>. On the other hand, biofuels can use grid electricity purchase and count the average grid GHG intensity in the GHG performance of the product. It will be of utmost importance for the further development of the bio-electrofuels technology to obtain a firm understanding of the legislative status of this type of product.

Based on the results of the project, summarized above, the following overall conclusion can be made:

- Integrated electrification of biofuel production, leading to so called bio-electrofuels, can greatly improve biomass resource efficiency.
- The most important electrification technologies that can lead to this improvement in efficiency are water electrolysis, high-temperature direct electric heating and heat pumps.
- Gasification-based biofuel production from lignocellulosic biomass shows the greatest potential for integrated electrification. The amount of transportation fuels that can be produced from the same amount of biomass can in many cases be doubled or tripled.
- Also other lignocellulosic-based production technologies show potential for integrated electrification with good efficiency improvements, but smaller than gasification
- The overall energy efficiency of the process is in general not negatively affected by the electrification. There are differences depending on the production technology with either small improvements in energy efficiency or small decreases.
- The production costs for bio-electrofuels are similar to or somewhat higher than the corresponding biofuels production costs, but lower than the corresponding electrofuels cost. This indicates that indirect electrification is cost-efficient.
- The greenhouse gas performance of all options studied – biofuels, bio-electrofuels and electrofuels – are in general good as long as the GHG footprint of the electricity used in the process is low.
- A scenario analysis for production to meet the demand of the future transport sector demand for liquid and gaseous fuels was made. The results indicate that improving biomass resource efficiency by indirect electrification leads to the possibility to meet demand based on domestic sustainable biomass resources, which was not possible using state-of-the-art biofuel production technology with lower carbon efficiency.
- Development of policy/incentives that promotes resource efficient use of limited biogenic resources in biorefineries is highly motivated to future-proof the biofuel production capacity being built up in the coming years. The efficient bio-electrofuel technologies may not be cost-competitive compared to pure biofuels given current market conditions.

---

<sup>7</sup> A delegated act to the Renewable Energy Directive is being developed by the European Commission, regarding sustainability criteria for RFNBOs. It was scheduled for December 2021 but at the writing of this report it has not been finalized. A leaked draft from the European Commission indicates severe demands on electricity, including either additionality in electricity production or only operating at time periods with a documented excess of renewable electricity in the grid.



## REFERENCES

- Alamia, Alberto, Anton Larsson, Claes Breitholtz, and Henrik Thunman. 2017. “Performance of Large-Scale Biomass Gasifiers in a Biorefinery, a State-of-the-Art Reference.” *International Journal of Energy Research* 41 (14): 2001–19. <https://doi.org/10.1002/er.3758>.
- Arvidsson, Maria, Matteo Morandin, and Simon Harvey. 2014. “Biomass Gasification-Based Syngas Production for a Conventional Oxo Synthesis Plant—Process Modeling, Integration Opportunities, and Thermodynamic Performance.” *Energy & Fuels* 28 (6): 4075–87. <https://doi.org/10.1021/ef500366p>.
- Baltrusaitis, Jonas, and William L Luyben. 2015. “Methane Conversion to Syngas for Gas-to-Liquids (GTL): Is Sustainable CO<sub>2</sub> Reuse via Dry Methane Reforming (DMR) Cost Competitive with SMR and ATR Processes?” *ACS Sustainable Chemistry & Engineering* 3 (9): 2100–2111. <https://doi.org/10.1021/acssuschemeng.5b00368>.
- Berglin, Niklas, Anders Lovell, Lennart Delin, and Janice Törmälä. 2011. “The 2010 Reference Mill for Kraft Market Pulp.” In *Tappi PEERS Conference*, 191–97. Portland, Oregon, USA.
- Börjesson, Pål. 2021. “Potential För Ökad Tillförsel Och Avsättning Av Inhemsk Biomassa i En Växande Svensk Bioekonomi - En Uppdatering.” Lund. <https://lup.lub.lu.se/record/29600a2a-724e-4e06-b407-2f5681040fec>.
- Brandberg, A., H. Hjortsberg, B. Sävbark, T. Ekbohm, C. J. Hjerpe, and I. Landälv. 2000. “BioMeeT. Planning of Biomass-Based Methanol Energy Combine - Trollhättan Region.” <https://www.osti.gov/etdeweb/biblio/20086721>.
- Brown, Thane. 2007. *Engineering Economics and Economic Design for Process Engineers*. Boca Raton, Florida, USA: CRC press, Taylor & Francis Group.
- Brynolf, Selma, Maria Taljegard, Maria Grahn, and Julia Hansson. 2018. “Electrofuels for the Transport Sector : A Review of Production Costs.” *Renewable and Sustainable Energy Reviews* 81 (February 2017): 1887–1905. <https://doi.org/10.1016/j.rser.2017.05.288>.
- Carrasco, Jose L, Sampath Gunukula, Akwasi A Boateng, Charles A Mullen, William J Desisto, and M Clayton Wheeler. 2017. “Pyrolysis of Forest Residues : An Approach to Techno-Economics for Bio-Fuel Production Q.” *Fuel* 193: 477–84. <https://doi.org/10.1016/j.fuel.2016.12.063>.
- Carvalho, Lara, Joakim Lundgren, Elisabeth Wetterlund, Jens Wolf, and Erik Furusjö. 2018. “Methanol Production via Black Liquor Co-Gasification with Expanded Raw Material Base – Techno-Economic Assessment.” *Applied Energy* 225 (November 2017): 570–84. <https://doi.org/10.1016/j.apenergy.2018.04.052>.
- Cintas, Olivia, Göran Berndes, Annette L. Cowie, Gustaf Egnell, Hampus Holmström, Gregg Marland, and Göran I. Ågren. 2017. “Carbon Balances of Bioenergy Systems Using Biomass from Forests Managed with Long Rotations: Bridging the Gap between Stand and Landscape Assessments.” *GCB Bioenergy* 9 (7): 1238–51. <https://doi.org/10.1111/gcbb.12425>.

Eichman, J, K Harrison, M Peters, J Eichman, K Harrison, and M Peters. 2014. “Novel Electrolyzer Applications : Providing More Than Just Hydrogen Novel Electrolyzer Applications : Providing More Than Just Hydrogen.” *NREL Report*.  
<http://www.nrel.gov/docs/fy14osti/61758.pdf>.

Ekbom, Tomas, Mats Lindblom, Niklas Berglin, and Peter Ahlvik. 2003. “Technical and Commercial Feasibility Study of Black Liquor Gasification with Methanol/DME Production as Motor Fuels for Automotive Uses - BLGMF.” Stockholm, Technical report Contract No. 4.1013/Z/01-087/2001. [https://doi.org/Contract No. 4.1013/Z/01-087/2001](https://doi.org/Contract%20No.%204.1013/Z/01-087/2001).

Energiforsk. 2021. “Konkurrensen Om Den Svenska Skogsråvaran.” *Energiforsk*.  
<https://energiforsk.se/konferenser/genomforda/konkurrensen-om-den-svenska-skogsravaran/>.

Energimyndigheten. 2019. “Kontrollstation 2019 För Reduktionsplikten.” <http://trafikverket.diva-portal.org/smash/get/diva2:1484716/FULLTEXT01.pdf>.

Fornell, Rickard. 2012. “Process Integration Studies on Kraft Pulp-Mill- Based Biorefineries Producing Ethanol.” Chalmers University of Technology, Heat and Power Technology, Department of Energy and Environment, Doctoral Thesis.  
<http://publications.lib.chalmers.se/records/fulltext/157451.pdf>.

FossilfrittSverige. 2021. “Strategi För Fossilfri Konkurrenskraft: BIOENERGI OCH BIORÅVARA.” <https://fossilfrittsverige.se/strategier/biostrategi/>.

Frankó, Balázs, Mats Galbe, and Ola Wallberg. 2016. “Bioethanol Production from Forestry Residues: A Comparative Techno-Economic Analysis.” *Applied Energy* 184 (2016): 727–36.  
<https://doi.org/10.1016/j.apenergy.2016.11.011>.

Geleynse, Scott, Kristin Brandt, Manuel Garcia-Perez, Michael Wolcott, and Xiao Zhang. 2018. “The Alcohol-to-Jet Conversion Pathway for Drop-In Biofuels: Techno-Economic Evaluation.” *ChemSusChem* 11 (21): 3728–41. <https://doi.org/10.1002/cssc.201801690>.

Glenk, Gunther, and Stefan Reichelstein. 2019. “Economics of Converting Renewable Power to Hydrogen.” *Nature Energy* 4 (3): 216–22. <https://doi.org/10.1038/s41560-019-0326-1>.

Gode, Jenny, Fredrik Martinsson, Linus Hagberg, and David Palm. 2011. “Miljöfaktaboken 2011 Uppskattade Emissionsfaktorer För Bränslen, El, Värme Och Transporter.” *Anläggnings- Och Förbränningsteknik*, 121.  
<https://energiforskmedia.blob.core.windows.net/media/17907/miljoefaktaboken-2011-vaermeforskrappport-1183.pdf%0Ahttp://www.sivl.ivl.se/download/18.372c2b801403903d2751c03/>.

Habermeyer, Felix, Esa Kurkela, Simon Maier, and Ralph Uwe Dietrich. 2021. “Techno-Economic Analysis of a Flexible Process Concept for the Production of Transport Fuels and Heat from Biomass and Renewable Electricity.” *Frontiers in Energy Research* 9 (November): 1–15.  
<https://doi.org/10.3389/fenrg.2021.723774>.

- Hannula, Ilkka. 2016. “Hydrogen Enhancement Potential of Synthetic Biofuels Manufacture in the European Context: A Techno-Economic Assessment.” *Energy* 104: 199–212. <https://doi.org/10.1016/j.energy.2016.03.119>.
- Hansson, Julia, Martin Hagberg, Magnus Hennlock, Kenneth B Karlsson, Raffaele Salvucci, Magnus Andersson, Steven Sarasini, Tanu Piriya Uteng, and Magnus Wråke. 2019. “Sustainable Horizons in Future Transport - with a Nordic Focus Project Summary 2015-2019.” [https://iea.blob.core.windows.net/assets/deebef5d-0c34-4539-9d0c-10b13d840027/NetZeroBy2050-ARoadmapfortheGlobalEnergySector\\_CORR.pdf](https://iea.blob.core.windows.net/assets/deebef5d-0c34-4539-9d0c-10b13d840027/NetZeroBy2050-ARoadmapfortheGlobalEnergySector_CORR.pdf).
- Holmgren, Kristina M., Thore S. Berntsson, Eva Andersson, and Tomas Rydberg. 2016. “Comparison of Integration Options for Gasification-Based Biofuel Production Systems - Economic and Greenhouse Gas Emission Implications.” *Energy* 111: 272–94. <https://doi.org/10.1016/j.energy.2016.05.059>.
- Hovsapian, Rob. 2017. “Role of Electrolyzers in Grid Services.” U.S. Department of Energy. [https://www.energy.gov/sites/prod/files/2017/06/f34/fcto\\_may\\_2017\\_h2\\_scale\\_wkshp\\_hovsapian.pdf](https://www.energy.gov/sites/prod/files/2017/06/f34/fcto_may_2017_h2_scale_wkshp_hovsapian.pdf).
- International Energy Agency. 2021. “Net Zero by 2050: A Roadmap for the Global Energy Sector.” *International Energy Agency*. <https://www.iea.org/reports/net-zero-by-2050>.
- Jafri, Yawer, Erik Furusjö, Kawnish Kirtania, and Rikard Gebart. 2016. “Performance of a Pilot-Scale Entrained-Flow Black Liquor Gasifier.” *Energy and Fuels* 30 (4): 3175–85. <https://doi.org/10.1021/acs.energyfuels.6b00349>.
- Jafri, Yawer, Elisabeth Wetterlund, Marie Anheden, Ida Kulander, Åsa Håkansson, and Erik Furusjö. 2019. “Multi-Aspect Evaluation of Integrated Forest-Based Biofuel Production Pathways: Part 2. Economics, GHG Emissions, Technology Maturity and Production Potentials.” *Energy* 172: 1312–28. <https://doi.org/10.1016/j.energy.2019.02.036>.
- Jafri, Yawer, Elisabeth Wetterlund, Sennai Mesfun, Henrik Rådberg, Johanna Mossberg, Christian Hulteberg, and Erik Furusjö. 2020. “Combining Expansion in Pulp Capacity with Production of Sustainable Biofuels – Techno-Economic and Greenhouse Gas Emissions Assessment of Drop-in Fuels from Black Liquor Part-Streams.” *Applied Energy* 279 (September): 115879. <https://doi.org/10.1016/j.apenergy.2020.115879>.
- la Fuente, Teresa de, Sara González-García, Dimitris Athanassiadis, and Tomas Nordfjell. 2017. “Fuel Consumption and GHG Emissions of Forest Biomass Supply Chains in Northern Sweden: A Comparison Analysis between Integrated and Conventional Supply Chains.” *Scandinavian Journal of Forest Research* 32 (7): 568–81. <https://doi.org/10.1080/02827581.2016.1259424>.
- Larsson, A., C. Gustavsson, and G. Gustafsson. 2020. “Co-Generation of Biojet in CHP Plants.” Energiforsk report, report no:2020-664. <https://energiforsk.se/en/programmes/biofuels-for-sweden-2030/reports/co-generation-of-biojet-in-chp-plants-2020-664/>.
- Larsson, Anton. 2014. “Fuel Conversion in a Dual Fluidized Bed Gasifier.” Chalmers University of Technology. <https://research.chalmers.se/publication/203166>.

Larsson, Anton, I. Gunnarsson, and F. Tengberg. 2018. “The GoBiGas Project - Demonstration of the Production of Biomethane from Biomass via Gasification.”

Liang, Zhiwu (Henry), Wichitpan Rongwong, Helei Liu, Kaiyun Fu, Hongxia Gao, Fan Cao, Rui Zhang, et al. 2015. “Recent Progress and New Developments in Post-Combustion Carbon-Capture Technology with Amine Based Solvents.” *International Journal of Greenhouse Gas Control* 40: 26–54. <https://doi.org/10.1016/j.ijggc.2015.06.017>.

Liu, Guangjian, Eric D. Larson, Robert H. Williams, Thomas G. Kreutz, and Xiangbo Guo. 2011. “Making Fischer-Tropsch Fuels and Electricity from Coal and Biomass: Performance and Cost Analysis.” *Energy and Fuels* 25 (1): 415–37. <https://doi.org/10.1021/ef101184e>.

Marsidi, Marc. 2019. “Industrial Mechanical Vapour Recompression (MVR).” <https://energy.nl/old/wp-content/uploads/2019/06/Technology-Factsheet-Industrial-mechanical-vapour-recompression.pdf>.

Mesfun, Sennai, Jan-Olof Anderson, Kentaro Umeki, and Andrea Toffolo. 2016. “Integrated SNG Production in a Typical Nordic Sawmill.” *Energies* 9 (5): 333. <https://doi.org/10.3390/en9050333>.

Miljödepartementet. 2021. “Statens Offentliga Utredningar (SOU 2021:48) - I En Värld Som Ställer Om - Sverige Utan Fossila Drivmedel 2040.” <https://www.regeringen.se/rattsliga-dokument/statens-offentliga-utredningar/2021/06/sou-202148/>.

Poluzzi, A., G. Guandalini, S. Guffanti, M. Martinelli, S. Moioli, P. Huttenhuis, G. Rexwinkel, et al. 2022. “Flexible Power and Biomass-To-Methanol Plants With Different Gasification Technologies.” *Frontiers in Energy Research* 9 (January): 1–23. <https://doi.org/10.3389/fenrg.2021.795673>.

Reuß, M., T. Grube, M. Robinius, P. Preuster, P. Wasserscheid, and D. Stolten. 2017. “Seasonal Storage and Alternative Carriers: A Flexible Hydrogen Supply Chain Model.” *Applied Energy* 200: 290–302. <https://doi.org/10.1016/j.apenergy.2017.05.050>.

Schmidt, O, A Gambhir, I Staffell, A Hawkes, J Nelson, and S Few. 2017. “ScienceDirect Future Cost and Performance of Water Electrolysis : An Expert Elicitation Study.” *International Journal of Hydrogen Energy* 42 (52): 30470–92. <https://doi.org/10.1016/j.ijhydene.2017.10.045>.

Smith, Robin. 2005. *Chemical Process Design and Integration*. West Sussex, England: John Wiley & Sons Ltd.

“Stora Källor För Biogen CO2 Lista.” 2019. 2019. <https://bioenergidningen.se/app/uploads/sites/2/2019/04/Stora-kallor-för-biogen-CO2-lista.pdf>.

Susan van Dyk, and Jack Saddler. 2021. *Progress in the Commercialization of Biojet /Sustainable Aviation Fuels (SAF): Technologies, Potential and Challenges*. IEA Bioenergy.

Svenska Kraftnät. 2021. “Långsiktig Marknadsanalys.” Stockholm. <https://www.svk.se/siteassets/om-oss/rapporter/2021/langsiktig-marknadsanalys-2021.pdf>.

SvenskKraftnät. 2022. “Mimer Primärreglering.” Online. 2022. <https://mimer.svk.se/PrimaryRegulation/PrimaryRegulationIndex>.

Svenskt Näringsliv. 2019. “Högre Elanvändning År 2045.”

[https://www.svensktnaringsliv.se/bilder\\_och\\_dokument/2spdr2\\_hogre-elanvandning-2045pdf\\_1138079.html/Hgre+elanvndning+2045.pdf](https://www.svensktnaringsliv.se/bilder_och_dokument/2spdr2_hogre-elanvandning-2045pdf_1138079.html/Hgre+elanvndning+2045.pdf).

Tews, Iva J., Yunhua Zhu, Corinne Drennan, Douglas C. Elliott, Lesley J. Snowden-Swan, Kristin Onarheim, Yrjo Solantausta, and David Beckman. 2014a. “Biomass Direct Liquefaction Options. TechnoEconomic and Life Cycle Assessment,” no. July. <https://doi.org/10.2172/1184983>.

———. 2014b. “Biomass Direct Liquefaction Options. TechnoEconomic and Life Cycle Assessment.” Pacific Northwest National Laboratory (PNNL), Richland, WA (United States). <https://doi.org/10.2172/1184983>.

Thunman, Henrik, Christer Gustavsson, Anton Larsson, Ingemar Gunnarsson, and Freddy Tengberg. 2019. “Economic Assessment of Advanced Biofuel Production via Gasification Using Cost Data from the GoBiGas Plant.” *Energy Science and Engineering* 7 (1): 217–29. <https://doi.org/10.1002/ese3.271>.

Trafikverkets. 2020. “Inriktningsunderlag Inför Transportinfrastrukturplaneringen För Perioden 2022 – 2033.” Borlänge.

Wetterlund, Elisabeth, Yawer Jafri, Johan M. Ahlström, Erik Furusjö, Karin Pettersson, Simon Harvey, and Elin Svensson. 2022. “FRAMTIDSSÄKRADE BIODRIVMEDEL.” [https://f3centre.se/app/uploads/FDOS-33-2022\\_k3\\_ExSum-220323.pdf](https://f3centre.se/app/uploads/FDOS-33-2022_k3_ExSum-220323.pdf).

Wismann, Sebastian T., Jakob S. Engbæk, Søren B. Vendelbo, Flemming B. Bendixen, Winnie L. Eriksen, Kim Aasberg-Petersen, Cathrine Frandsen, Ib Chorkendorff, and Peter M. Mortensen. 2019a. “Electrified Methane Reforming: A Compact Approach to Greener Industrial Hydrogen Production.” *Science* 364 (6442): 756–59. <https://doi.org/10.1126/science.aaw8775>.

Wismann, Sebastian T., Jakob S. Engbæk, Søren B. Vendelbo, Flemming B. Bendixen, Winnie L. Eriksen, Kim Aasberg-Petersen, Cathrine Frandsen, Ib Chorkendorff, and Peter M. Mortensen. 2019b. “Electrified Methane Reforming: A Compact Approach to Greener Industrial Hydrogen Production.” *Science* 364 (6442): 756–59. <https://doi.org/10.1126/science.aaw8775>.

“Wood Fuel and Peat Prices.” 2018. Örebro.

[https://www.energimyndigheten.se/globalassets/statistik/priser/tradbransle\\_och\\_torvpriser\\_en0307\\_2018-03-05.pdf](https://www.energimyndigheten.se/globalassets/statistik/priser/tradbransle_och_torvpriser_en0307_2018-03-05.pdf).

Xie, Nan, Bin Chen, Chenghua Tan, and Zhiqiang Liu. 2017. “Energy Consumption and Exergy Analysis of MEA-Based and Hydrate-Based CO<sub>2</sub> Separation.” *Industrial and Engineering Chemistry Research* 56 (51): 15094–101. <https://doi.org/10.1021/acs.iecr.7b03729>.

Zhang, Xiao Bin, Jian Ye Chen, Lei Yao, Yong Hua Huang, Xue Jun Zhang, and Li Min Qiu. 2014. “Research and Development of Large-Scale Cryogenic Air Separation in China.” *Journal of Zhejiang University: Science A* 15 (5): 309–22. <https://doi.org/10.1631/jzus.A1400063>.

## APPENDIX 1. INTERMITTENT ELECTRIFICATION AND HYDRO-GEN STORAGE

This appendix contains details to describe methodology and support conclusions in chapter 5.

### ELECTRICITY PRICE SCENARIOS

To summarize the impact on electricity supply and demand of the presented scenarios Figure 47, Figure 48 and Figure 49 illustrate the essential differences between the scenarios. Compared to today’s consumption all of the scenarios assume an increased electricity demand as a result of electrification within transports and industry. For scenario EP, the electricity production in SE3 will increase significantly by 2045 in comparison to the other scenarios. Furthermore, the production capacity is also expected to increase for all scenarios, mostly due to the expansion of solar power.

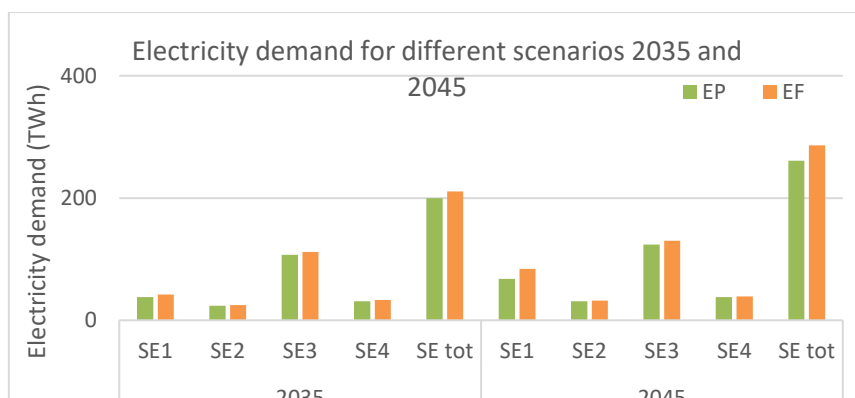


Figure 59. The projected electricity demand for 4 different scenarios divided by the electricity trading zones over the years 2035 and 2045, based on data from Svenska Kraftnät (Svenska Kraftnät 2021).

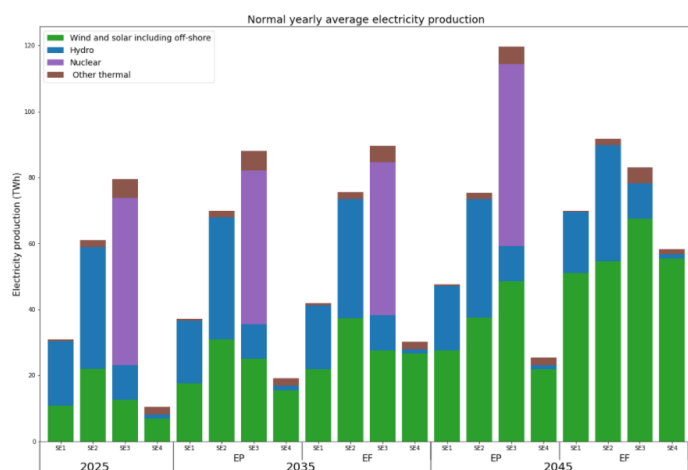
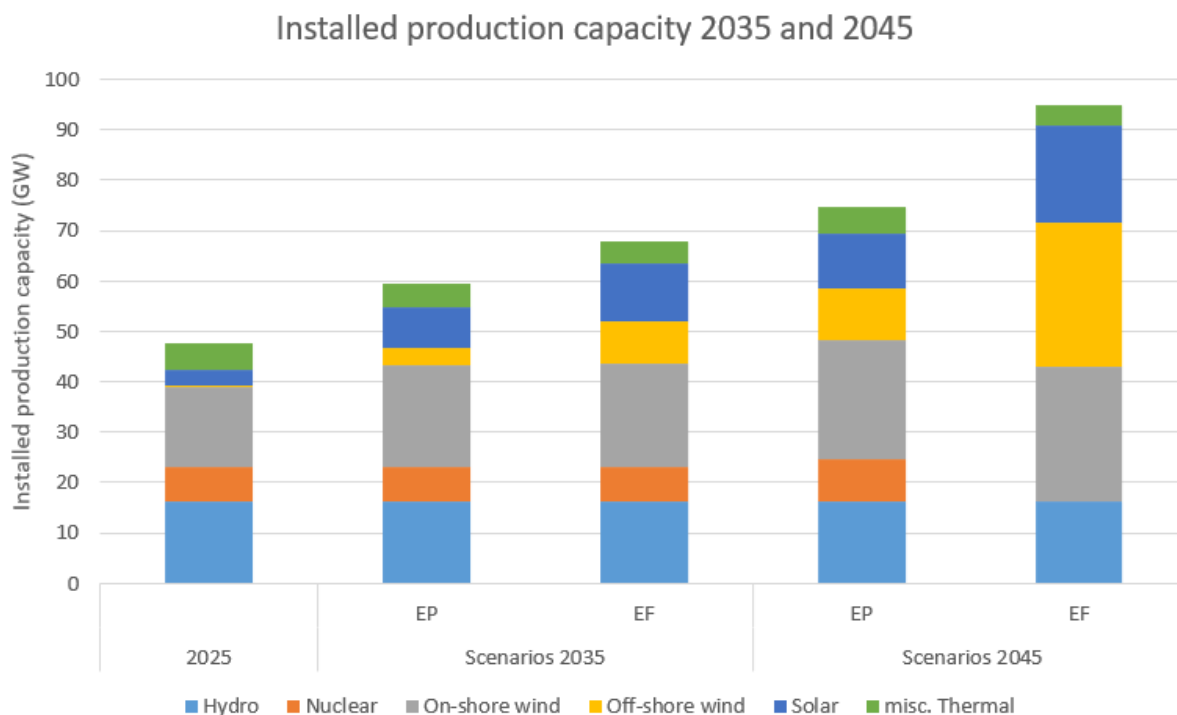


Figure 60. The normal yearly average electricity production for 2025, 2035 and 2045, based on data from Svenska Kraftnät (Svenska Kraftnät, 2021).



**Figure 61.** The projected installed production capacity divided over the different scenarios, based on data from Svenska Kraftnät (Svenska Kraftnät, 2021).

Through simulations conducted by the TSO Svenska Kraftnät based on the scenarios and different weather years, a normal energy balance was obtained as can be seen in Figure 50. In 2035 we can see that the balance is approximately the same as today for all zones, except for SE1, which in the two higher-electrification scenarios is simulated to be a net consumer instead of net producer. For 2045, the balance varies a lot depending on the scenario except for SE2 and SE3, which remain net producers and consumers respectively. SE1 will either become a net producer or consumer depending on the degree of electrification within the steel and iron industry. For SE4 the situation depends on how much off-shore wind is going to be located in the region. If the expansion is fully implemented, the zone will have a large electricity surplus, otherwise it will remain a net consumer of the approximate same magnitude as today.

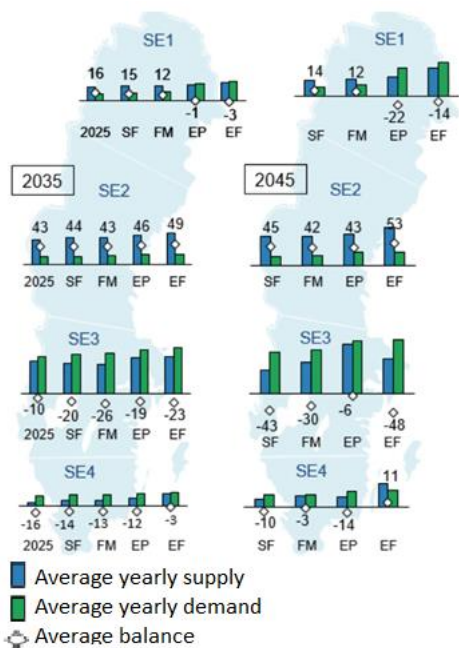


Figure 62. The simulated normal energy balance in TWh for the different scenarios by 2035 and 2045, (Svenska Kraftnät, 2021).

The normal average prices of electricity simulated for the different scenarios and trading zones are presented in Figure 51.

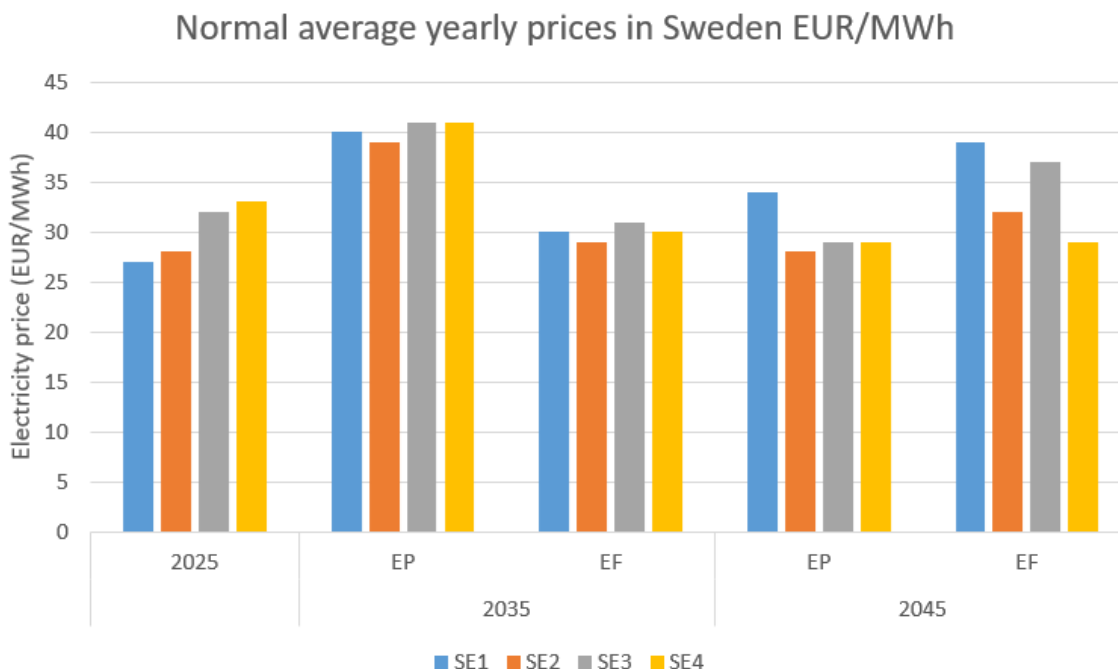


Figure 63: Normal average yearly prices for the different scenarios by 2035 and 2045, based on data from Svenska Kraftnät (Svenska Kraftnät, 2021).

## METHODOLOGY FOR ELECTRICITY PRICE MINIMIZATION

In Equation 1, the problem is mathematically described.

$$\begin{aligned}
 \min_P \quad & \sum_{i=1}^N P_i \cdot price_i \\
 \text{s.t.} \quad & P_{stor,i} - P_i = -P_{use} & \forall i \in N \\
 & E_{stor,i} - P_{stor,i} - E_{stor,i-1} = 0 & \forall i \in N \\
 & P_i = \begin{cases} P_i & \text{if } price_i < maxbuy \\ else 0 & \end{cases} & \forall i \in N \\
 & 0 \geq P_i \geq P_{use} + P_{oversize} & \forall i \in N \\
 & -P_{use} \geq P_{stor,i} \geq P_{oversize} & \forall i \in N \\
 & 0 \geq E_{stor,i} \geq storsize \cdot 24 & \forall i \in N
 \end{aligned} \tag{1}$$

Table 1 describes all of the variables and parameters that have been used in this study.

Variable/Parameter	Description	Value, [Unit]
$P_i$	The power purchased from the grid at time step $i$	[MWh/h]
$N$	The optimization horizon	8736, [h]
$price_i$	The spot price of electricity at time step $i$	Values from simulations (Svenska kraftnät, 2021), [€/MWh]
$P_{stor,i}$	The power going into or out off the storage at time step $i$ .	[MWh/h]
$E_{stor,i}$	The state of charge at time step $i$	[MWh]
$maxbuy$	The highest price at which the electrolyzer is allowed to purchase electricity from the grid	10-1000, [€/MWh]
$P_{oversize}$	Electrolyzer over capacity compared to the constant demand	10-100, [%]
$P_{use}$	The constant demand required for the production process	1 (would yield the same result for any value), [MWh/h]
$Storsize$	The size of the storage	2 or 5, [days]

## APPENDIX 2. EQUIPMENT COST FOR MAJOR PROCESS UNITS

Process section	Scaling parameter	Scaling exp.	Base size (S <sub>0</sub> )	Base cost (C <sub>0</sub> ) M€ <sup>a</sup>	Base year		Reference
Feedstock handling and feeding system							
Gasification feed handling system	production, MW <sub>th</sub>	0.65	100	31	2014		(Thunman et al. 2019)
Belt dryer	production, MW <sub>th</sub>	0.65	100	7	2014		(Thunman et al. 2019)
Gasification feeding system	production, MW <sub>th</sub>	0.60	20	6	2014		(Thunman et al. 2019)
Air separation unit (ASU)	oxygen, ton/day	0.75	576	27	2013		(Mesfun et al. 2016)
Liquefaction feed handling & prep	feedstock, ton <sub>wet</sub> /h	0.77	65	10	2014		(Tews et al. 2014b)
Main conversion units							
Entrained flow gasifier (black liquor)	BL, tBLS/day	0.70	500	24	2017		(Jafri et al. 2020)
Dual fluidized bed gasifier	biomass feed, MW <sub>th</sub>	0.60	100	60	2020		BioShare
Fluidized bed gasifier	biomass feed, MW <sub>th</sub>	0.60	170	70	2020		BioShare
Hydrothermal liquefaction reactor	feed, ton <sub>DM</sub> /day	0.70	500	114	2014		(Tews et al. 2014b)
Fast pyrolysis reactor	feed, ton <sub>DM</sub> /h	0.40	10	12	2000		(Tews et al. 2014b)
Hydrogen plant	production, ton <sub>H<sub>2</sub></sub> /day	0.70	16	31	2014		(Tews et al. 2014b)
Intermediate product refining units							
Compressor	feed, kmol/h	0.70	285	4	2014	b	(Thunman et al. 2019)
Conventional steam reforming (SMR)	feed, kmol/h	0.60	31 733	74	2014		(Baltrusaitis and Luyben 2015)
Electrified steam reforming (eSMR)	feed, kmol/h	0.60	31 733	37	2014	c	
Water gas shift (WGS)	raw syngas, Nm <sup>3</sup> /h	0.65	59 000	6	2009		(Jafri et al. 2020)
Acid gas removal (amine wash)	shifted syngas, Nm <sup>3</sup> /h	0.65	15 695	2.5	2018		(Jafri et al. 2020)
Zinc bed	HHV biomass, MW <sub>th</sub>	0.65	216	2.3	2012		(Arvidsson, Morandin, and Harvey 2014)
H <sub>2</sub> S scrubber	feed, kmol/h	0.70	285	1	2014	b	(Thunman et al. 2019)
PEM electrolyser	electricity input, MW	1	1	0.8	2016	d	(Glenk and Reichelstein 2019)
SOEC electrolyser	Electricity input, MW	1	1	1.2	2018		(Brynnolf et al. 2018)
SMR/rWGS	feed, kmol/h	0.60	31 733	74	2014	e	(Baltrusaitis and Luyben 2015)

Carbon capture (amine technology)	separated CO <sub>2</sub> , kton	1	1	0.05	2015		(Brynnolf et al. 2018)
Mechanical vapor recompression (MVR)	heat delivered, MW <sub>th</sub>	1	1	0.5	2018		(Marsidi 2019)
Biofuel synthesis							
Fischer Tropsch synthesis reactor	syngas feed, Nm <sup>3</sup> /h	0.75	70 630	56	2007	f	(Liu et al. 2011)
Methanol Synthesis reactor	MeOH, ton/day	0.65	465	26	2017		(Jafri et al. 2020)
Synthetic natural gas reactors	syngas feed, kmol/h	0.70	285	5.2	2014	b	(Thunman et al. 2019)
Final product refining and upgrading							
HTL oil upgrading	HTL oil flow, ton/day	0.70	184	16	2014		(Tews et al. 2014b)
Pyrolysis oil upgrading	Pyro oil flow, ton/day	0.70	360	57	2014		(Tews et al. 2014b)
Fischer Tropsch upgrading	FT crude, ton/day	0.65	6	15	2007		(Liu et al. 2011)
Methanol upgrading	MeOH, ton/day	0.65	465	17	2017		(Jafri et al. 2020)

<sup>a</sup>Base cost other than Euro converted to Euro equivalent using average annual exchange rate of the reference year.

<sup>b</sup>Original cost reported for 20 MW biofuel product plant capacity. The scaling parameter was converted to molar flow.

<sup>c</sup>Assumed to be half of that of SMR due to the significant size reduction expected with the design of eSMR configuration (Wismann et al. 2019b). Besides, no side-fired combustor is need for eSMR configuration which further reduces the capital cost compared to traditional SMR.

<sup>d</sup>PEM electrolyser cost refers to projected cost for 2030, in line with the timeline this study considers.

<sup>e</sup>Following internal discussion with project partners, it is possible to run a steam reformer in reverse water-gas-shift (rWGS) mode by fine tuning the operating parameters (temperature, pressure, steam, catalyst) to favour desired products. The cost of rWGS is thus assumed to be the same as that of steam-methane reformer.

<sup>f</sup>FT synthesis cost recalculated to reflect the configuration used in this study. The source reported aggregated cost for FT synthesis, ATR, FT refining and recycle compressor. Cost for reformer and recycle compressor are deducted.

## APPENDIX 3. CAPEX AND SPECIFIC INVESTMENT

Track	Process configuration	Specific investment			
		[k€/MW-biofuel]	TFCI [M€]		
E-fuels	eFT		5 962	858	
	eMeOH		4 874	700	
	eSNG		4 121	829	
	eSNG		4 121	829	
BLGFT	Base	SMR	3 981	498	
		xSMR	3 675	530	
	No WGS	PEM	3 275	696	
		SOEC	3 601	765	
	rWGS	PEM	3 271	1 295	
		SOEC	3 981	1 577	
	Base	eSMR	3 868	502	
		xeSMR	3 425	547	
	No WGS	PEM	3 159	737	
		SOEC	3 501	816	
BLGMeOH	rWGS	PEM	3 086	1 429	
		SOEC	3 785	1 752	
	Base	Base	2 856	458	
		PEM	2 514	679	
	No WGS	SOEC	2 865	774	
		PEM	2 397	1 094	
	rWGS	SOEC	2 973	1 357	
		Base	2 785	171	
	EtOH	MVR		3 080	189
		MVR + rWGS	PEM	3 202	350
MVR + rWGS		SOEC	3 605	394	
Base			3 692	252	
HTL	HTL biogas	PEM	3 663	250	
		SOEC	3 814	260	
	No biogas	PEM	3 663	250	
		SOEC	3 814	260	
Pyro	Base		4 889	93	
		PEM	4 898	94	
	No biogas	SOEC	5 141	98	
			2 044	184	
DFBSNG	Base	Preheat	2 038	184	
		PEM	1 994	211	
	No WGS post	SOEC	2 117	224	
		PEM	2 107	279	
	No WGS pre	SOEC	2 377	315	
		PEM	2 251	409	
rWGS	SOEC	2 673	485		

	Base	SMR	5 108	301
		eSMR	3 653	309
DFBFT	No WGS	PEM	3 807	483
		SOEC	4 110	522
	rWGS	PEM	3 843	509
		SOEC	4 176	554
O2FBSNG	Base		1 909	306
	No WGS post	PEM	1 959	342
		SOEC	2 011	351
	No WGS pre	PEM	2 239	737
		SOEC	2 617	862
	rWGS	PEM	2 306	893
O2FBFT	Base	SOEC	2 752	1 066
		SMR	4 827	506
	No WGS	eSMR	3 240	494
		PEM	4 005	1 148
ATJ	Base	SOEC	4 137	1 186
		SMR	3 163	432
	MVR		3 475	475
	MVR + rWGS	PEM	3 423	854
	MVR + rWGS	SOEC	3 838	958

## APPENDIX 4. MVR APPLICATION TO LIGNOCELLULOSIC ETHANOL PROCESS

### PRETREATMENT

To remove the demand of steam for pretreatment an MVR could be interesting since there is low-pressure steam leaving the flash tanks in this system. The two main questions for MVR integration are if there is enough flash steam, and if the temperature lift is realistic. One other aspect to consider for practical use is the risk of accumulation of compounds in the flash steam when recycling. A description of the relevant flows in a SO<sub>2</sub>-catalysed steam explosion pretreatment is shown in Figure 64.

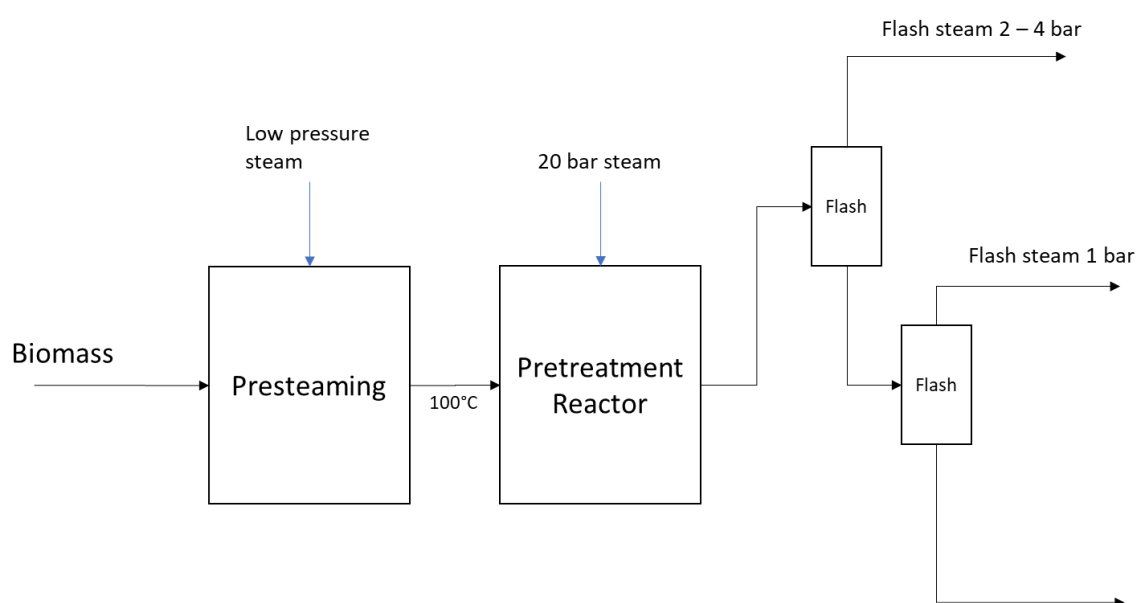


**Figure 64. Block flow diagram of potential vapor streams in SO<sub>2</sub>-catalysed steam explosion pretreatment of softwood with 2 flash drums at different pressures.**

With regards to the temperature lift a good measure of finding a realistic lift (or pressure increase) is to look at the Coefficient of Performance (COP). The COP is equal to the amount of heat  $Q_h$  at high temperature that you can get out from an input of electricity  $W$  (c.f. Figure 3). Typical values for the Coefficient of Performance obtained in industry for MVR heat pumps are at least 3.5, but COPs above 10 are achievable (Klop, 2015).

Simulations in SuperPro Designer have been made for steam pretreatment of lignocellulosic biomass to study the effect of pressure/temperature of flash steam and the integration of an MVR. The results indicate that it is possible to cover the 20-bar steam demand in the pretreatment reactor with flash steam using vapor recompression. The pressure increase, and thus temperature lift, will need to be high, however. Most likely temperature lifts of 90-100°C and a pressure increases of 18 bar would be needed to match the steam demand and the production of recompressed flash steam. The COP for this MVR would most likely lie below 3.5, but not too far away from a COP of 3.

The 20 bar steam is covered using an MVR and flash steam, but the steam needed for pre-steaming will not be covered by the atmospheric flash drum. Thus, the problem of supplying steam to the pretreatment is not entirely solved by the MVR approach. An MVR with a conservative COP of 3 is assumed to replace the 20 bar steam demand of the pretreatment process.

## DISTILLATION

A number of scientific studies have assessed the best designs of distillation systems for ethanol production. The consensus in these studies is that three internally integrated distillation columns are the best design when considering both heat demand and investment costs. There are also commercial designs in 1<sup>st</sup> generation ethanol plants, e.g., at Agroetanol in Norrköping Sweden and many other places around the world (Vogelbusch, 2021), who have come to this conclusion. MVR-integrated distillation systems have also been presented in several of the studies conducted but based on the assumptions in these investigations the MVR option is expensive compared to heat integrated distillation given the price of electricity and the cost of the heat pump.

In (Humbird D., 2021) a design of an ethanol distillation system was developed in Aspen Plus together with commercial suppliers (Figure 65). Applying an MVR heat pump with a COP of around 4 in this system would reduce the reboiler demand to approximately 35% of the original steam demand. It is also stated in the report that the reboiler demand in this case is high in order to recover as much ethanol as possible and should also be noted that the demand in the Beer column is very much dependent on the concentration of ethanol in the Beer (in this case the concentration was approximately 5%).

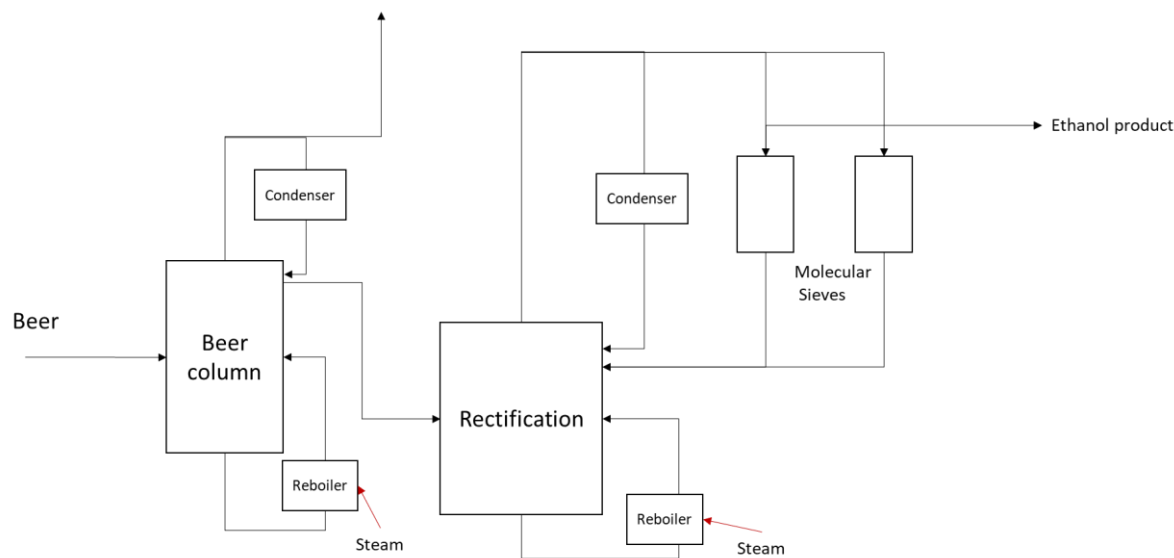


**Figure 65 Distillation system design according to (Humbird D., 2021).**

There are many degrees of freedom when designing distillation columns and the further upgrading of ethanol across the azeotrope of ethanol and water (at 90-95% ethanol concentration). An MVR with COP 3 is assumed to replace the steam demand of the reboilers.

## DRYING

If drying of the solid by-product fraction in the ethanol plant is needed, e.g. as in the reference case where pellets are seen as the product of choice, then heat pumps that recompress the energy in the exhaust from the drier and use it to heat the feed stream (e.g. steam or air) are of interest. There are a number of existing industrial applications of heat pumps in combination with drying (c.f. (IEA, 2014)) and typical reductions of steam demand mentioned are 50 – 60%. Of course, there are also a lot of possibilities to design drying systems to reduce or even remove the steam demand, but since this level of detail is not the focus of this assessment, and since the reference process utilizes steam drying, we can, based on existing systems in industry, conclude that at least a 50% reduction of steam can be easily obtained in a typical ethanol process.

## APPENDIX 5. ADDITIONAL DATA FOR PROCESS MASS AND ENERGY BALANCES

This appendix contains detailed process modelling results that were excluded from chapter 6 to improve readability. Specific tables and figures are always referred to from the main text, to provide the correct context.

**Table 26 Lignocellulosic ethanol carbon and energy balance.**

Case (acronym)	EtOH		EtOH_MVR		EtOH_MVR_H2		
	Carbon	Energy	Carbon	Energy	Carbon	Energy	Energy
	kg/h	MW	kg/h	MW	kg/h	MW	MW
						SOEC	PEM
<b>Input</b>							
Feedstock	13 402	137	13 402	137	13 402	137	137
Electricity		0		9		84	92
<b>Main output</b>							
Ethanol	3 028	48	3 028	48	3 028	48	48
Biogas/SNG	658	14	658	14	2 987	61	61
Pellets	3 873	42	6 208	68	6 206	68	68
Electricity		2		0		0	0
<b>Other</b>							
Ferm. CO2	1 669		1 669				
AD CO2	720		720				
Flue gas	3 293		968		968		
District heat		4		4		5	5
Cold utility		28		24		50	59
Wastewater	160		151		213		

**Table 27 Lignocellulosic ethanol to Jet fuel carbon and energy balance.**

Scenario	EtOH2Jet		EtOH2Jet_H2		
	Carbon	Energy	Carbon	Energy	
	kg/h	MW, HHV	kg/h	MW, HHV	
				SOEC	PEM
Input (background process)					
Feedstock	31 639	324	31 636	324	324
Electricity		0		197	216
Output (background process)					
Ethanol	7 136	113	7 136	113	113
Biogas/SNG export	1552	32	7 050	145	145
Pellets	9 151	100	14 636	160	160
Electricity		6		0	0
Fermentation CO <sub>2</sub>	3 940				
AD CO <sub>2</sub>	1 699				
Flue gas	7 772		2 284		
District heat		9		3	3
Wastewater	378		519		
Cold utility		64		99	119
Input (ATJ)					
Ethanol	7 136	113	7 136	113	113
Biogas	938	17	0	0	0
Electricity		1		18	19
Output (ATJ)					
Jet	6 266	93	6 266	93	93
Diesel	820	12	820	12	12
Other (ATJ)					
Flue gas	987				
District heat		8		6	6
Cold utility		18		20	21
Wastewater	49		49		

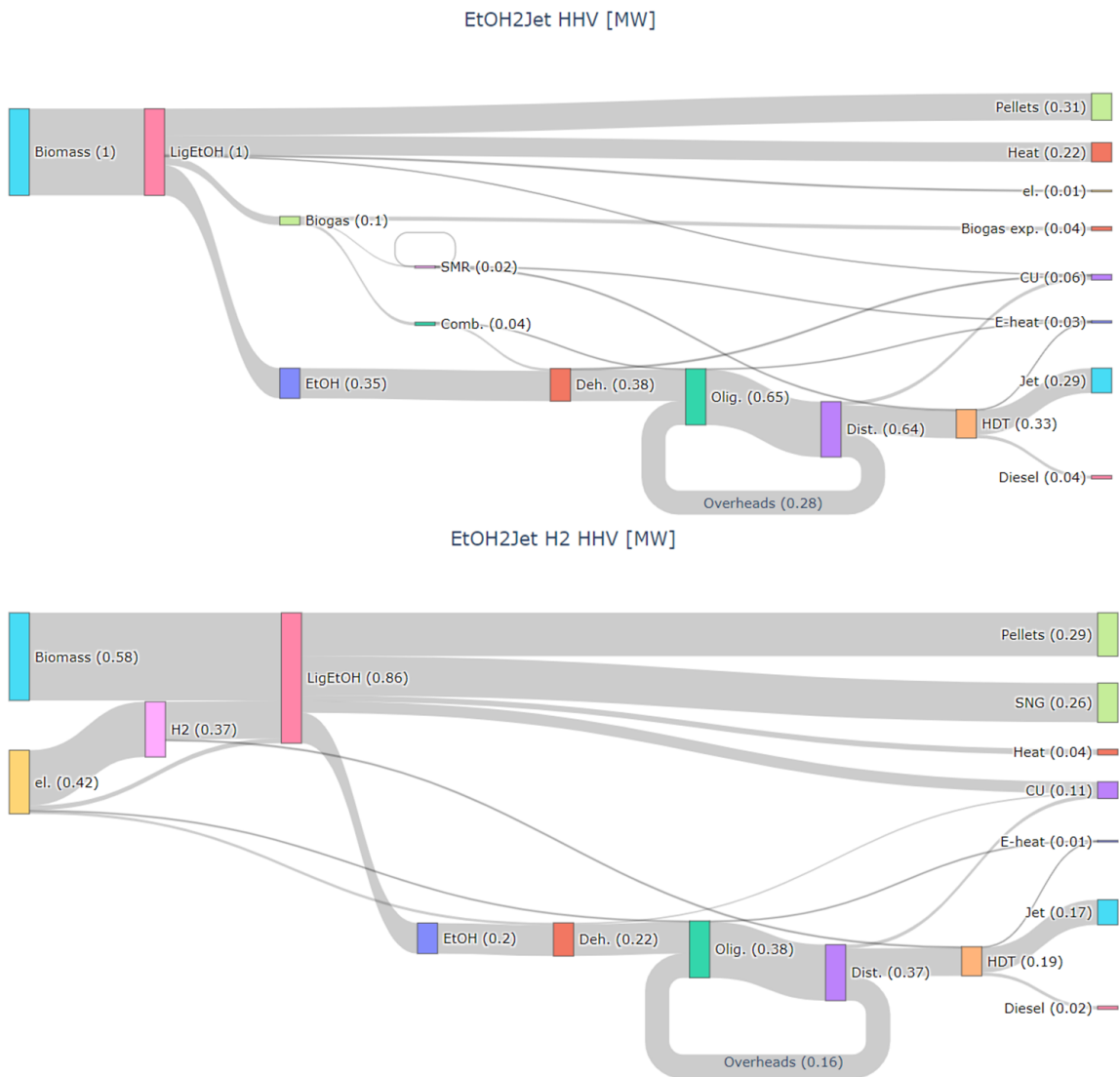


**Figure 66 Energy Sankey diagrams – lignocellulosic ethanol to jet fuel (including indicative balances for the background ethanol plants).**

**Table 28 HTL carbon and energy balance.**

Scenario	HTL_biogas		HTL_H2			HTL_xH2		
	Carbon	Energy	Carbon	Energy		Carbon	Energy	
	kg/h	MW	kg/h	MW		kg/h	MW	
				SOEC	PEM		SOEC	PEM
<b>Input</b>								
Feedstock	7 392	94	7 392	94	94	7 392	94	94
Biogas	1 866	38	968	20	20			
Electricity		1		20	21		36	38
<b>Output</b>								
Gasoline	3 229	49	3 229	49	49	3 229	49	49
Diesel	828	11	828	11	11	828	11	11
Heavies	666	8	666	8	8	666	8	8
Electricity								
Biogas						233	5	5
<b>Other</b>								
Char	611	6	611	6	6	611	6	6
Flue gas	2 863		1 941			740		
AD CO2	233		233			233		
DH		9		9	9		9	9
CU & losses		49		50	52		42	44
Wastewater	829		852			852		



Figure 67 Energy Sankey diagrams – HTL and upgrading.

**Table 29 Fast pyrolysis carbon and energy balance.**

Scenario	Pyro_biogas		Pyro_H2		
	Carbon	Energy	Carbon	Energy	
	kg/h	MW	kg/h	MW	
				SOEC	PEM
Input					
Feedstock	2 354	27	2 354	27	27
Biogas	357	7	0	0	0
Electricity		0		7	9
Output					
Gasoline	623	10	623	10	10
Diesel	467	7	467	7	7
Heavies	236	3	236	3	3
Electricity		1.69		0.00	0.00
Other					
Flue gas	1 367		971		
District heat		1.27		1.75	1.75
CU & losses	7	13	25	14	15
Wastewater	12		34		

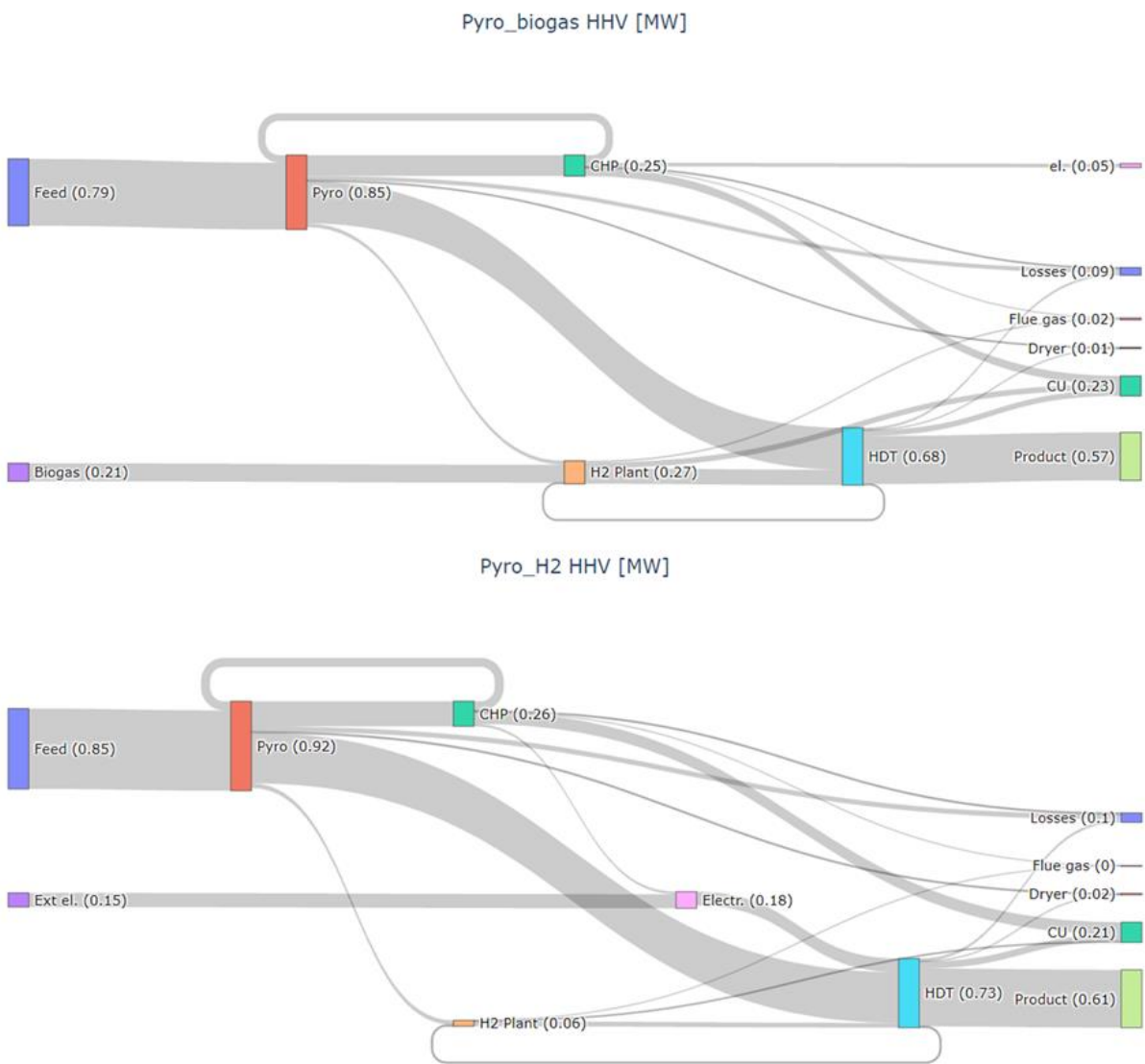


Figure 68 Energy Sankey diagrams – fast pyrolysis.

**Table 30 BLG Methanol carbon and energy balance.**

Scenario	BLGMeOH		BLGMeOH_noWGS			BLGMeOH_rWGS		
	Carbon	Energy	Carbon	Energy		Carbon	Energy	
	kg/h	MW	kg/h	MW		kg/h	MW	
				SOEC	PEM		SOEC	PEM
Changes to mill BAU								
Replacement feed	25 989	291	27 064	304	304	30 165	338	338
Electricity		16		173	192		481	533
Output								
MeOH	9 542	160	16 084	270	270	27 172	456	456
Electricity		0		0	0		0	0
Secondary								
Steam to mill								
LPS		61		56	56		44	44
MPS		-2		-4	-4		-10	-10
IPS		0		0.0	0.0		0.0	0.0
District heat		4		6	6		14	14
Green liquor	3 214		3 214			3 214		
Conc. CO2	18 018		12 016			0.02		
off gases	1 398		1 615			2 490		
Cold utility		71		110	114		188	200
Wastewater	1498		740			794		
Non energy co-product								
Oxygen, kg/h		0		0	0		854	854

**Table 31 BLG FT carbon and energy balance – SMR configuration.**

Scenario	BLGFT_SMR		BLGFT_xSMR		BLGFT_xSMR_noWGS			BLGFT_xSMR_rWGS		
	Carbon	Energy	Carbon	Energy	Carbon	Energy		Carbon	Energy	
	kg/h	MW	kg/h	MW	kg/h	MW		kg/h	MW	
						SOEC	PEM		SOEC	PEM
Changes to mill BAU										
Replacement feed	27 268	306	31 668	355	25 354	284	284	20 796	233	233
Electricity		6		2		126	140		514	569
<b>Output</b>										
Main										
FTP	7 826	120	9 057	139	13 259	204	204	24 796	381	381
Electricity		0		0		0	0		0	0
Secondary										
Steam to mill										
LPS		18		15		6	6		0	0
MPS		34		38		56	56		90	90
IPS		0		-28		1.6	1.6		2.2	2.2
District heat		29		31		22	22		38	38
Green liquor	3 201		3 201		3 201			3 201		
Conc. CO2	18 387		19 146		14 427			14		
Flue gas	3 654		1 497		2 024			4 944		
Cold utility		72		82		94	98		172	185
Wastewater	600		767		759			714		
Other co-product										
Oxygen, kg/h		0		0		0	0		958	958

**Table 32 BLG FT carbon and energy balance – eSMR configuration.**

Scenario	BLGFT_eSMR		BLGFT_xeSMR		BLGFT_xeSMR_noWGS			BLGFT_xeSMR_rWGS		
	Carbon	Energy	Carbon	Energy	Carbon	Energy		Carbon	Energy	
	kg/h	MW	kg/h	MW	kg/h	MW		kg/h	MW	
						SOEC	PEM		SOEC	PEM
Changes to mill BAU										
Replacement feed	27 458	308	32 851	368	27 137	304	304	28 350	318	318
Electricity		11		17		145	158		590	646
Output										
Main										
FTP	8 133	125	9 996	154	14 588	225	225	28 843	444	444
Electricity		0		0		0	0		0	0
Secondary										
Steam to mill										
LPS		16		11		2	2		0	0
MPS		35		42		60	60		75	75
IPS		0		-36		-9.7	-9.7		-29.4	-29.4
District heat		30		32		24	24		42	42
Green liquor	3 201		3 201		3 201			3 201		
Conc. CO2	18 557		19 602		14 974			1 418		
Flue gas	3 198		0		0			0		
Cold utility		73		89		103	106		209	222
Wastewater	570		870		906			208		
Other co-product										
Oxygen, kg/h		0		0		0	0		1 024	1 024

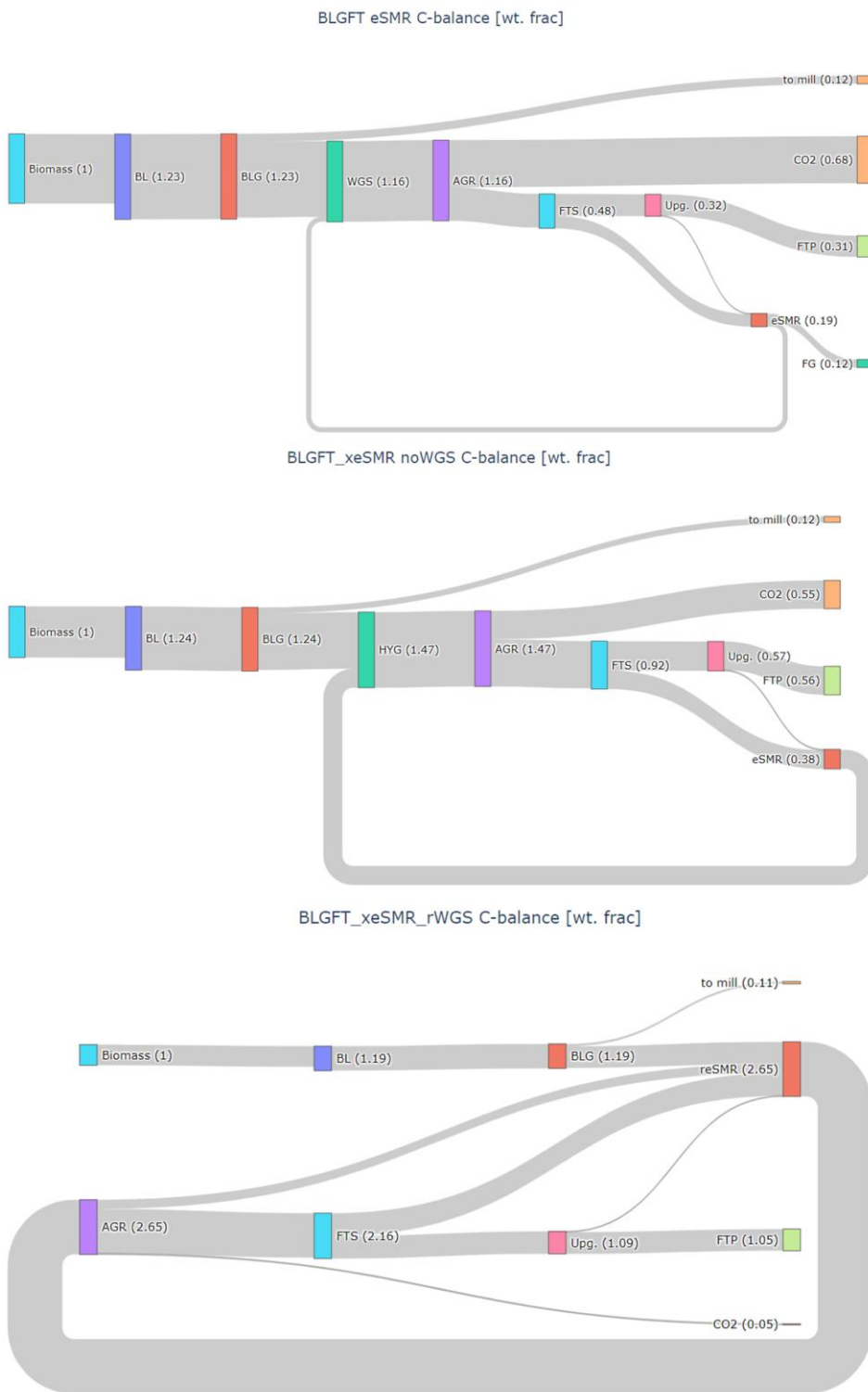


Figure 69 Carbon Sankey diagrams – BLG FT cases under eSMR configuration.

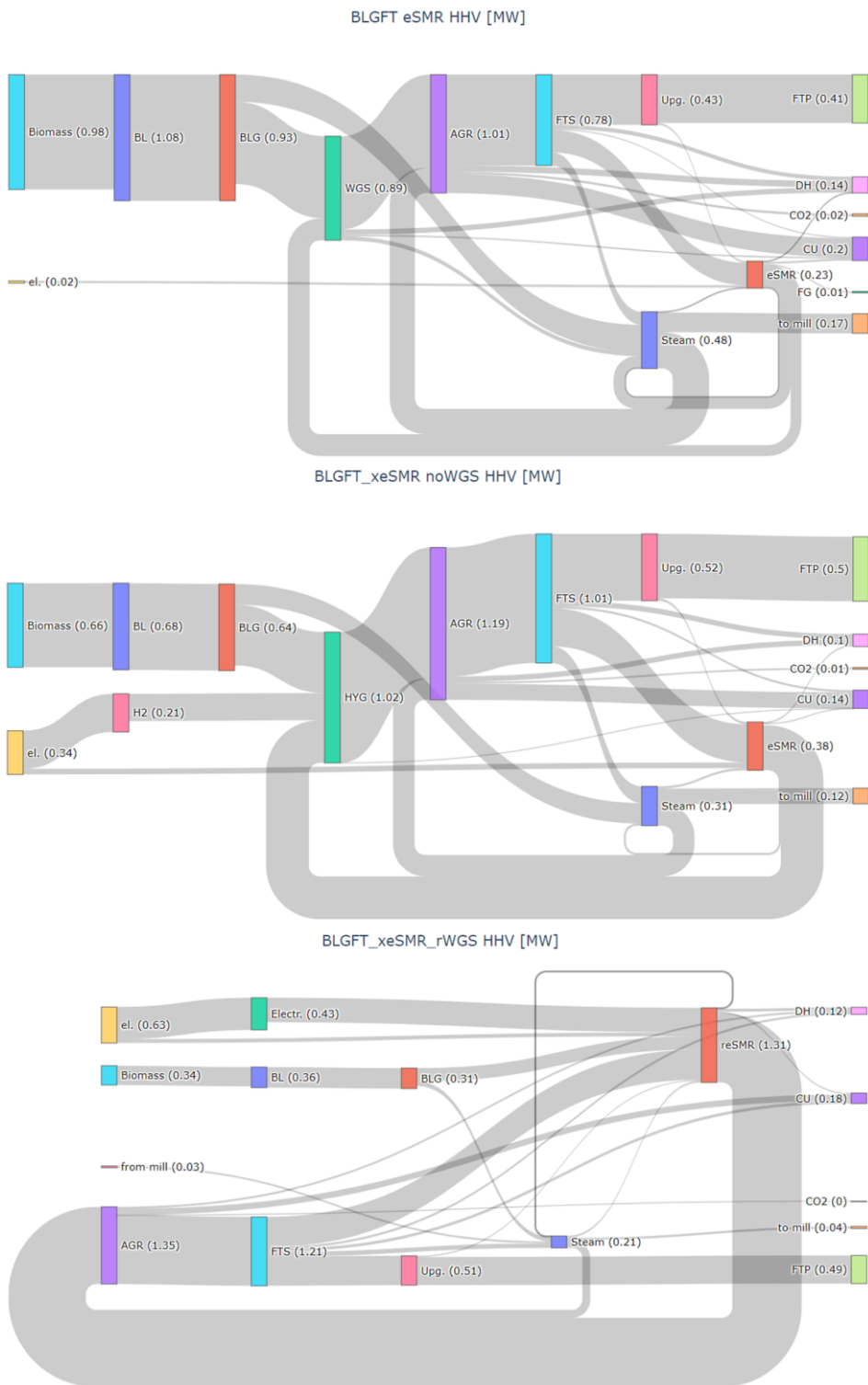


Figure 70 Energy Sankey diagrams – BLG FT cases under eSMR configuration.

**Table 33: Summary of marginal energy flows, mass flows and efficiencies of simulated DFB-SNG cases.**

Marginal Energy flows (MW)	DFB-SNG Base	DFB-SNG 1	DFB-SNG 2a	DFB-SNG 2b	DFB-SNG 3a	DFB-SNG 3b	DFB-SNG 4a	DFB-SNG 4b
Biomass	115.0	113.7	105.0	109.2	98.5	107.9	92.6	109.0
RME	5.6	5.6	5.6	5.6	5.6	5.6	5.6	5.6
Electricity	9.2	10.5	37.6	33.5	86.0	75.0	174.6	151.0
SNG	90.2	90.2	105.8	105.8	132.5	132.5	181.5	181.5
DH	5.0	5.0	0.7	1.0	6.1	5.0	17.7	11.8
<b>Marginal Carbon flows (kg/s)</b>								
Marginal Carbon flows (kg/s)	DFB-SNG Base	DFB-SNG 1	DFB-SNG 2a	DFB-SNG 2b	DFB-SNG 3a	DFB-SNG 3b	DFB-SNG 4a	DFB-SNG 4b
Biomass	3.14	3.11	2.87	2.98	2.69	2.95	2.53	2.98
RME	0.11	0.11	0.11	0.11	0.11	0.11	0.11	0.11
SNG	1.26	1.26	1.46	1.46	1.84	1.84	2.49	2.49

**Table 34: Summary of marginal energy flows, mass flows and efficiencies of simulated DFB-FT cases.**

Marginal Energy flows (MW)	DFB-FT Base	DFB-FT 1	DFB-FT 2a	DFB-FT 2b	DFB-FT 3a	DFB-FT 3b
Biomass	99.0	101.1	104.4	104.4	104.2	104.2
RME	5.6	5.6	5.6	5.6	5.6	5.6
Electricity	13.53	48.58	135.40	123.82	147.75	134.68
FTP	58.96	84.69	126.90	126.90	132.57	132.57
DH	16.88	25.82	53.27	43.13	56.66	45.20
<b>Marginal Carbon flows (kg/s)</b>						
Marginal Carbon flows (kg/s)	DFB-FT Base	DFB-FT 1	DFB-FT 2a	DFB-FT 2b	DFB-FT 3a	DFB-FT 3b
Biomass	2.70	2.76	2.85	2.85	2.85	2.85
RME	0.11	0.11	0.11	0.11	0.11	0.11
FTP	1.07	1.54	2.30	2.30	2.41	2.41

**Table 35: Summary of marginal energy flows, mass flows and efficiencies of simulated O<sub>2</sub>FB-SNG cases.**

Energy flows (MW)	O <sub>2</sub> FB- SNG Base	O <sub>2</sub> FB-SNG 1a	O <sub>2</sub> FB-SNG 1b	O <sub>2</sub> FB-SNG 2a	O <sub>2</sub> FB-SNG 2b	O <sub>2</sub> FB-SNG 3a	O <sub>2</sub> FB-SNG 3b
Biomass	270.0	270.0	270.0	270.0	270.0	270.0	270.0
Electricity	-0.96	23.05	19.31	287.99	248.28	391.30	338.98
SNG	160.1	174.5	174.5	329.32	329.32	387.3	387.3
DH	68.24	71.19	67.91	117.47	83.18	133.96	88.92
Carbon flows (kg/s)	O <sub>2</sub> FB- SNG Base	O <sub>2</sub> FB-SNG 1a	O <sub>2</sub> FB-SNG 1b	O <sub>2</sub> FB-SNG 2a	O <sub>2</sub> FB-SNG 2b	O <sub>2</sub> FB-SNG 3a	O <sub>2</sub> FB-SNG 3b
Biomass	6.69	6.69	6.69	6.69	6.69	6.69	6.69
SNG	2.19	2.40	2.40	4.56	4.56	5.35	5.35

**Table 36: Summary of marginal energy flows, mass flows and efficiencies of simulated O<sub>2</sub>FB-FT cases.**

Energy flows (MW)	O <sub>2</sub> FB-FT Base	O <sub>2</sub> FB-FT 1	O <sub>2</sub> FB-FT 2a	O <sub>2</sub> FB-FT 2b
Biomass (marginal)	270.0	270.0	270.0	270.0
Electricity	-6.89	59.55	343.13	305.4
FTP	104.77	152.59	286.70	286.70
DH	100.72	113.09	197.39	164.34
Carbon flows (kg/s)	O <sub>2</sub> FB-FT Base	O <sub>2</sub> FB-FT 1	O <sub>2</sub> FB-FT 2a	O <sub>2</sub> FB-FT 2b
Biomass	6.69	6.69	6.69	6.69
FTP	1.90	2.77	5.28	5.28

## APPENDIX 6. PRODUCTION COST BUILD-UP

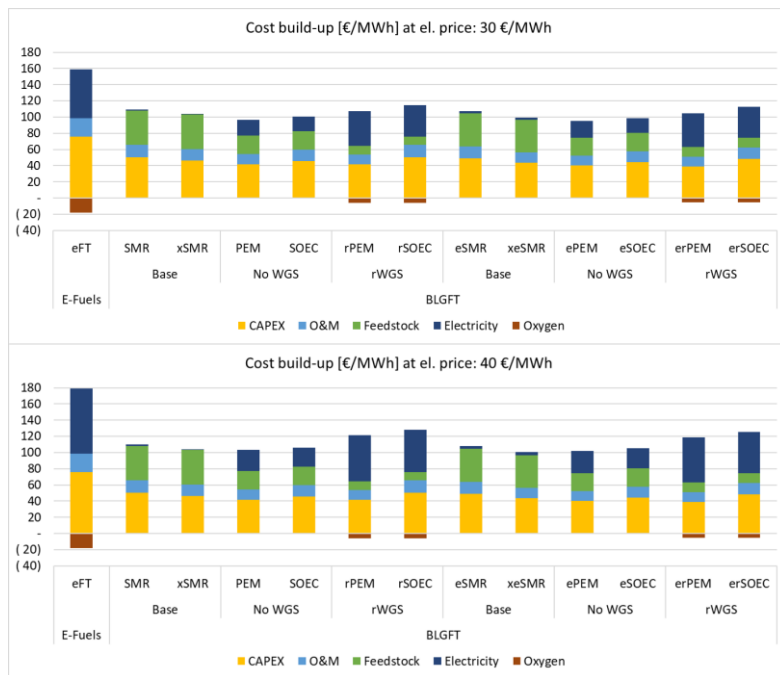


Figure 71 Production cost build-up for BLGFT tracks compared to eFT.

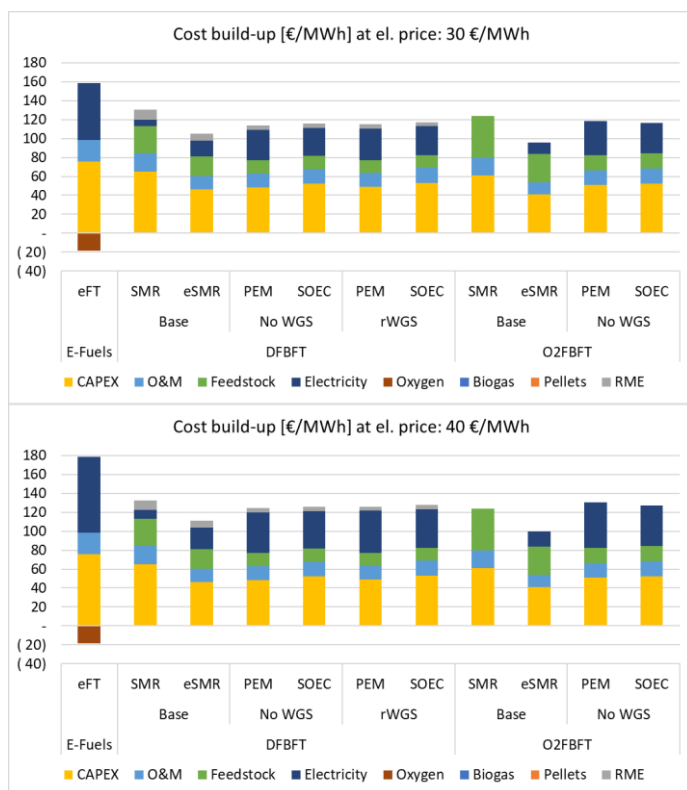


Figure 72 Production cost build-up for fluidized bed FT tracks compared to eFT.

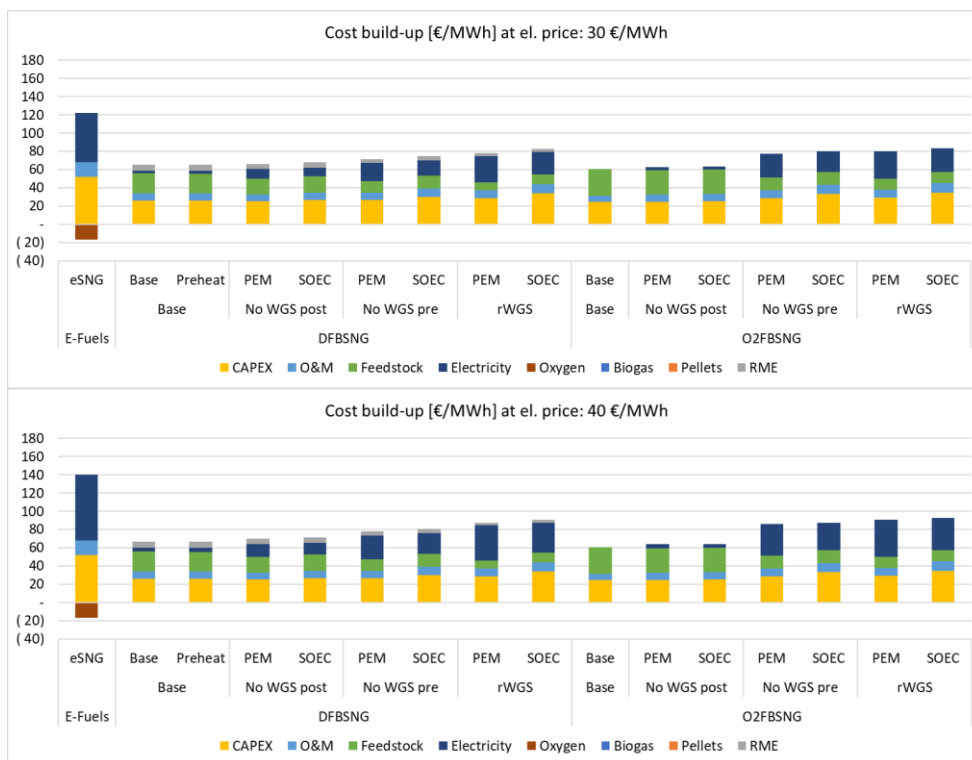


Figure 73 Production cost for SNG tracks compared to eSNG.

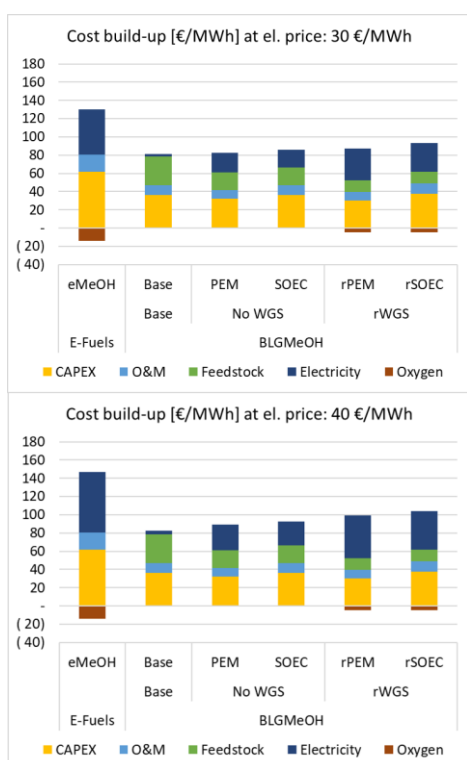


Figure 74 Production cost build-up for methanol tracks compared to eMeOH

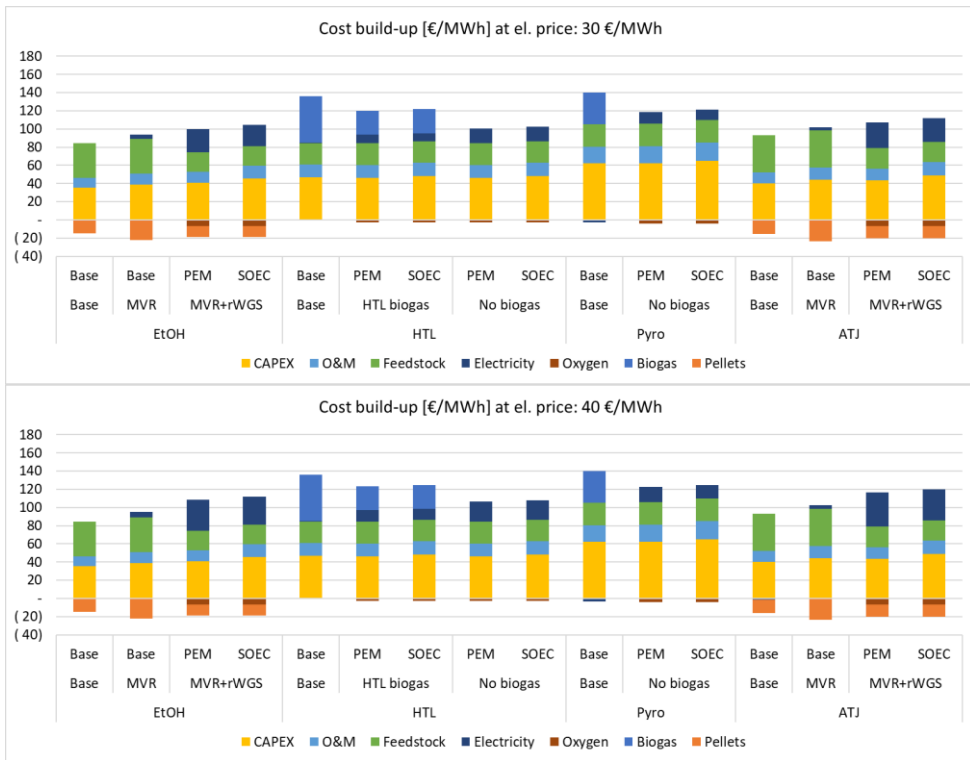


Figure 75 Production cost build-up for liquefaction tracks

